Report
P-18-15
June 2019

Full-scale test of the Dome Plug for KBS-3V deposition tunnels

Monitoring, function tests and analysis of bentonite components

Mattias Åkesson
Torbjörn Sandén
Reza Goudarzi
Daniel Malmberg

SVENSK KÄRNBRÄNSLEHANTERING AB

SWEDISH NUCLEAR FUEL
AND WASTE MANAGEMENT CO

Box 3091, SE-169 03 Solna
Phone +46 8 459 84 00
skb.se

SVENSK KÄRNBRÄNSLEHANTERING

ISSN 1651-4416
SKB P-18-15
ID 1674161
June 2019

Full-scale test of the Dome Plug for KBS-3V deposition tunnels

Monitoring, function tests and analysis of bentonite components

Mattias Åkesson, Torbjörn Sandén, Reza Goudarzi,
Daniel Malmberg

Clay Technology AB

Keywords: Bentonite seal, Filter section, Backfill, Tightness, KBP1016.

Abstract

The deposition tunnels in a planned repository for spent nuclear fuel will be sealed with a plug at the end of the tunnels to withstand the swelling of the backfill and to seal off out-flowing groundwater. A full-scale Dome plug was installed during spring 2013 at Äspö HRL. The principle design of the plug includes several components, among which the most important are the concrete dome, the bentonite seal and the filter section. The test also included a section with backfill behind the filter section. This report describes:

- the monitoring of the bentonite components i.e. bentonite seal and backfill from test start until the test dismantling of the plug in the end of 2017,
- the performed function tests on tightness and strength,
- the sampling of the bentonite seal and backfill during excavation,
- the predictive modelling and following comparison with results on density and degree of saturation distribution determined during excavation.

The sampling, function tests and evaluation of the concrete dome are described in an own report (Malm et al. 2019).

Monitoring

The monitoring of the bentonite components has included sensors measuring Relative Humidity, Total pressure, Pore Pressure and Displacement. In addition, the applied water pressure and inflow to the filter section have been registered together with the leakage past/through the plug.

The measurements have shown that both the seal and the backfill started to take up water immediately after installation. After the filter fill-up and the later water pressure increase in the filter section up to 4 MPa, the saturation rates increased and after about two years test duration the Relative Humidity sensors indicated that both the bentonite seal and the backfill were largely saturated. The registered swelling pressures have been somewhat lower than expected, between a couple of hundreds kPa and up to 1 800 kPa. The displacement sensors have registered a small movement upstream, approximately 30 mm at the end of the monitoring period, of both the bentonite seal and the filter section and these movements were later confirmed in conjunction with the dismantling.

The water tightness of the plug has been continuously measured during the test time. The leakage collected in a weir in front of the plug has been determined to between one and three liters per hour. It is however not exactly known how much of this leakage that has been coming through the plug or in the interface concrete-rock and how much that has been coming via fractures in the rock.

Function tests

Gas tightness. A decision was made that the Dome plug experiment should be used to verify the gas tightness requirement (see description in Section 1.3.3). The test was started by draining the water from the filter section and then fill it with helium gas to an overpressure of 0.4 bar. By monitoring the gas pressure evolution and also by using sniffer leak search along the entire front surface of the concrete plug it was verified that the seal was gas tight at 0.4 bar overpressure.

Strength test. A preliminary design basis has been that the plug shall withstand a total pressure of 7 MPa (hydrostatic pressure of 5 MPa and swelling pressure from the backfill of 2 MPa). The total pressure during the test time has been somewhat lower, between 5 and 6 MPa, and it was therefore decided to increase the applied water pressure in the filter section in order to test the strength. The water pressure was increased in steps for three weeks up to 8 MPa (total pressure including the swelling pressure from the bentonite was thus >9 MPa). No cracking or fracturing of the concrete could be observed visually. The concrete dome has been investigated with e.g. different methods of non-destructive testing, core drilled samples etc. The results from these tests are reported in Malm et al. (2019). The leakages past the plug and through the rock increased, however, strongly when the water pressure was increased but was after a water pressure decrease to 4 MPa back to the same level as before the strength test started.

Sampling of bentonite components

The sampling of the bentonite seal showed that it was completely saturated. There were, however, remaining large differences in density between the central parts (former block stack) and the periphery (former pellet filling) even if it was obvious that the differences had decreased when comparing with the density of the different components at installation. The homogenization of the bentonite had thus proceeded which also was expected.

It was during excavation observed that the bentonite seal had swelled and compacted the filter section inside (gravel filling) and also moved the LECA wall a few centimeters upstream towards the backfill.

The backfill section was also largely saturated but there were some central parts with a lower degree of saturation. The differences in density between the central parts and the pellet filled parts at the periphery were similar to what was determined for the bentonite seal.

Modelling

Numerical modelling of the dome plug was performed in order to predict the state of the bentonite seal at the time of the dismantling. This entailed some modifications of an earlier blind predictive model that was presented in Börgesson et al. (2015a). This model included representation of bentonite backfill and seal (both blocks and pellets) as well as filter materials (Leca beams and gravel). The mechanical processes of the bentonite-based materials were modelled with the thermoelastoplastic constitutive laws, based on the Barcelona Basic Model (BBM).

The hydro-mechanical modeling has shown a fairly good ability to predict the overall evolution of RH, swelling pressures and displacements. However, the hydro-mechanical model could not converge if a boundary condition with 4 MPa water pressure was applied, and it was therefore necessary to use an atmospheric pressure boundary in order to obtain a solution. This appears to be one of the reasons for why the rate of hydration was underestimated, possibly together with a circumventing water supply to the seal from the side toward the concrete beams. The extent of homogenization was in fairly good agreement with the experimental data if the model was allowed to run to a hydration state more similar to the experiment. However, the lowest dry densities in the HM model significantly exceeded the lowest values observed in the in experimental data, which may be a consequence of the absence of wall friction in the model, since wall friction tend to counteract the homogenization processes.

The consistency between the installed dry density, the measured effective stresses and the dismantling data were evaluated. This shows that the measured dry density distribution in the bentonite seal and the dimensions of this at the time of dismantling were in good agreement with the average dry density of the seal at the installation. A corresponding comparison for the backfill showed however that the equivalent dry density at the dismantling was 7 % lower than the average dry density at the installation. This discrepancy seems to originate from the low dry densities found in the pellets filled slot adjacent to the Leca wall. The swelling pressures at the end of the monitoring period were related to the measured dry density values in samples taken close to 15 of the total pressure sensors. This was found to be consistent with established swelling pressure relations for approximately half of the sensors. However, four of the sensors in the seal close to the concrete beams showed too low pressure levels in relation to the dry density, and three of the sensors in the pellets filling close to the Leca wall showed too high pressure levels. Finally, an evaluation of the filter pressure data and the displacement at the Leca/backfill interface showed that these variables were correlated, which supports the notion that the pressurization of the filter contributed to the compression of the gravel filling.

Sammanfattning

I det planerade slutförvaret för utbränt kärnbränsle kommer deponeringstunnlarna att tätas med en plugg i slutet på tunnlarna. Pluggens uppgift är att stå emot svälltrycket från återfyllningen samt att täta för vattenflöden. En valvplugg i full skala installerades våren 2013 i Äspö HRL. Designen inkluderar ett flertal komponenter av vilka de viktigaste är betongvalvet, bentonittätningen samt filtersektionen. I försöket ingår även en sektion med återfyllning innanför filtret. Denna rapport beskriver:

- övervakning samt datainsamling av tryckutveckling, vattenmättnad etc hos bentonitkomponenterna från det att försöket startade och fram tills brytningen i slutet av 2017,
- de utförda funktionstesterna när det gäller täthet och hållfasthet hos pluggen,
- provtagningen av bentonittätningen och återfyllningen i samband med brytningen av försöket,
- resultat från modellering av homogenisering och vattenmättnad samt jämförelser med de bestämningar som gjorts i samband med brytningen.

Provtagning, funktionstester samt utvärdering av betongvalvet är beskrivet i en egen rapport (Malm et al. 2019).

Övervakning och datainsamling

Under testtiden har data registrerats som visar utvecklingen av relativ fuktighet, totaltryck, portryck samt förskjutningar. Utöver detta har även det pålagda vattentrycket, inflödet till filtersektionen samt läckagen över pluggen registrerats.

Mätningarna har visat att både bentonittätningen och återfyllningen började att ta upp vatten omedelbart efter installationen. Efter det att filtret fyllts upp med vatten och senare också trycksatts till 4 MPa, ökade vattenupptaget och efter ca 2 års test indikerade givarna för relativ fuktighet att både tätning och återfyllning till stora delar var vattenmättad. De registrerade svälltrycken har varit lägre än väntat, från några hundra kPa och upp till ca 1 800 kPa. Förskjutningsgivarna har visat att bentonittätningen har svällt och pressat filtersektionen inklusive LECA väggen inåt. Detta har också senare bekräftats i samband med brytningen.

Tätheten hos pluggen har registrerats kontinuerligt under testtiden. Det vattenläckage som samlades innanför en invallning framför pluggen har varit i storleksordningen 1–3 liter/h. Det är emellertid inte helt klart om detta vatten har läckt genom pluggen eller vid dess kontaktytor mot berget, eller om det har kommit genom sprickor i berget.

Funktionstester

Gastäthet. Innan brytningen fattades det ett beslut att detta experiment skulle användas för att verifiera det krav på gastäthet som fanns, se sektion 1.3.3. Testet startades med att filtersektionen dränerades på vatten och därefter fylldes med heliumgas till ett övertryck på 0.4 bar. Genom att registrera hur gastrycket utvecklades över tid och även genom att använda en läcksökare som registrerade helium kunde det verifieras att tätningen var gastät 0.4 bars övertryck.

Hållfasthet. Ett preliminärt designkrav har varit att pluggen skall kunna stå emot ett totaltryck på 7 MPa (ett hydrostatiskt tryck på 5 MPa och ett svälltryck från återfyllningen på 2 MPa). Det totaltryck som har registrerats under huvuddelen av testtiden har varit mellan 5 och 6 MPa och det bestämdes därför att det pålagda vattentrycket i filtret skulle ökas för att kunna verifiera pluggens hållfasthet. Vattentrycket ökades i steg upp till 8 MPa (totaltrycket inklusive svälltrycket var alltså >9 MPa). Visuellt kunde inga sprickor registreras på betongens yta. Betongvalvet undersöktes senare med olika metoder, både icke-förstörande provtagning samt genom att man borrade ut kärnor för närmare undersökning i laboratorium. Resultaten från dessa undersökningar finns rapporterade i Malm et al. (2019). Läckagen över pluggen och genom berget ökade kraftigt i samband med tryckhöjningen men återgick senare till samma nivå som innan tryckökningen när trycket åter hade sänkts till 4 MPa.

Provtagning av bentonitkomponenterna

Provtagningen av bentonittätningen i samband med brytningen visade att denna var helt vattenmättad. Det fanns emellertid fortfarande stora skillnader i densitet mellan de centrala delarna (tidigare blockstapel) och de yttre delarna närmast berget (tidigare pelletsfyllning) även om det var tydligt att skillnaderna hade minskat i jämförelse med de olika komponenternas densitet vid tiden för installationen. Homogeniseringen av bentonittätningen hade alltså fortgått som förväntat. I samband med brytningen observerades också att bentonittätningen hade svällt och pressat samman filtersektionen (grusfyllningen) och även flyttat LECA-väggen några centimetrar in mot återfyllningen.

Återfyllningen var också till stora delar vattenmättad men det fanns partier i de centrala delarna med något lägre vattenmättnadsgrad. Skillnaden i densitet mellan de centrala delarna och de pelletsfyllda yttre delarna var liknande den som fanns i bentonittätningen.

Modellering

Numerisk modellering av valvpluggen har utförts för att prediktera tillståndet hos bentonittätningen vid tiden för brytning. Detta innefattade en modifiering av en tidigare genomförd prediktiv simulering, presenterad av Börgesson (2015a). Modellen inkluderade både bentonittätningen och återfyllningen (både block och pellets) samt även de båda filtermaterialen (Leca balkar och grusmaterialet). De mekaniska processerna hos de bentonitbaserade komponenterna modellerades med en materialmodell vilken baseras på den s.k. Barcelona Basic Model (BBM).

Den här typen av hydromekaniska modeller har visat sig ha en ganska god förmåga att prediktera den övergripande utvecklingen av relativ fuktighet, svälltryck och förskjutningar. Det var dock inte möjligt att ställa upp en hydro-mekanisk modell som kunde konvergera tillsammans med ett randvillkor med 4 MPa vattentryck, och det var därför nödvändigt att använda en atmosfärisk tryckrand för att erhålla en lösning. Detta tycks vara en av anledningarna till att vattenupptagstakten underskattades. En annan förklaring kan vara att bentonittätningen även tycktes få tillgång till vatten från baksidan dvs. från betongbalkarna. Homogeniseringen av bentonitkomponenterna stämde ganska bra överens med provtagningsresultaten om man lät modellen fortgå tills dess att vattenupptaget i modellen var jämförbart med det i försöket. De lägsta densiteterna i HM-modellen var dock betydligt högre än de som observerades i försöket vilket kan vara en konsekvens av att väggfriktion inte var inkluderad i modellen, eftersom väggfriktion tenderar till att motverka homogeniseringsprocesserna.

Samstämmigheten mellan installerad densitet, uppmätta effektivspänningar samt brytningsdata har utvärderats. Denna utvärdering visar att den uppmätta torrdensitetsfördelningen i bentonittätningen och dimensionerna för denna vid tiden för brytningen stämde bra överens med medeltorrdensiteten hos bentonittätningen vid tiden för installationen. En motsvarande jämförelse för återfyllningen visade dock att den ekvivalenta torrdensiteten för denna var ca 7 % lägre än medeltorrdensiteten vid tiden för installationen. Denna avvikelse tycks härröra från den låga densiteten hos pelletsfyllningen i spalten närmast LECA-väggen. Det uppmätta svälltrycket vid slutet av övervakningsperioden har jämförts med torrdensiteten hos prov tagna i närheten av femton av de installerade tryckgivarna. Värdena visade sig stämma bra med de etablerade samband mellan torrdensitet och svälltryck för ungefär hälften av givarna. Fyra av tryckgivarna i bentonittätningen närmast betongbalkarna visade emellertid för låga tryck i förhållande till de uppmätta torrdensiteterna och tre av tryckgivarna i pelletsfyllningen närmast LECA-väggen visade för höga värden. En utvärdering av filtertryck och registrerade förskjutningar av gränsytan mellan LECA-väggen och återfyllningen visade på en tydlig korrelation, vilket stöder idén om att trycksättningen av filtret har bidragit till kompressionen av grusfyllningen.

Contents

1 Introduction

1.1 Background

The deposition tunnels in a planned repository for spent nuclear fuel will be sealed with a plug at the end of the tunnels in order to withstand the swelling of the backfill and to seal off out-flowing groundwater. The principle design of the plug includes several components, among which the most important are the concrete dome, the bentonite seal and the filter. The groundwater leakage past the plug has to be small enough in order to build up a water pressure behind the plugged volume, thereby removing the hydraulic gradients from the deposition holes and tunnels, and to prevent loss of bentonite from the deposition holes due to erosion throughout the operational phase of the repository. In addition, the construction site must be kept free from water during construction of the plug system and while the concrete dome cures until it is finally grouted for a tight contact to rock. Wet tunnels therefore require a filter section which can drain the water coming from the inner parts of the tunnel and temporarily let it by-pass the plug.

These issues and demands were addressed in the joint SKB and Posiva project "System design of dome plug for deposition tunnels". The project has aimed at ensuring that the reference configuration of the KBS-3V deposition tunnel end plug works as intended, and within the framework of this project a full-scale test, denoted "DOMPLU", has been performed at 450 m depth at Äspö Hard Rock Laboratory in cooperation between SKB and Posiva (Grahm et al. 2015).

The Dome plug was installed during spring 2013. During the test time, data from more than 100 sensors have been continuously registered and leakages pass the plug or through the rock have been measured. The dismantling of the plug started in November 2017. Before the dismantling started, several tests have been performed e.g. a test with the aim to determine the gas tightness of the plug and one test with the aim to demonstrate the strength of the plug.

The purpose of this report is to present results from the Domplu field test which relate to the bentonite-based components and the filter section behind the Dome plug. The installed bentonite components, filter materials, instrumentation and equipment used for leakage measurement are presented in Chapter 2. Results from the monitoring of sensors and the special function tests is described in Chapter 3. The dismantling operation, the sampling program and the results from these activities are presented in Chapter 4. The numerical modeling is presented in Chapter 5. Evaluations regarding the compliance of requirements and design premises, the consistency of different data sets, and the validity of used material models are presented in Chapter 6. Finally, some comments and conclusions are given in Chapter 7.

1.2 General design

The full-scale test consists of several components, each with its own purpose, Figure 1-1. The innermost component is a 1.1 m backfill zone which consists of a stack of bentonite blocks with a surrounding pellet filling. The next component is the filter section which is composed of 0.3 m thick LECA-beams and a 0.3 m layer of gravel (2–4 mm). The filter serves for drainage of groundwater during construction as well as for artificial wetting of the bentonite seal when the drainage is finally closed. The gravel and the bentonite seal are separated by a geo-textile which also facilitates distribution of water into the seal. Pre-fabricated concrete beams are positioned on the downstream side of the bentonite seal to facilitate installation and to have a clear delimiter towards the in situ cast concrete dome. The bentonite seal consists of a 0.5 m stack of highly compacted MX-80 bentonite blocks with a surrounding MX-80 pellet filling closest to the rock.

The restraining concrete structure is designed as an unreinforced octagonal dome plug, cast in situ by low-pH concrete. The diameter of the concrete dome is 8.8 m while the concrete thickness is 1.79 m in the hub. An important feature of the dome plug is the internal cooling system which enable shrinkage of the dome prior to the contact grouting of the joint between the plug and the rock, which in turn has contributed to an efficient sealing of the plug. A preliminary design basis is that the plug shall withstand 7 MPa of total pressure.

Before the plug installation started, coarse groundwater inflow measurements to the plug location were carried out (Grahm et al. 2015). The total inflow from the backwall to the front of the slot was determined to 5.2 l/h. Consequently, the assumed rock requirement to not allow any water bearing fractures at the DOMPLU location could not be fulfilled.

Besides extensive monitoring of the concrete dome structure, the inner plug components are instrumented with sensors for measurement of total pressure, pore pressure, relative humidity and displacements at several positions. The bentonite-based components and the filter were installed in January 2013, while the concrete dome was cast in March 2013. Pressurization by natural groundwater inflow began in October 2013. The artificial pressurization was increased to 4 MPa in February 2014 and was maintained at this level until June 2017.

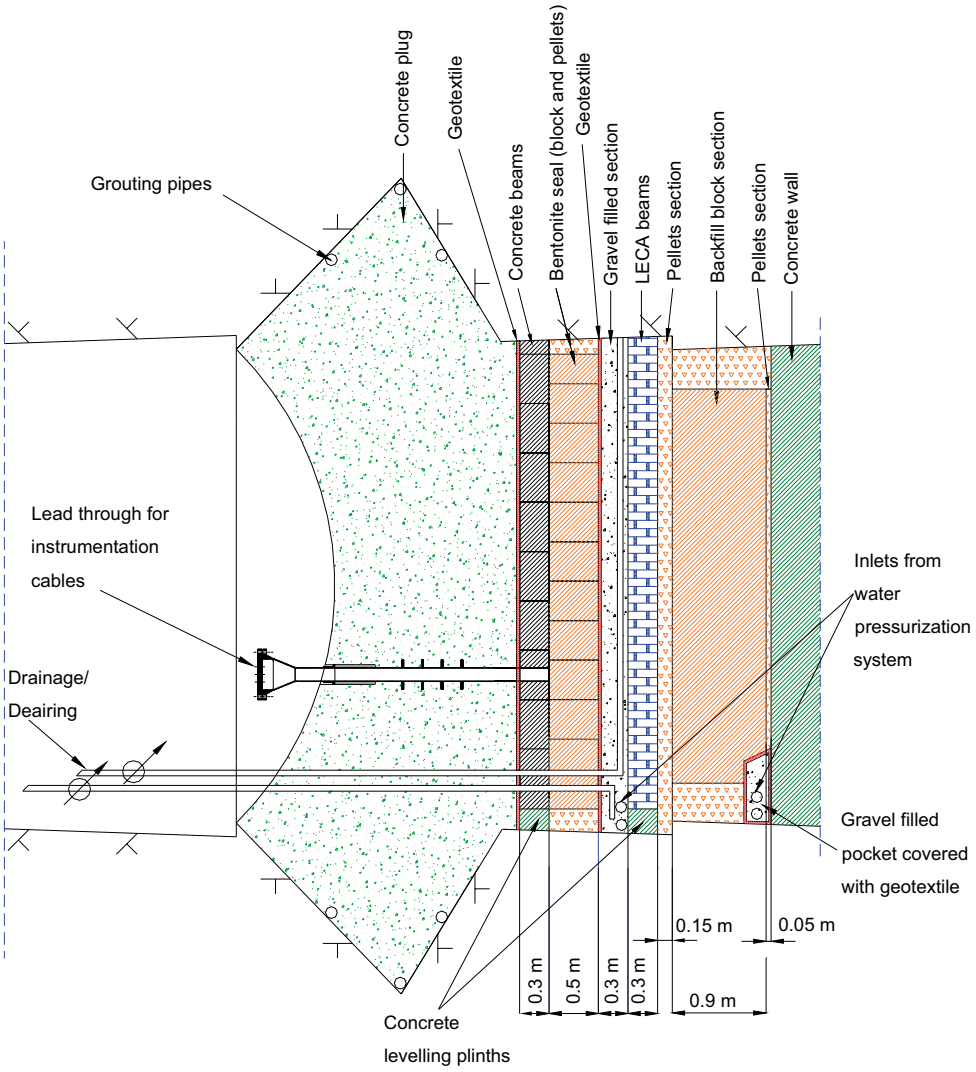

Figure 1-1. *Schematic drawing of the Domplu plug and the different materials included.*

1.3 Requirements on the plug

1.3.1 General

The two main functions of the plug apply to the operational phase (Posiva SKB 2017):

1. The plug shall keep the backfill in place. The plug shall withstand the swelling pressure from the backfill and also the hydrostatic pressure at repository level.
2. The plug shall restrict water flow from deposition tunnels to prevent piping and erosion that may lead to transport of buffer and backfill materials.

To fulfill the demands on the plug functions, requirements have thus been set regarding the strength of the plug and regarding the tightness of the plug. The Domplu project has included tests regarding these requirements. There are also other requirements on the plug e.g. regarding the material composition of the concrete plug but these are not considered in this report.

1.3.2 Strength of the plug

In Posivas case, the design basis load carrying capacity of the plug is 7.5 MPa, derived from the sum of swelling pressure from the backfill, 3 MPa, and the hydrostatic pressure 4.5 MPa (Posiva SKB 2017).

The reference design total pressure of the Dome plug was 7 MPa. This value is based on a water pressure of 5 MPa in combination with a swelling pressure of 2 MPa in the bentonite (Grahm et al. 2015).

1.3.3 Tightness of the plug

Water leakage

Water leakages past the plug may lead to piping and erosion in the buffer and backfill. These processes could lead to unacceptable losses of material.

The current technical design requirement regarding the tightness of the plug was formulated by Posiva and SKB (2017; Section 6.5.3) as: "*200 m^3 total outflow before the backfill is saturated*". This is further discussed in Section 6.1.

Gas tightness

In addition to restricting the water flow from the deposition tunnel, "*the plug also needs to be reasonably gas tight to stop convection of air during the operational period*" (Posiva SKB 2017). SKB defines gas-tight as a situation where no gas phase is present in the hydraulically sealing part of the plug and that the requirement for gas tightness can be assumed to be fulfilled if a water column is maintained in the filter section of the plug throughout the operational period of the entire repository.

The issue with gas tightness has been investigated within this project where a special test has been performed. The results from this test is reported in detail in Åkesson (2018).

2 Description of components and instrumentation

2.1 General

This chapter briefly describes the different components i.e. bentonite seal, filter section and backfill, regarding design, dimensions and installed density. The different sensors and their positions are also described. A more detailed description regarding design and installation process etc is available in Grahm et al. (2015).

2.2 Components

2.2.1 Bentonite seal

The bentonite seal consists of blocks and pellets, both manufactured of MX-80 bentonite, a sodium dominated bentonite produced by American Colloid Company (Karnland et al. 2006). The blocks were stacked according to a decided pattern, see drawing provided in Figure 2-1. Bentonite pellets were used as a floor levelling material to even out the rough rock surface and thereby provide a suitable surface on which the blocks could be stacked. Pellets were also used to fill all gaps between the blocks and the rock walls and the ceiling.

The blocks were compacted by uniaxial compression to a size of 500 × 571 × 300 mm with a pressure of 27 MPa. The design height 300 mm of a seal block was chosen to comply with the 600 mm height of a concrete beam. The total design depth of the bentonite seal for DOMPLU is 500 mm.

The bentonite blocks had after compaction an average dry density of 1 682 kg/m^3. The initial water content of the raw material was 17 %. The bentonite pellets had a water content of 10 % and the dry density of the pellet filling was 900 kg/m^3.

2.2.2 Filter section

The filter section consists of two material layers, a stiff draining material made of 300 mm thick LECA beams and a 300 mm thick layer of a geological draining material (gravel 2–4 mm). In addition, a geotextile is positioned between the gravel filling and the bentonite seal to prevent the bentonite from swelling into the voids of the filter. The photo provided in Figure 2-2 shows the different filter components and the bentonite seal outside.

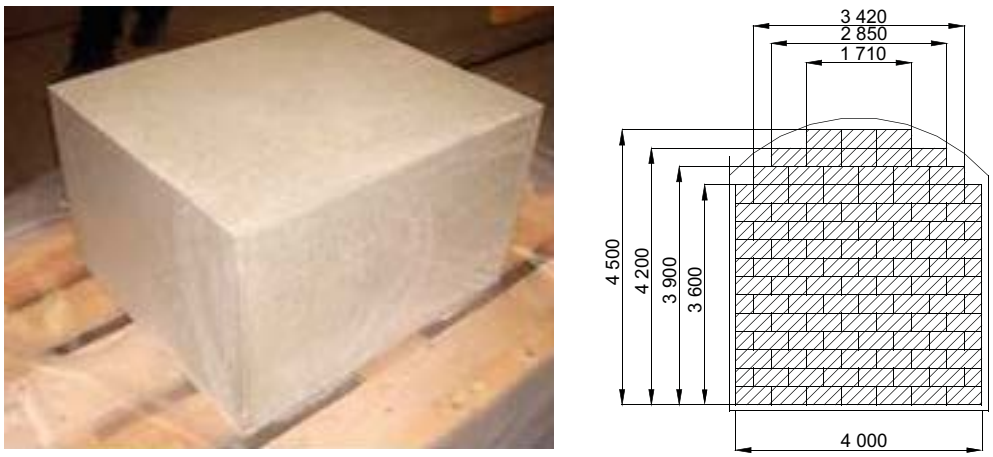

Figure 2-1. *Left: Photo of a bentonite block that was used for the sealing section. Right: Schematic drawing of the block stack for the bentonite seal.*

Figure 2-2. *Photo taken during installation of the different components. From left: the LECA wall (1), the gravel filter (2), the geotextile (3), the bentonite seal consisting of block (4A) and pellets (4B) and the concrete beams (5).*

2.2.3 Bentonite backfill

The backfill section was built according to the reference design i.e. it included a central block stack with pellets filling up the gaps between block and rock. Bentonite pellets were also used as a floor levelling material to even out the rough rock surface and thereby provide a suitable surface on which the blocks could be stacked (same principle as for the bentonite seal). The blocks used in this experiment were, however, considerably smaller than in the reference design. The blocks used were manufactured in brick size (300 × 150 × 75 mm). The photo provided in Figure 2-3 was taken during the installation that largely was made manually.

In addition to the block stack, two vertical sections, one positioned just behind the LECA wall (thickness of 150 mm) and another positioned between the block stack and the tunnel end (thickness of 50 mm) were filled with bentonite pellets. The motive for this pellet filling was to reduce the overall dry density and the swelling pressure on the concrete plug.

The backfill blocks were manufactured of bentonite from Ashapura, India. The blocks had a water content of approximately 17 % and a dry density of 1 750 kg/m^3. The pellets used in the backfill were commercially available under the trademark Cebogel (see Sandén et al. 2008). They are manufactured of bentonite from Milos, Greece. The Cebogel pellets had a water content of 16 % and the dry density of the pellet filling was 900 kg/m^3.

2.2.4 Compilation of material data

The properties of the bentonite seal and the backfill regarding e.g. swelling pressure and hydraulic conductivity are to a large extent depending on the installed mean dry density in the sections. The as-built data from the installation can be found in (Grahm et al. 2015). A compilation of the material data and the calculated volumes and mean dry density of the bentonite-based components is given in Table 2-1 (Åkesson 2017).

Figure 2-3. *Photo taken during the installation of backfill. To the left in the photo, the LECA wall can be seen. Between the LECA wall and the backfill blocks there is a pellet filled gap with a thickness of 150 mm and between the blocks and the tunnel end there is another pellet filled gap with a thickness of about 50 mm. The three steel tubes laying on the backfill blocks are displacement sensors.*

Table 2-1. Dry density and volume for bentonite-based components.

Quantity	Bentonite seal		Backfill	
	Blocks	**Pellets**	**Blocks**	**Pellets**
Material	MX-80		Asha NW BFL-L 2010	Cebogel
Dry density	1 682 kg/m^3	~900 kg/m^3	1 750 kg/m^3	~900 kg/m^3
Volume*	8.4 m^3	1.5 m^3	14.8 m^3	8.5 m^3
Mean dry density**	1 560 kg/m^3		1 440 kg/m^3	

* Based on areas and depths of block stacks and tunnel profiles.

** Calculated as weighted means.

2.3 Monitoring

2.3.1 General

Behind the concrete dome, there is a sealing section, a filter section (filter section) and a section simulating a small part of the backfill. The sealing section consists of bentonite blocks and bentonite pellets that during water uptake will swell and seal against the rock. The filter section consists of a geotextile, a gravel filling and a wall made of LECA beams. Drainage tubes through the plug have made it possible to control the pressure in the filter and to test the plug function when exposed to high water pressures. The backfill is approximately one meter long, installed according to the present reference design i.e. bentonite blocks are piled in the main part of the tunnel and bentonite pellets are filling up the gaps between blocks and rock. In order to monitor the status of the different components, sensors of different types have been placed in both the bentonite seal, the filter section and in the backfill.

2.3.2 Sensor description

The purpose of the measurements is to:

- Follow the saturation process of the bentonite.
- Monitor the development and distribution of swelling pressure.
- Evaluate the sealing function.
- Follow displacements between the material zones.

The following sensor types were installed:

- Total pressure (swelling pressure + water pressure) 20 pcs
- Pore pressure 6 pcs
- Relative humidity 16 pcs
- Displacement 3 pcs

The transducers are all designed to resist an outer pressure of at least 10 MPa. To prevent leakages through the cables, these are led in steel tubes from the sensor body, through the bentonite and then into special "lead throughs" installed in the rock and in the plug, see description in Grahm et al. (2015). All instruments were manufactured in acid proof steel.

Total pressure

The transducer uses a pressure sensitive diaphragm with a vibrating wire attached to it. The transducer is special designed, shaped as an ice hockey puck. The same type of transducer has been used within other full-scale tests at Äspö HRL e.g. the Lasgit test.

A photo showing a sensor is provided in Figure 2-4a.

Model: Geokon 4800-1x-10 MPa. **Dimensions:** D=63 mm, t=16 mm.

Pore pressure

The transducer uses a pressure sensitive diaphragm with a vibrating wire attached to it. The transducer is a standard type. The sensitive part of each transducer is protected with a filter.

A photo showing a sensor is provided in Figure 2-4b.

Model: Geokon 4500SH-3-10 MPa. **Dimensions:** D=19.1 mm, L=133 mm.

Relative Humidity

These transducers are manufactured by Sensiron and then modified by Aitemin in order to achieve a digital output signal which makes it possible to have cable lengths up to 100 m. The transducer is of capacitive type. The sensitive part of each transducer is protected with a filter.

A photo showing a sensor is provided in Figure 2-5a.

Model: Aitemin SHT75 V3. **Dimensions:** D=12 mm, L=87 mm.

Displacement

The relative displacement of the different sections is registered with sensors from Geokon.

A photo showing a sensor is provided in Figure 2-5b.

Model: Geokon 4435-1X-50. **Dimensions:** 1 000 mm, 1 300 mm, 1 600 mm.

A compilation of all sensors is provided in Table 2-2 and 2-3. The different ID codes for every sensor and a brief description of the positions is specified. In the last three columns, the serial numbers and the values from the function control that was made in conjunction with the installation, are provided.

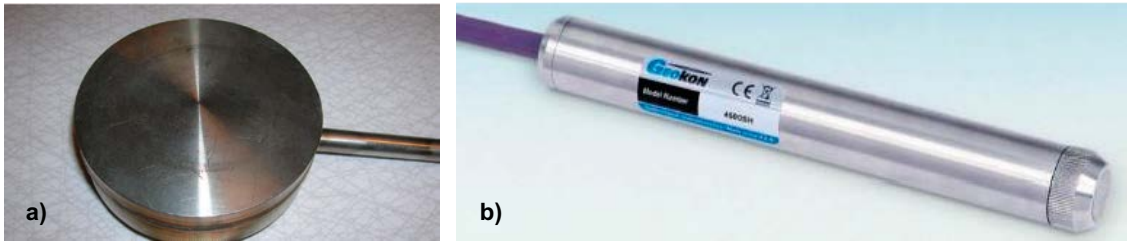

Figure 2-4. *a) Total pressure sensor (Geokon 4800-1x-10 MPa), b) pore pressure sensor (Geokon 4500SH-3-10 MPa).*

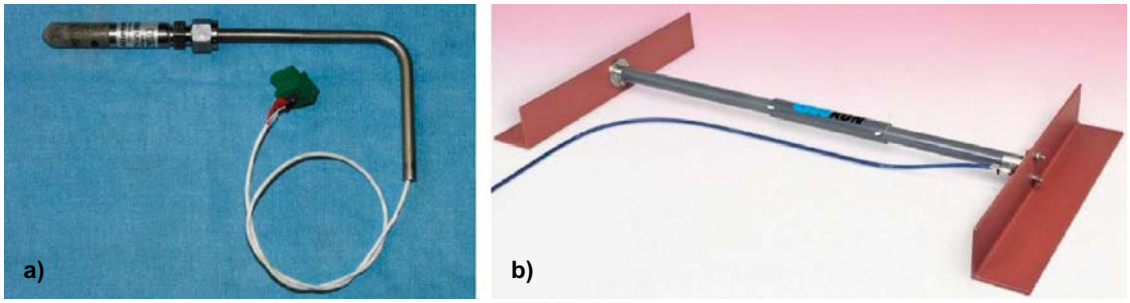

Figure 2-5. *a) Relative humidity sensors (Aitemin SHT75 V3), b) Deformation sensors (Geokon 4435-1X-50).*

Table 2-2. Compilation of data for sensors measuring total pressure, pore pressure and displacement.

Sicada ID code	Mark	Manufacturer	Section	Measuring	Position	Remark	Serial no.	Function control	
								Frequency	Temp.
PXDP10001	PPL10001	Geokon	1	Total pressure	Between bentonite block and concrete		1200466	3719.8	11.6
PXDP10002	PPL10002	Geokon	1	Total pressure	Radial pressure against rock	Molded to rock surface	1200464	3594.0	11.7
PXDP10003	PPL10003	Geokon	1	Total pressure	Between bentonite block and concrete		1200465	3678.6	12.2
PXDP10004	PPL10004	Geokon	1	Total pressure	Radial pressure against rock	Molded to rock surface	1200469	3714.3	11.8
PXDP10005	PPL10005	Geokon	1	Total pressure	Between bentonite block and concrete		1200458	3814.1	11.7
PXDP10006	PPL10006	Geokon	4	Total pressure	Between bentonite block and filter		1200470	3709.9	11.9
PXDP10007	PPL10007	Geokon	4	Total pressure	Radial pressure against rock	Molded to rock surface	1200455	3758.9	12.9
PXDP10008	PPL10008	Geokon	4	Total pressure	Between bentonite block and filter		1200468	3538.1	13.4
PXDP10009	PPL10009	Geokon	4	Total pressure	Radial pressure against rock	Molded to rock surface	1200463	3636.5	12.7
PXDP10010	PPL10010	Geokon	4	Total pressure	Between bentonite block and filter		1200459	3838.7	11.6
PXDP10011	PPL10011	Geokon	5	Total pressure	Between LECA and backfill		1200467	3443.3	13.2
PXDP10012	PPL10012	Geokon	5	Total pressure	Radial pressure against rock	Molded to rock surface	1200454	3741.2	12.9
PXDP10013	PPL10013	Geokon	5	Total pressure	Between LECA and backfill		1200474	3980.2	11.9
PXDP10014	PPL10014	Geokon	5	Total pressure	Radial pressure against rock	Molded to rock surface	1200460	3656.3	13.9
PXDP10015	PPL10015	Geokon	5	Total pressure	Between LECA and backfill		1200456	3774	14.2
PXDP10016	PPL10016	Geokon	9	Total pressure	Between backfill and concrete		1200472	3774.4	13.3
PXDP10017	PPL10017	Geokon	3	Total pressure	Ceiling	Molded to rock surface	1200462	3738.6	11.9
PXDP10018	PPL10018	Geokon	8	Total pressure	Floor	Molded to rock surface	1200473	3826.2	12.3
PXDP10019	PPL10019	Geokon	3	Total pressure	Floor	Molded to rock surface	1200461	3804.5	13.3
PXDP10020	PPL10020	Geokon	9	Total pressure	Between backfill and concrete		1200457	3549.7	13.2
PXDD10001	DPL10001	Geokon	5–9	Displacement	Concrete-Leca	20 cm from centre	1147048	OK	OK
PXDD10002	DPL10002	Geokon	4–9	Displacement	Concrete-bentonite sealing		1147050	OK	OK
PXDD10003	DPL10003	Geokon	5–9	Displacement	Concrete-Leca	40 cm from centre	1147049	3984.9	11.9
PXDU10001	UPL10001	Geokon	Plug	Pore pressure	Positioned on rock surface	Membrane against gap	1200864	8937.6	12.4
PXDU10002	UPL10002	Geokon	Plug	Pore pressure	Positioned on rock surface	Membrane against gap	1200865	9214.8	11.8
PXDU10003	UPL10003	Geokon	1	Pore pressure	Positioned on rock surface	Membrane against gap	922420	8246.5	11.9
PXDU10004	UPL10004	Geokon	1	Pore pressure	Positioned on rock surface	Membrane against gap	922428	8637.3	11.5
PXDU10005	UPL10005	Geokon	9	Pore pressure	Positioned on rock surface	Membrane against gap	1200862	8945.3	12.6
PXDU10006	UPL10006	Geokon	9	Pore pressure	Positioned on rock surface	Membrane against gap	922430	8472.5	12.7

Table 2-3. Compilation of data for sensors measuring relative humidity.

Sicada ID code	Mark	Manufacturer	Section		Position	Remark	Serial no.	Function control	
								Frequency	Temp.
PXDW10001	WPL10001	Aitemin SHT75 V3	2	RH	50 cm from block surface	Borehole in block	16948 134/12	54.9–58.1	12.9–14.2
PXDW10002	WPL10002	Aitemin SHT75 V3	2	RH	20 cm from block surface	Borehole in block	16949 135/12	54.9–58.1	12.9–14.2
PXDW10003	WPL10003	Aitemin SHT75 V3	3	RH	20 cm from block surface	Borehole in block	16956 142/12	54.9–58.1	12.9–14.2
PXDW10004	WPL10004	Aitemin SHT75 V3	3	RH	50 cm from block surface	Borehole in block	16947 133/12	54.9–58.1	12.9–14.2
PXDW10005	WPL10005	Aitemin SHT75 V3	3	RH	50 cm from block surface	Borehole in block	16951 137/12	54.9–58.1	12.9–14.2
PXDW10006	WPL10006	Aitemin SHT75 V3	3	RH	20 cm from block surface	Borehole in block	16961 147/12	54.9–58.1	12.9–14.2
PXDW10007	WPL10007	Aitemin SHT75 V3	2	RH	20 cm from block surface	Borehole in block	16957 143/12	54.9–58.1	12.9–14.2
PXDW10008	WPL10008	Aitemin SHT75 V3	2	RH	50 cm from block surface	Borehole in block	16945 131/12	54.9–58.1	12.9–14.2
PXDW10009	WPL10009	Aitemin SHT75 V3	6	RH	20 cm from block surface	Borehole in block	16954 140/12	54.9–58.1	12.9–14.2
PXDW10010	WPL10010	Aitemin SHT75 V3	6	RH	50 cm from block surface	Borehole in block	16959 145/12	54.9–58.1	12.9–14.2
PXDW10011	WPL10011	Aitemin SHT75 V3	6	RH	20 cm from block surface	Borehole in block	16946 132/12	54.9–58.1	12.9–14.2
PXDW10012	WPL10012	Aitemin SHT75 V3	6	RH	50 cm from block surface	Borehole in block	16952 138/12	54.9–58.1	12.9–14.2
PXDW10013	WPL10013	Aitemin SHT75 V3	7	RH	20 cm from block surface	Borehole in block	16958 14412	54.9–58.1	12.9–14.2
PXDW10014	WPL10014	Aitemin SHT75 V3	7	RH	50 cm from block surface	Borehole in block	16950 136/12	54.9–58.1	12.9–14.2
PXDW10015	WPL10015	Aitemin SHT75 V3	7	RH	20 cm from block surface	Borehole in block	16953 139/12	54.9–58.1	12.9–14.2
PXDW10016	WPL10016	Aitemin SHT75 V3	7	RH	50 cm from block surface	Borehole in block	16962 148/12	54.9–58.1	12.9–14.2

2.3.3 Sensor positions

The sensors are positioned in nine main sections according to Figure 2-6. Note that the scale is excessive in the x-direction in order to facilitate the presentation of the different measuring sections. The individual sensor positions in each section are shown in Figure 2-7 and Figure 2-8.

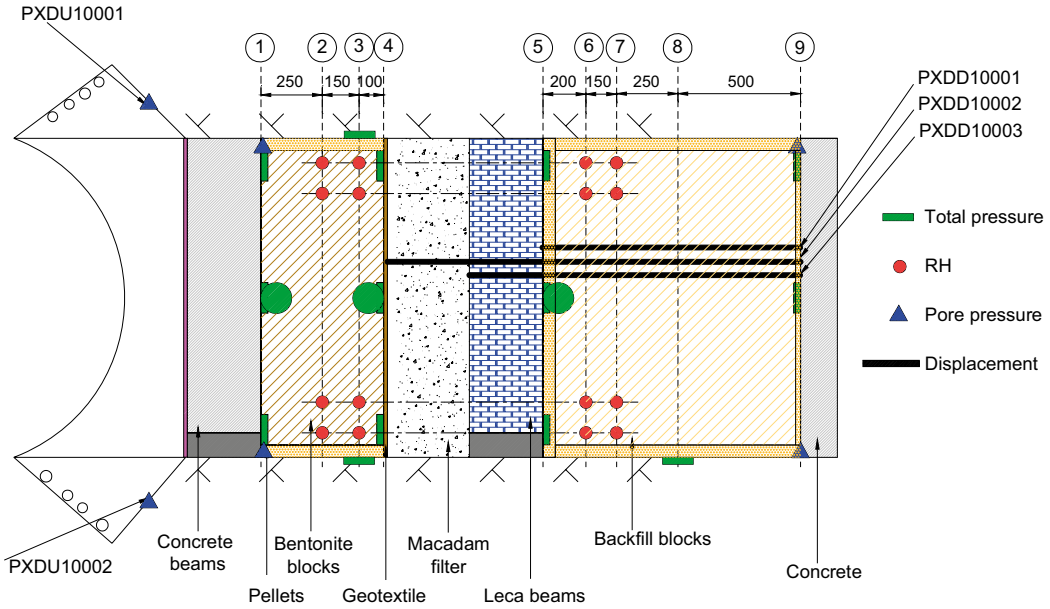

Figure 2-6. Schematic drawing showing the sensor positions in bentonite seal and in the backfill.

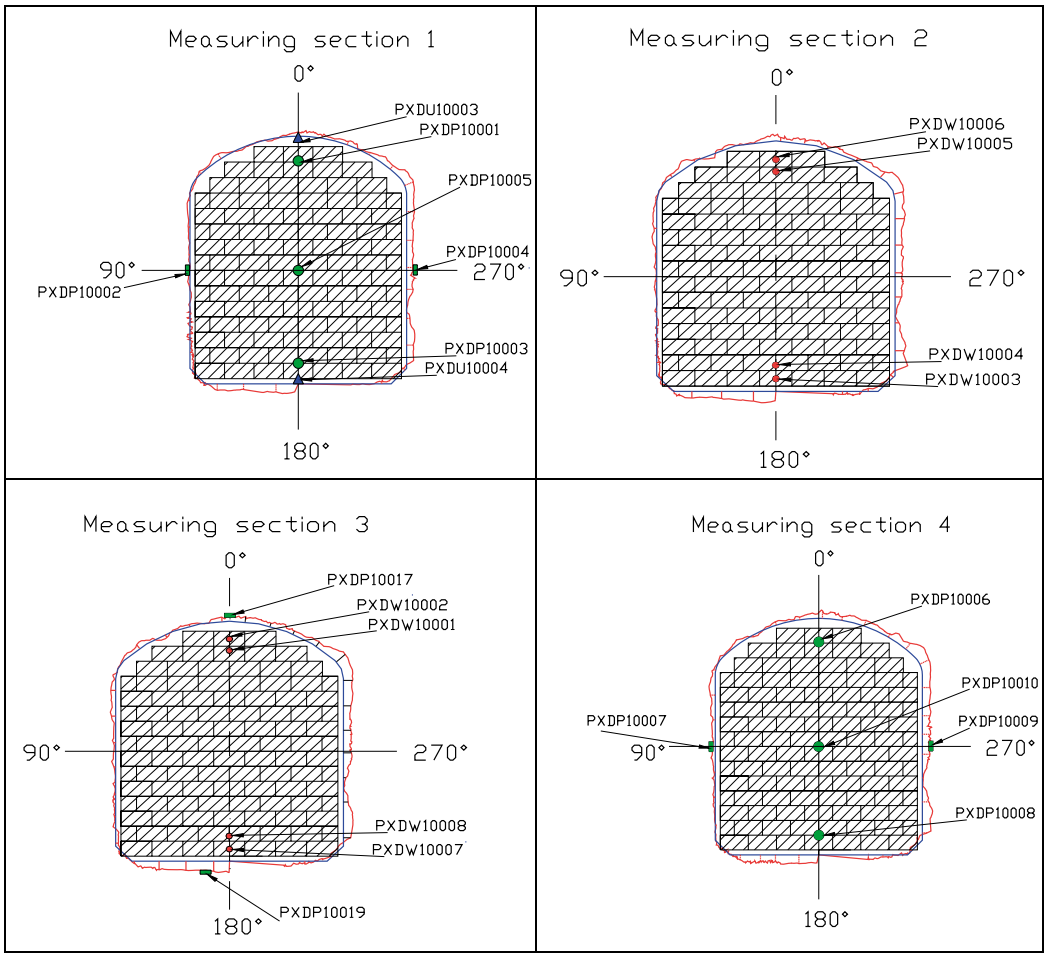

Figure 2-7. Sensor positions in the bentonite seal.

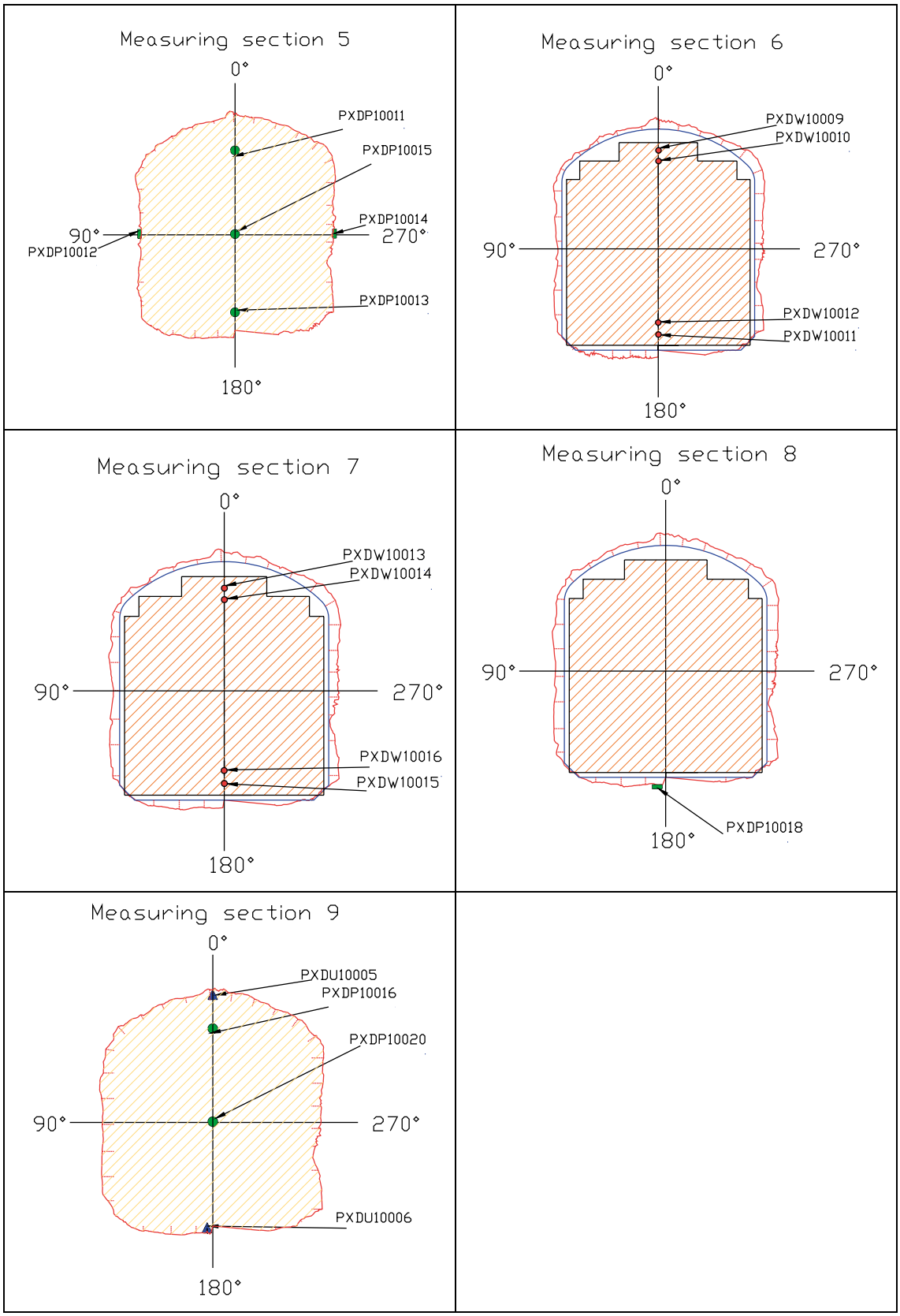

Figure 2-8. *Sensor positions in the backfill.*

2.3.4 Leakage and applied water pressure

In order to supply the filter sections behind the concrete plug with a high water pressure, water has continuously been pumped in during the test time. The inflowing water and the returning water was registered. Leakages has been registered/measured at three positions:

1. **Across the plug**. Leakages across the concrete dome have been collected in a weir in front of the plug. The seepage water from the weir has been automatically transferred to a scale that weighs the leakage mass for on-line recording, Figure 2-9. The photos are taken from Grahm et al. (2015).
2. **In rock fracture**. Leakages were also detected in a rock fracture positioned about five meters from the plug at the entrance of the niche. Water has been manually collected and measured from this fracture, Figure 2-10.
3. **Through cable bundle**. A small amount of water has leaked through a cable bundle within the concrete dome. This water has been manually collected and measured, Figure 2-9.

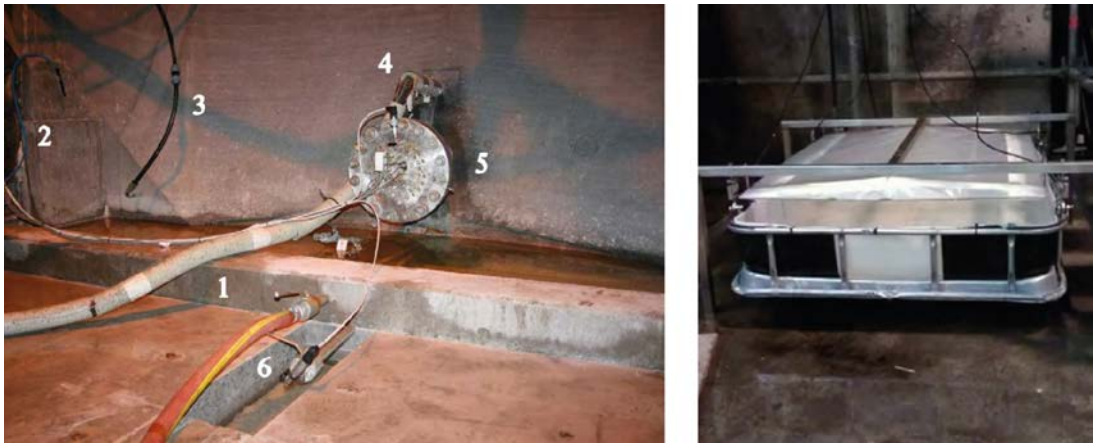

Figure 2-9. *Left: Photo showing the water tight weir in front of the plug (1). Position (4) in the photo shows the cables coming from sensors within the concrete dome. The leakages through the cable bundle were measured separately. Right: Photo showing the vessel where water from the weir was collected and automatically weighed. The photos are taken from Grahm et al. (2015).*

Figure 2-10. *Photo showing the rock fracture where water was collected. A steel tube was glued to the rock surface and the leakage water measured.*

3 Sensor data and special function tests

3.1 General

Besides extensive monitoring of the concrete dome structure, the inner plug components were instrumented with sensors for measurement of total pressure, pore pressure, relative humidity and displacements at several positions. The bentonite-based components and the filter were installed in January 2013, while the concrete dome was cast in March 2013. Pressurization by natural groundwater inflow began in October 2013. The artificial pressurization was increased to 4 MPa in February 2014 and was maintained at this level until June 2017 when several special tests started, see description in Section 3.4.

In this chapter all data from the different sensors positioned in the bentonite seal, the filter section and in the backfill are presented. In addition, results from some special function tests that were made just before the dismantling of the plug started, also are presented.

3.2 Water pressurization scheme

Monitoring results have responded to the pressurization of the system by injection of water into the filter and backfill, followed by saturation and development of swelling pressure in the watertight seal and backfill transition zone. The pressurization sequence has been marked in the graphs to clarity and to aid understanding of the system responses:

1. **January 30, 2013 (day 1).** All sensors behind the concrete delimiter have been positioned and connected to the data acquisition system. The last concrete beam was put in place two days later.
2. **March 13, 2013 (day 42).** Casting of the concrete dome.
3. **May 27, 2013 (day 117). Draining test and filter fill-up 1.** In order to give the bentonite seal access to water as soon as possible and also to simulate the worst groundwater case in the final repository, it was decided to inject water through the gravel-filled pocket at the back of the tunnel behind the backfill (Figure 1-1). The plan was to enable a channel to form through the pellet filling to the filter section, from which the water then would be drained. At the same time, it was important to not erode any bentonite into the gap between the concrete dome and the rock since this gap should be grouted with cement. Initially a constant water flow of 5 l/min was applied. A large outflow of bentonite slurry through the lead through pipe in the concrete dome occurred the next day (the cone and flange were still not mounted) and the inflow was stopped. A new attempt was performed with an inflow rate of 1.0 l/min, but the system failed again to drain also this flow rate. The filter section was believed to have been partly filled during this procedure. It was subsequently decided to postpone further activities until the grouting of the plug had been performed.
4. **June 11 and 19, 2013 (days 132 and 140).** Contact grouting of the plug.
5. **July 16, 2013 (day 167. Draining test and filter fill-up 2.** After having back-flushed the drainage pipe, a constant flow of 1.4 l/min was applied from the inside of the backfill. The draining then functioned well for one day. The next day the drainage pipe had clogged, and the flow was mainly running through the de-airing pipe i.e. the filter section was full of water. The inflow was thereafter kept constant but after about 12 days it was discovered that also the de-airing pipe had clogged. A leakage was then observed through the sensor cable lead through pipe (through the dome) and the flow was stopped. Approximately 240 kg bentonite was lost[1]. It is believed that the finely meshed copper net placed over the drainage tube endings inside the gravel filling was the reason for the problem with clogging.

[1] The origin of this bentonite mass is unknown. No erosion channels were found during the dismantling operation.

6. **August 6, 2013 (day 188). Filter fill-up 3.** The draining- and de-airing pipes were back flushed, and the filter was completely filled from the outside. The water pressure in the filter was slowly raised to 7 m head and then maintained at this level. No draining test was done in this procedure and no water flow rate was applied through the backfill.
7. **August 26, 2013 (day 208).** A lid was mounted on the lead through tube in the plug. In addition, an extra pipe was installed inside in order to measure the water pressure inside the lead through.
8. **September 30, 2013 (day 243). Shutoff of the drain.** The valves on the draining and de-airing pipes from the filter section were closed. Natural water pressure increase was allowed to occur as water entered from the surrounding rock.
9. **October 7, 2013 (day 250, activity no.5 in the graphs).** Installation of safety valve (6 bar). The natural water pressure increase is now allowed to increase up to 6 bars.
10. **November 6, 2013 (day 280, activity no.6 in the graphs).** Installation of safety valve (10 bar). The natural water pressure increase is now allowed to increase up to 10 bars.
11. **December 2, 2013 (day 306).** Start of pump system. The water pressure is artificially increased in steps.
12. **February 17, 2014 (day 383)**. The water pressure behind the plug has reached 4 MPa. The pressure has then been kept at this level for the remaining test time.
13. **June 2, 2017 (day 1 583).** The final day for the project. A new project is started to handle the termination and evaluation of the test.

January 30, 2013 is set as day 1 in the graphs provided in Chapter 3. In addition, day 117, 167, 188, 243, 250 and 280 are all indicated.

3.3 Sensor data from bentonite seal, filter section and backfill

The evolution of the sensors data and other continuous measurements during the monitoring period, i.e. between 2013-01-30 and 2017-06-02, is presented in this section.

Relative humidity

The initial RH level in the seal blocks was 72–76 % (Figure 3-1), and this was in good agreement with independent retention curve measurement for MX-80 bentonite with a water content of 17 %, (e.g. Dueck and Nilsson 2010). The corresponding initial RH level in the backfill blocks was 61–67 % (Figure 3-2), and this was also in agreement with independent tests on Asha bentonite with a water content of about 17 %, (e.g. Johannesson et al. 2008). During the first 167 days, the increase of RH was generally quite slow. However, a more rapid increase was observed from start in sensors PXDW10001, PXDW10007 and PXDW10008 in section 3 in the seal near the filter. This early RH increase indicated that there was a significant natural water inflow into the tunnel. In addition, after day 117 (when the first filter fill-up was performed) a more rapid increase was also observed in sensor PXDW10009 and PXDW10011 in section 6 in the backfill near the filter.

After day 167–188 (with the second fill-up) the RH increase was generally more rapid. This was most noticeable in the sections close to the filter (i.e. section 3 and 6), but also in sections more distant from the filter (i.e. section 2 and 7). The slowest RH increases were found for the backfill sensors PXDW10014 and PXDW10016 in section 7, and sensor PXDW10012 in section 6. After day 787, all sensors had either reached 100 % or failed, except for three sensors in the backfill (i.e. sensors PXDW10014, PXDW10016 and PXDW10012). At the end of the monitoring phase (2017-06-02), one sensor (PXDW10014) was still operational and showed 96 %.

Temperature

Two cooling events were observed at day 42 and 146 (Figure 3-3). The second was the most noticeable with temperatures falling to a level of 9 ºC. These events were caused by active cooling of the concrete plug during the casting and the contact grouting of this component. After day 300, the temperatures generally varied in an interval between 14 and 16 ºC. A seasonal variation was observed with three maxima corresponding to the summers of 2014, 2015 and 2016, respectively.

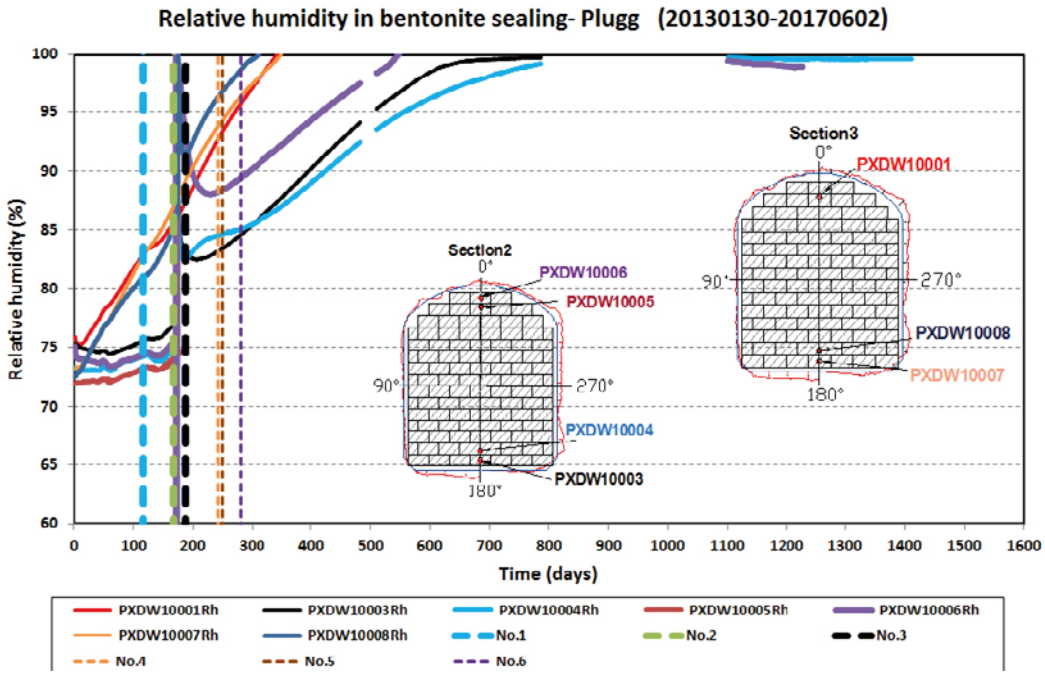

Figure 3-1. *RH measurements in bentonite seal.*

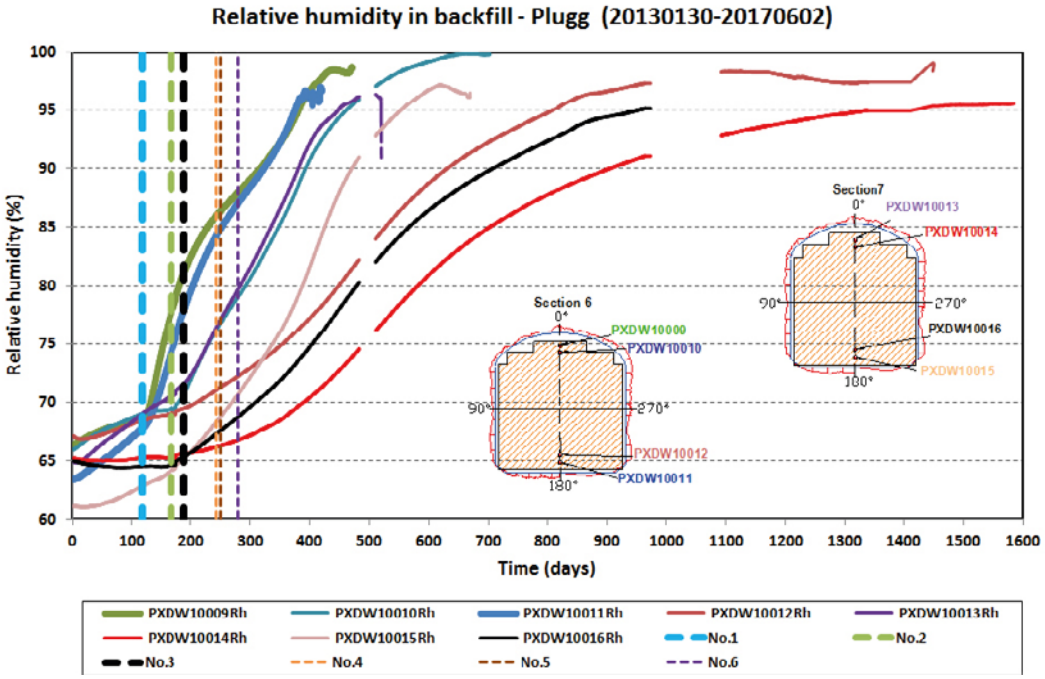

Figure 3-2. *RH measurements in backfill.*

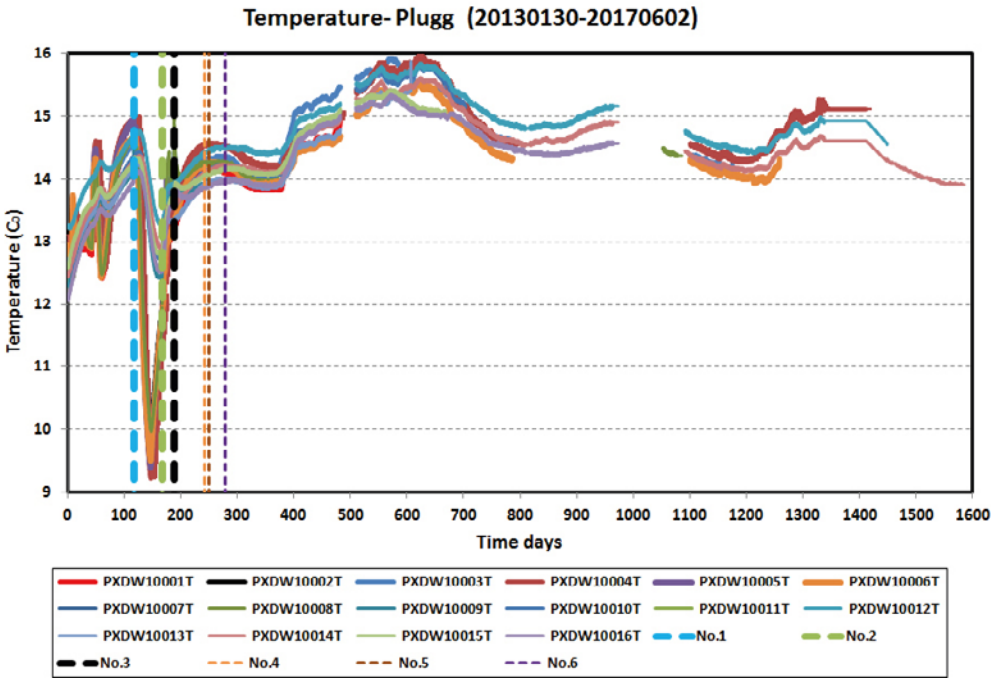

Figure 3-3. *Temperature measurements in bentonite seal and backfill.*

Total pressure

Reliable pressure results could first be monitored after day 287. This was caused by initial difficulties to evaluate the signal from the pressure sensors. After this, the buildup of total pressures followed the increase of water pressure applied to the filter until a level of 4 MPa was reached at day 383 (Figure 3-4 and Figure 3-5).

After day 383, all total pressures increased more or less to levels higher than the filter pressure. At the end of the monitoring phase (2017-06-02) the difference (i.e. the effective stress) was between 0.2 and 1.9 MPa the for different sensor positions, except for one sensor at the back of the backfill (PXDP10020) which increased much more. At the end of the monitoring phase the effective stress at this position was 5.2 MPa. An involuntary pressure drop occurred at day 1 444, and this affected the total pressure for a few months.

Pore pressure

Similar to the total pressure sensors, reliable pore pressures could first be monitored after day 287. The buildup of pore pressures also followed the filter pressure increase until 4 MPa was reached (Figure 3-6). Subsequent to this, the pore pressures were generally lower than the filter pressure. Sensor PXDU10001, at the upstream interface between the concrete plug and the rock, generally showed a pore pressure level 1 MPa lower than the filter pressure. The corresponding difference for the other functional sensors did generally not exceeded 0.4 MPa. The reduced pressure levels may be caused by a pressure gradient (through the rock) or by measurement inaccuracies. A difference of 1 MPa indicates a significant lowering and therefore appears to be caused by a gradient. Differences smaller than 0.4 MPa can on the other hand be regarded as insignificant.

A pressure sensor was also installed in the lead-through tube through the concrete plug. This pressure sensor generally displayed a smoother evolution which possibly was caused by trapped air in the tube (Figure 3-6). This pressure increase was relatively slow after 4 MPa was reached in the filter and reached a level of almost 4 MPa after day 700. The difference between this and the filter pressure decreased with time, and at the end of the monitoring period the pressure was virtually identical with the filter pressure.

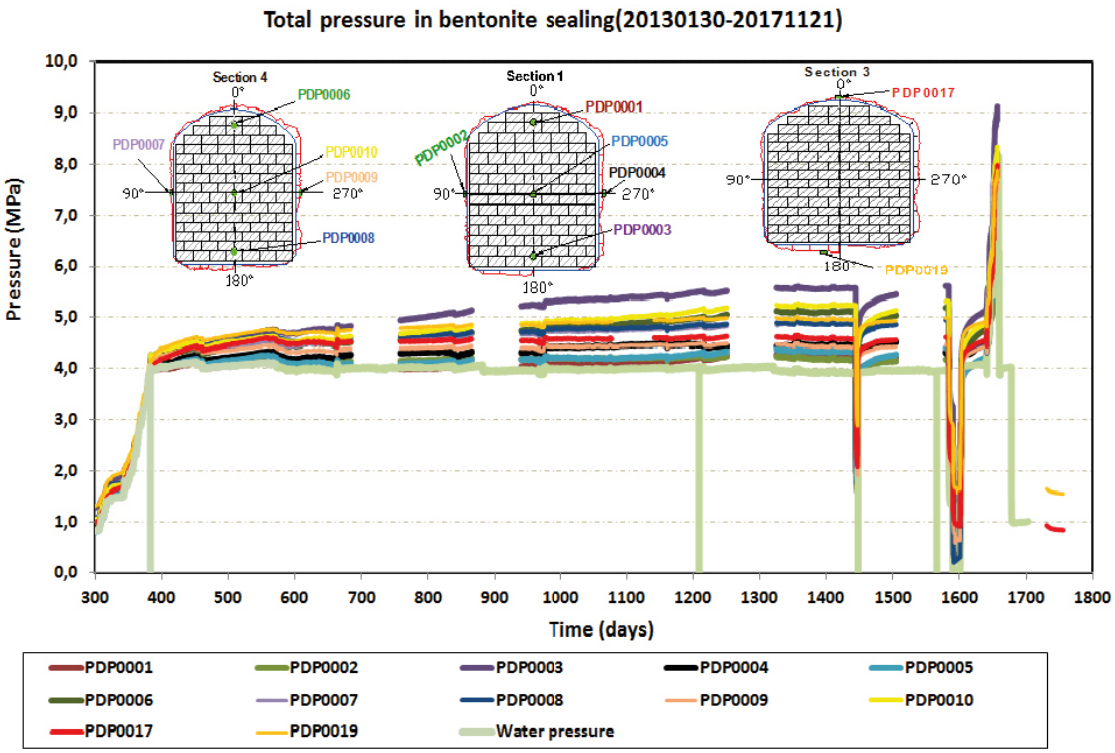

Figure 3-4. *Total pressure measurements in bentonite seal section 1, 3 and 4.*

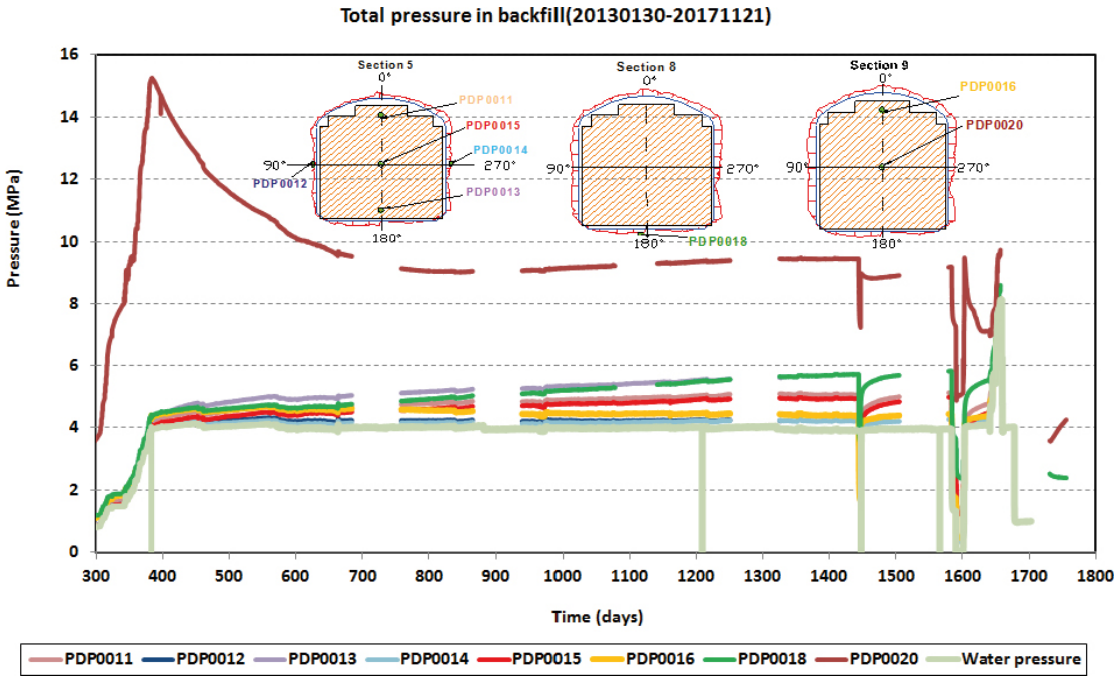

Figure 3-5. *Total pressure measurements in backfill.*

Displacements

All three sensors measuring displacement displayed a response from the start of the monitoring period (day 0), see Figure 3-7. The sensors followed each other quite closely up to day 167 at which time a displacement of 12 mm inward into the tunnel had been reached.

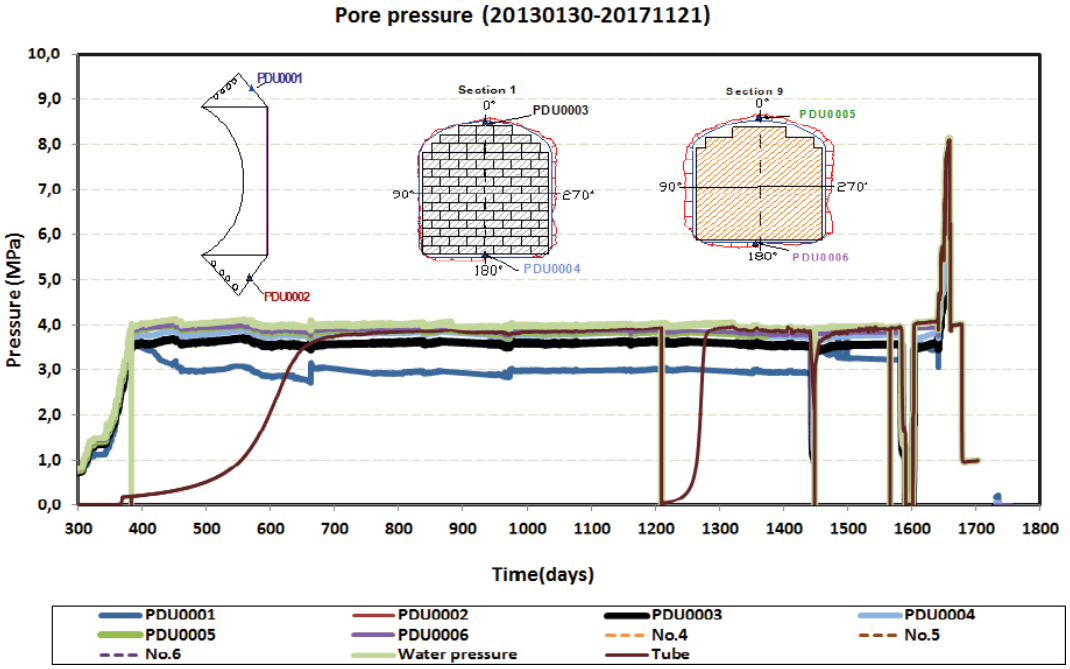

Figure 3-6. *Pore pressure measurements in bentonite seal and backfill.*

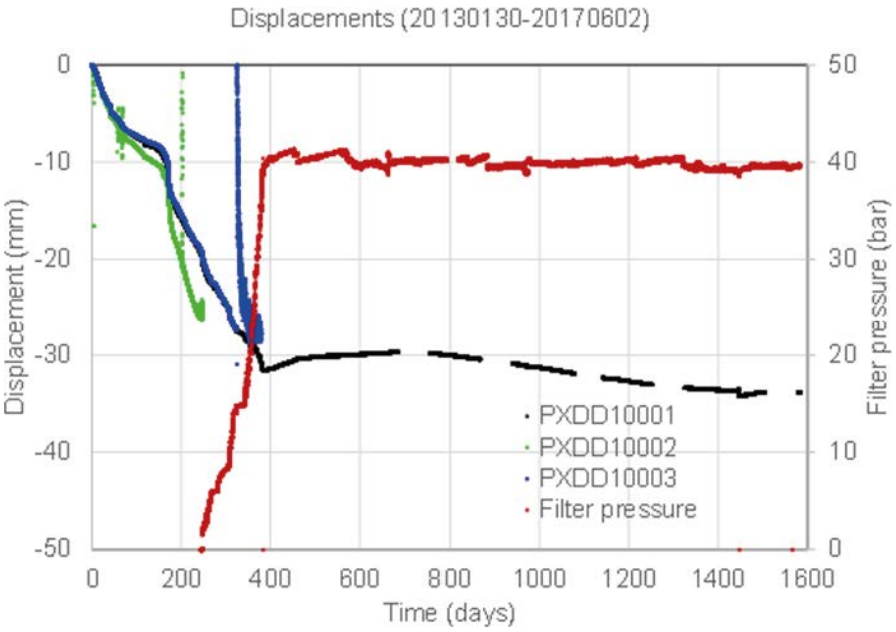

Figure 3-7. *Displacement of bentonite seal (2) and leca wall (1 and 3) relative the inner concrete wall. Filter pressure evolution shown for comparison.*

After that, sensor PXDD10002 displayed values slightly higher than the other two, indicating the compression of the gravel filling. However, sensors PXDD10002 and PXDD10003 failed before day 325. At around day 383, PXDD10001 reached a level of 30 mm, which leveled out thereafter. This event coincided with the filter pressure reaching a level of 4 MPa. An evaluation of this and similar correlations are presented in Chapter 6.

Water inflow and leakages

The evolution of the water inflow and the water pressure applied to the filter is shown in Figure 3-8. In order to increase the filter pressure up to a level of 4 MPa, the inflow rate had to be increased up to approximately 100 liters per hour. During the test period, when a constant filter pressure was maintained, the inflow decreased within 200 days to a level of approximately 20–25 liters per hour.

The leakage from the pressurized filter was measured as three separate flow rates (see Figure 3-9 and Figure 3-10): i) into the rock and out through a fracture in the main tunnel perpendicular to the experiment tunnel; ii) along cable lead-through in the concrete (not to be confused with the lead though pipe from the seal); and iii) past the concrete plug and collected in the embankment in front of the concrete plug. The leakage through the fracture was initially 50 l/h, but this decreased within 200 days to approximately 5–10 liters per hour. Both the leakage along the cable and past the plug, which began when the filter pressure exceeded 3.1 MPa, were initially 15–20 liter per hour. The leakage along the cable decreased significantly down to 1 liter per hour, while the leakage past the plug was approximately 1–3 liters after day 600.

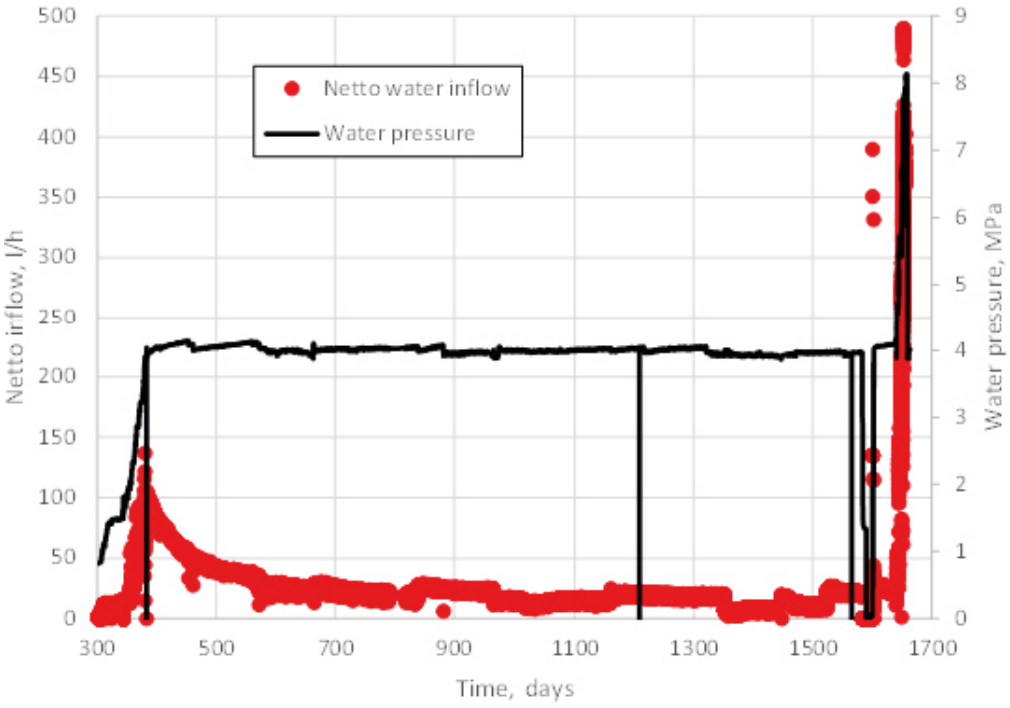

Figure 3-8. *The net water inflow to the filter section and water pressure plotted versus time.*

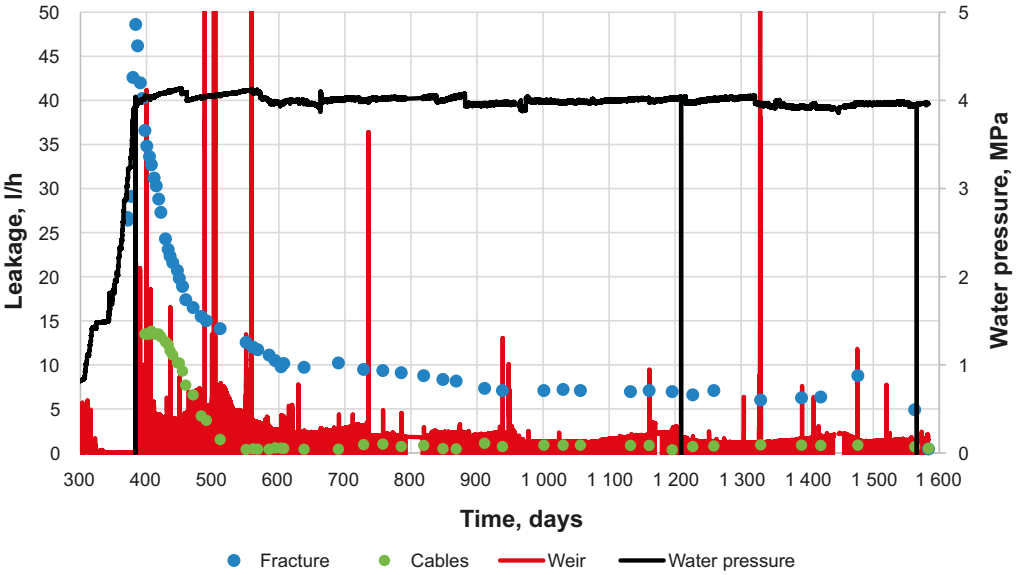

Figure 3-9. *Determined leakages and water pressure plotted versus time.*

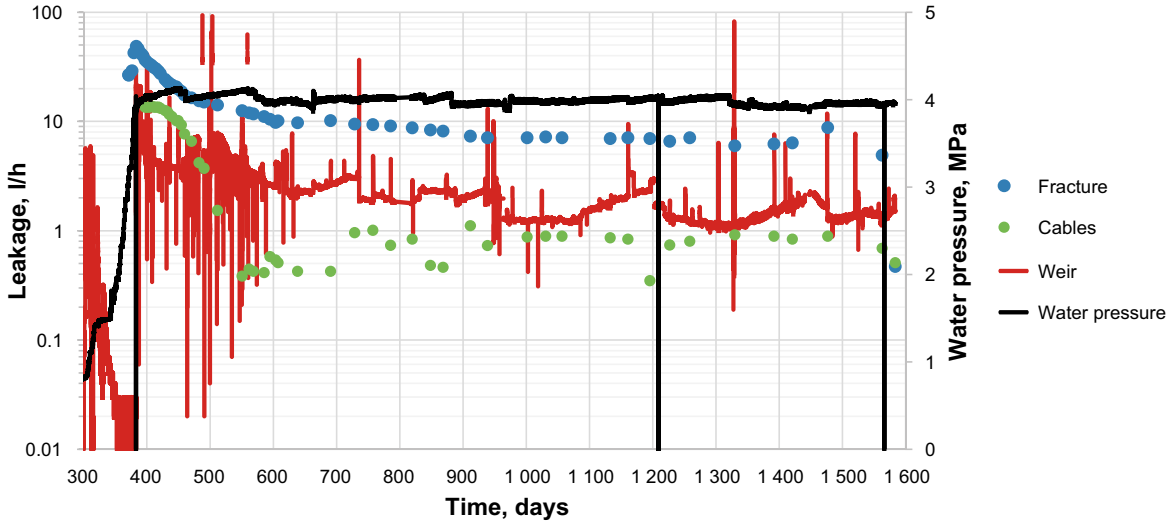

Figure 3-10. *Determined leakages and water pressure plotted versus time (logarithmic x-axis).*

Failed sensors and logging

The reliability of the sensor function and the sensor logging was different for different sensor types. A compilation of last relevant measurements, and periods without any logging is shown in Table 3-1.

The RH sensors were generally very reliable, although the output signal disappeared once they reached saturated conditions (or above 95 % in a few cases), and at the end of the monitoring period only one sensor was still operational. One RH sensor (PXDW10002) did not work from the start. The evolution of the RH measurements was interrupted by logging failure during three major periods. The pressure sensors were also very reliable, although the difficulties of evaluating the signal meant that no results could be obtained before day 285. One pore pressure sensor leaked and had to be cut at day 252. The total pressure sensor PXDP10020 initially showed very high results and it therefore was considered to be unreliable. At the end of the monitoring phase however, it showed a pressure level that was consistent with the dry density level determined after the dismantling (see Section 6.2), and the possibility that it actually was functional should therefore be kept open.

The evolution of the pressure measurements was interrupted by logging failure during six major periods. Finally, the displacement sensors displayed reliable results as long as they didn't reach the limit of the measuring range. This occurred for sensor PXDD10002 and PXDD10003 quite early during the monitoring period, but sensor PXDD10001 was apparently functional throughout the test. Logging failure interruption occurred during almost the same periods as for the pressure sensors.

Table 3-1. Last measurement of sensors and periods without logging.

Sensor type	Last measurement (day)	Logging missing (days)
RH sensors	PXDW10002: 0	482–510
	PXDW10005: 174	973–1 091
	PXDW10008: 312	1 411–1 448
	PXDW10001: 343	
	PXDW10007: 350	
	PXDW10011: 420	
	PXDW10009: 471	
	PXDW10013: 519	
	PXDW10015: 668	
	PXDW10010: 701	
	PXDW10003: 786	
	PXDW10006: 1 227	
	PXDW10004: 1 411	
	PXDW10012: 1 448	
	PXDW10016: 1 486	
Pressure sensors	PXDU10002: 252	0–285
		361–382
		684–758
		865–939
		1 250–1 324
		1 504–1 578
		1 656–
Displacement	PXDD10002: 247	684–758
	PXDD10003: 324	865–939
		1 077–1 141
		1 250–1 324
		1 504–1 578
		1 656–

3.4 Special function tests

Before starting the dismantling of the Dome Plug it was decided to perform a number of special tests on the function of the plug which were related to the requirements on the plug (see Section 1.3):

- **Gas tightness test**. One of the requirements on the plug is that it "needs to be reasonably gas tight to stop convection of air during the operational period" (Posiva SKB 2017). After a request from SSM it was decided to use the Dome Plug experiment to verify and demonstrate the gas tightness requirement.
- **Strength test**. One of the objectives with the experiment has been to demonstrate that the plug works under realistic conditions up to the reference design total pressure of 7 MPa. A water pressure of 4 MPa has been maintained for more than three years and together with the swelling pressure from the bentonite seal this gives a total pressure of 5 MPa. By increasing the water pressure to 6 MPa the total pressure will be 7 MPa (reference pressure). As a last test the water pressure was increased to 8 MPa (corresponding to a total pressure of 9 MPa) to demonstrate the strength of the plug.

- **Hydraulic tightness of the plug**. The current technical design requirement regarding the tightness of the plug was formulated by Posiva and SKB (2017; section 6.5.3) as: "*200 m³ total outflow before the backfill is saturated*". The leakages over the plug have been monitored since the water pressure was increased i.e. for more than three years. The decreases and increases of the water pressure in the filter section (see tests above) resulted in certain movements of the plug. These movements were monitored, and it was also investigated how they influenced the leakages over the plug. The old data and the new collected in conjunction with the pressure increase/ decrease have been evaluated.

In conjunction with the function tests, the water leaking across the plug and through the rock-fracture (see Section 2.3.4), as well as the ground water used for pressurization, were sampled and analyzed through evaporation with the objective to assess the occurrence of bentonite erosion. However, the differences in dry mass between the leakage samples and the reference sample were very small (less than 0.1 g/L) which showed that the bentonite concentration and therefore also the erosion rate was negligible. This result was further supported by the absence of bentonite sediment in the weir.

3.4.1 Gas tightness test

A decision was made that the Dome plug experiment should be used to verify the gas tightness requirement (see description in Section 1.3.3). SKB has earlier presented analyses which indicated that diffusion through an air-filled slot appeared to be the mechanism that potentially can contribute to the most significant inflow rates of oxygen through the tunnel plug. Such processes are however very slow, and in order to test whether the plug is gas tight or not, it was decided that a gas pressure difference would be applied over the plug. SKB defines gas-tight as a situation where no gas phase is present in the hydraulically sealing part of the plug and that the requirement for gas tightness can be assumed to be fulfilled if a water column is maintained in the filter section of the plug throughout the operational period of the entire repository.

A gas tightness test was therefore implemented by draining the water from the filter; pressurization of the filter with helium gas to 0.4 bar gauge and by monitoring the gas pressure evolution. During a period of 18 hours it was found that the gas pressure increased with 3 kPa, which indicated that a noticeable inflow of water occurred during this measurement. The monitoring was also complemented with a sniffer leak search along the entire front surface of the concrete plug. No detectable concentrations were however found. The test therefore verified that the seal was gas tight. The performed test on gas tightness is described in detail in Åkesson (2018).

3.4.2 Strength test

General

The reference design total pressure of the Dome plug was 7 MPa. This value is based on a water pressure of 5 MPa in combination with a swelling pressure of 2 MPa in the bentonite (Grahm et al. 2015). During the water pressure increase phase (October 2013) it was discovered that the leakages in the rock became large when increasing the pressure above 4 MPa and it was therefore decided to not increase the pressure further but instead maintain a water pressure level of 4 MPa. The registered swelling pressure in the bentonite seal varies a lot depending on position, between 0.1 to 1.6 MPa, see description of monitoring data in Section 3.3. An average swelling pressure of 1 MPa, means that the total pressure acting on the plug during the test time has been about 5 MPa.

Before dismantling the plug test, it was decided to increase the applied water pressure in the filter section in a first step to 6 MPa, resulting in a total pressure of 7 MPa, and in a second step to a maximum of 8 MPa which gives a total pressure of 9 MPa. This pressure is well above the reference pressure and was made in order to demonstrate the strength of the plug.

Experimental

After having finished the gas tightness test (described in Section 3.4.1) the filter section was re-filled with water that again was pressurized to 4 MPa. The water used for re-filling was mixed with uranine in a special pump station. The target uranine concentration of the water was set to 10 mg/liter. The uranine is used as a fluorescent tracer and was added in order to facilitate the identification of new leakage ways around the plug and in the rock that were expected due to the planned increase of the water pressure. The water pressure was kept at 4 MPa for more than five weeks in order to stabilize the registered inflows and outflows. After this time, the water pressure was increased in steps during a period of 17 days (29th of June to 16th of August) up to 8 MPa. During the pressure increase time a number of observations/measurements were made in order to verify the function of the plug at these conditions:

- Visual observations of the exposed concrete dome.
- Measurements of movements of the concrete dome.
- Leakage measurements including UV lamp to detect all positions.

Visual observations

No cracking or large movements of concrete could be noted through visual observation of the concrete dome. It should be mentioned that a detailed investigation of the concrete was made in a later stage of the project including both nondestructive tests and core drilling. The results from these tests are not included in this report.

Movements

Four sensors registering the displacement of the plug were mounted against the concrete dome before starting the gas tightness test. The approximate sensor positions are shown in the photo provided in Figure 3-11.

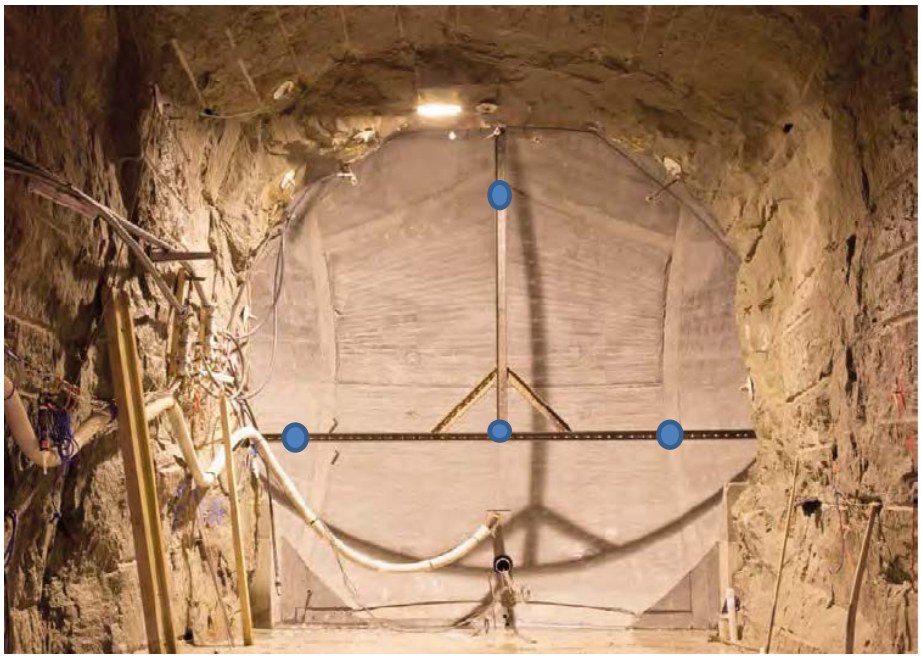

Figure 3-11. *Photo showing the approximate position of the four displacement sensors mounted on the dome plug.*

The graph provided in Figure 3-12 shows the registered displacement of the plug during the time of the special tests that were performed after June 2nd: The measurements can be divided in four phases:

- Phase 1: Gas tightness test (June 2nd to June 20th). The water pressure decreases from 4 MPA to 0 MPa resulted in a small movement of the concrete dome upstream of between 0.4 to 0.9 mm. After having performed the gas tightness test the water pressure was again increased to 4 MPa which resulted in a movement of between 0.4 to 0.9 mm downstream i.e. the position of the concrete dome was more or less reset to the original.
- Phase 2: Reset the filter pressure to 4 MPa and await stable inflow/outflow conditions (June 21th to July 28th). During this test phase the water inflow/outflow was measured continuously, see description in Section 3.4.3. However, the displacement sensors were all affected of the test conditions (high relative humidity and saline water dripping on them) which resulted in that they all failed to register displacement. Unfortunately, this was not discovered/checked before starting the water pressure increase in the next phase.
- Phase 3: Strength test (July 29th to August 18th). Only one of the displacement sensors (upper) was working during the main time of the water pressure increase phase. The measured movement when increasing the pressure from 4 to 8 MPa was approximately 0.4 mm downstream which was almost the same as registered when decreasing the pressure with 4 MPa but in the other direction which is judged to be logical. Before decreasing the water pressure again, new sensors were mounted which means that the movements during the pressure decrease could be registered. The movements shown in the graph, Figure 3-12, are adjusted so that the final measured values were set to the same as the expected starting value (July 1st). It is clearly shown in the graph that the movements registered during the water pressure increase from 4 to 8 MPa are for all sensor positions in the same range as registered during the water pressure decrease from 4 to 0 MPa.
- Phase 4: Reset the filter pressure to 4 MPa and await stable inflow/outflow conditions (August 19th and to September 11th). During this test phase the water inflow/outflow was measured continuously, see description in Section 3.4.3.

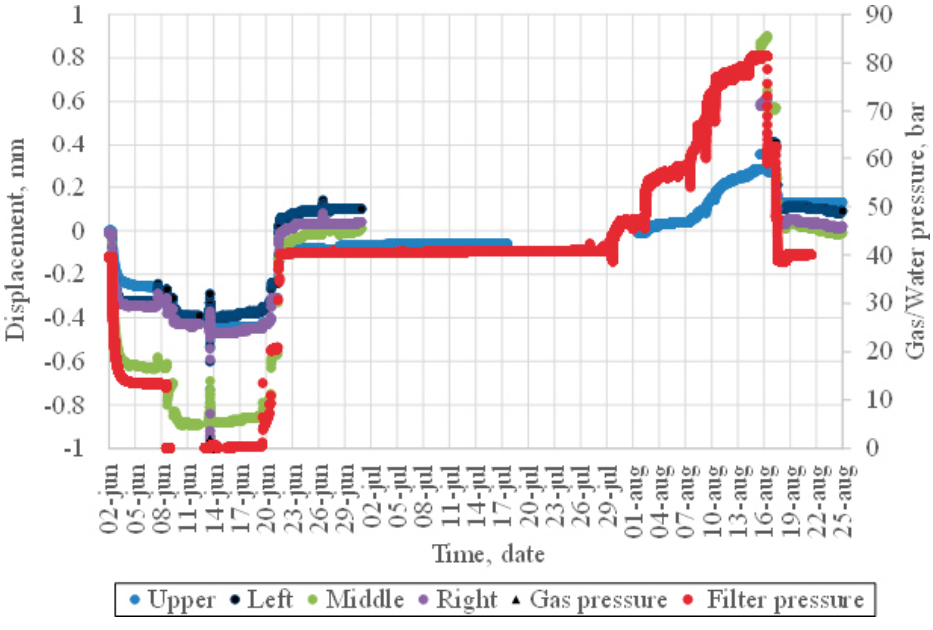

Figure 3-12. *Applied water pressure in the filter section and displacement measurements plotted versus time.*

3.4.3 Hydraulic tightness of the plug

Uranine detection

After the gas tightness test, all water injected to the filter was mixed with uranine in a special pump station. The uranine is used as a fluorescent tracer and by using an UV (ultraviolet) lamp it was possible to detect new water leakages during the test. Measurements were made at two occasions, June 28th when the water pressure in the filter was reset to 4 MPa and August 8th when the water pressure was increased to 6 MPa. Due to safety reasons no measurement was made when the water pressure was 8 MPa in the filter.

June 28th, 4 MPa water pressure

Water leakages were found at a number of positions, see Figure 3-13 and Figure 3-14. Many of these positions were the same as have been detected earlier in the project but by using the uranine water and an UV lamp it was possible to say that the origin of the water was from the filter section. The main identified leakages were:

- Some minor leakages were found at the top of the plug, 10 to 11 o'clock.
- Some minor leakages were also found on the other side of the top of the plug, 13 to 14 o'clock.
- A large number of leakage points were detected on the right wall side, see photo provided in Figure 3-13.
- The largest outflow was detected from the right corner at the entrance to the tunnel, no. 5 in Figure 3-13.

Figure 3-13. *Left: Water leakages can mainly be detected at four positions in the interface between concrete and rock, see green marked areas on the photo. Right: Photo showing the areas were water leakages could be detected with the UV lamp. The photo is taken on the right side of the tunnel with the dome to the left in the photo.*

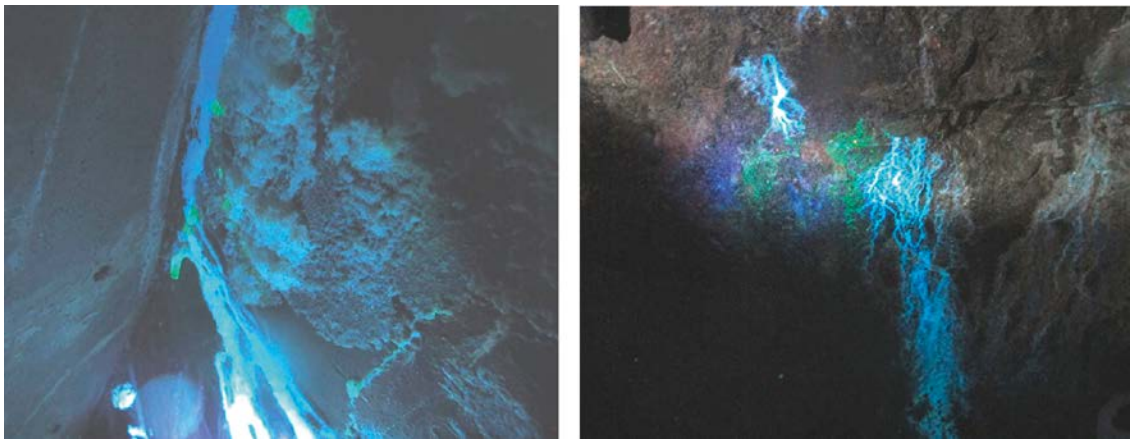

Figure 3-14. *Example of leakages detected with the UV lamp. Left: Small leakage in the interface between rock and concrete (about one o´clock, see Figure 3-13). Right: Small leakage on the rock wall on the right side about 2 meters from the plug (no.2 Figure 3-13).*

August 8th, 6 MPa water pressure

A new detection was made with the UV lamp when the water pressure in the filter had reached 6 MPa. It was at this time obvious that the number of leakage points had increased. The water in the weir in front of the plug, collecting all water leakages from the interface between concrete and rock and also leakages through the concrete, was clearly green colored, Figure 3-15. There were also a large number of small leakages from the ceiling in front of the plug. These water drops fell down on the floor that also was colored, see photo provided in Figure 3-15. The ceiling had earlier been considered dry (at 4 MPa water pressure).

The water leakage from the rock corner had largely increased as a result of the water pressure increase and the water coming out from the pipe (collecting water from the rock) was also clearly colored by the uranine (Figure 3-16).

Leakage measurements

The leakages past the concrete dome and through the rock from the filter section has been continuously registered during almost four years, see graph provided in Figure 3-10. The leakage measurements have continued during the performance of the special tests described in this section which have included variations in the applied water pressure in the filter, Figure 3-17. The results from the leakage measurements can be compiled as follows:

- The decrease in water pressure during the performance of the gas tightness test, June 2nd to June 20th, resulted in that all leakages decreased to zero.
- The applied water pressure was after that again increased to 4 MPa, June 21st to July 28th. After a few weeks the measured leakages in the weir, through the cables and in the rock fracture had been restored to the values registered during the time before June 2nd.
- The strength test of the plug, July 29th to Aug 18th, included a water pressure increase up to 8 MPa in the filter section. During this test period all registered leakages increased largely especially through the rock fracture. The maximum leakage in the rock fracture was determined to 257 l/h (7–8 l/h during the original 4 MPa test period), through the cables to 15 l/h (1 l/h) and in the weir to 13 l/h (1–2 l/h).
- The water pressure was decreased to 4 MPa Aug 19th and the leakages decreased again to values close to the one registered during the original 4 MPa test period (the number of measurements is limited).

Figure 3-15. *Left: The water standing in the weird in front of the plug has been colored by the uranine content in the leakage water. Right: Water has started to leak from the ceiling and are then dripping on the floor that is colored.*

Figure 3-16. *The water from the rock corner, see no.5 in Figure 3-13 is collected into a tube. The water is clearly colored by the uranine content.*

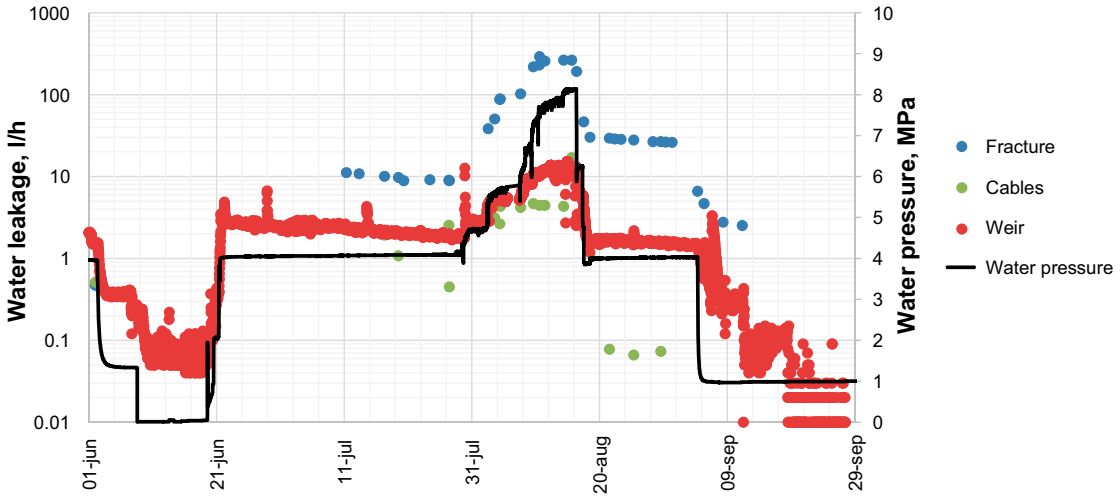

Figure 3-17. *Applied water pressure and measured leakages from weir, rock fracture and from cables plotted versus time.*

During the original test period until June 2nd, 2017, a net water injection of 20–25 liters per hour has been needed to maintain the 4 MPa water pressure, Figure 3-8. The corresponding inflow data registered from June 2nd and forward i.e. during the performance of the special function tests are provided in Figure 3-18. As shown in the graph, the water inflow had to be increased to more than 400 l/h in order to keep the water pressure in the filter at 8 MPa.

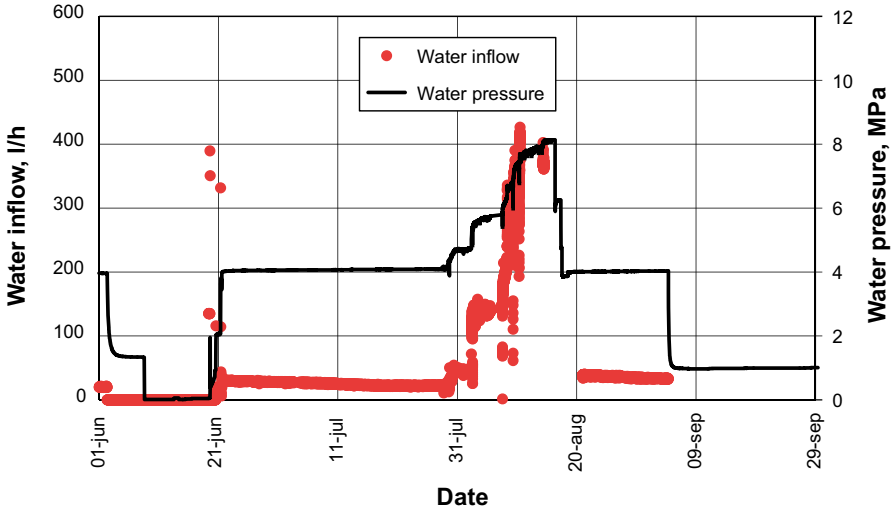

Figure 3-18. *Applied water pressure and water inflow to filter plotted versus time.*

4 Termination and sampling of bentonite seal, filter section and backfill

4.1 General

The disassembly of the Dome plug started with removal of the concrete dome. This work is described in an own report together with the performed measurements and analysis on the concrete (Malm et al. 2019).

This chapter describes the removal and sampling of the different components behind the concrete dome, see schematic drawing of the plug design in Figure 1-1. The photo provided in Figure 4-1 shows the concrete beam wall after removal of the concrete dome. The performed work can be divided in two parts:

1. Removal and sampling of components in front of the LECA wall i.e. the concrete beams, the bentonite seal and the filter section consisting of gravel filling. These parts were removed more or less in parallel i.e. after removal of one concrete beam the bentonite behind was sampled and then removed before the next concrete beam was removed. At three different occasions a vacuum truck was used to empty the filter section from the gravel filling.
2. Removal and sampling of the LECA wall and the backfill behind. This work was also made in parallel i.e. after removal of a LECA beam, the backfill behind was sampled before the next beam was removed.

4.2 Removal of concrete beams

The uppermost concrete beam was at the time for installation casted around the periphery i.e. concrete was pushed into the remaining gap between the beam and the rock. The beam was crushed by use of a hydraulic hammer, the same as was used for removal of the concrete dome, and then removed. The following beams were removed by using a hydraulic hammer carried by an excavator. The hammer was used to crush the ends of the beam which then could be lifted away, see photos in Figure 4-2. After removal of one concrete beam the bentonite behind was sampled and removed before the work with removal of the next concrete beam was started.

Figure 4-1. *Photo showing the concrete beam wall after removal of the concrete dome.*

Figure 4-2. *Left: A hydraulic hammer was used on both ends of each concrete beam to crush the concrete. Right: After crushing the concrete at both ends the steel anchoring to the rock was cut and the beam could then be lifted away by a large loading machine.*

4.3 Bentonite seal

4.3.1 General

The bentonite seal is positioned behind the concrete beams and is one of the most important parts in the plug design in order to achieve a tight plug. The seal consisted of both bentonite blocks positioned in the central area and of bentonite pellets filling up the remaining gaps between blocks and rock. The bentonite pellets were also used to even out the floor in order to achieve a foundation for the block stack.

During excavation of the bentonite seal, the following have been checked/measured:

- The contact between bentonite and rock have been checked. Any signs for channels, missing bentonite due to erosion etc have been checked.
- The thickness of the seal has been measured. The seal section had at installation a thickness of 500 mm. According to displacement measurements during test time, the bentonite blocks have swelled and compacted the filter section behind and moved the LECA wall.

In addition, many samples have been taken from the bentonite seal:

- The water content and density distribution have been determined in approximately 450 points in the bentonite seal.
- A special investigation has been made to investigate the cation distribution within the bentonite seal.

4.3.2 Removal of bentonite

After having taken out all samples from the bentonite behind a concrete beam, see description in Section 4.3.5, the rest of the bentonite was removed by use of a special hook carried by an excavator, see photos provided in Figure 4-3.

4.3.3 Contact between bentonite seal and rock

The bentonite was in tight contact with the rock surface all around the tunnel contour and bentonite was filling up the complete seal section i.e. no empty voids or channels could be found. It was obvious that the bentonite blocks had swelled and compacted the pellet filling against the rock, see also results from the determinations of density in Section 4.3.5.

The photo provided in Figure 4-4 shows the contact between bentonite and the rock surface at the ceiling. The vertical surface to the right is excavated to facilitate the sampling. The orange dots marks where samples are planned to be taken.

Figure 4-3. *Upper left: A scissor platform was used during sampling of the bentonite. Upper right: The exposed bentonite has been sampled. Lower left: A special "hook" was used to remove the remaining bentonite above the next concrete beam. Lower right: The main part of the bentonite has been removed, leaving the outer parts close to the rock wall for sampling.*

Figure 4-4. *Photo taken during the excavation of the former pellet filled slot at the ceiling. The bentonite has swelled and is everywhere in good contact with the rock surface.*

4.3.4 Thickness of bentonite seal

The bentonite seal blocks had initially a thickness of 500 mm. As mentioned earlier, the data registered during test time have indicated that the bentonite seal has swelled and compressed the filter section and pushed the LECA wall upstream, see graph provided in Figure 3-7. The registered data indicate that the bentonite seal has swelled upstream about 26 mm. This should, however, be seen as the minimum movement since it was judged that the sensor had exceeded its range and then failed. Measurements during excavation and sampling showed that the bentonite seal had increased its thickness to between 560 and 620 mm.

The uppermost half meter of the bentonite seal stretched out over the top of the filter section and forward against the LECA wall. This was due to difficulties, during installation, to achieve a vertical standing section of the gravel filling behind the bentonite seal, Figure 4-5.

4.3.5 Water content and density distribution

Sampling of the bentonite

Two different sampling techniques have been used, Figure 4-6:

1. The central area of the seal, where bentonite blocks originally were stacked, was sampled using a core drill. The cores were taken through the whole thickness of the seal i.e. every core included samples from all five sections planned to be sampled. This method is known to work well on dense bentonite but was somewhat time consuming since it was necessary to pull out the core drill many times during the operation in order to get rid of powder. An air flow was also used to blow out powder from the drilled track. The cores were transported to the laboratory and samples were then sawed out by using a band saw.
2. The former pellet filled slots around the tunnel contour had a lower density and was sampled using hand-held tools/machines to expose a smooth surface close to the sampling position and then a half-pipe was pushed in by help of a hammer. The half bentonite core could then be broken loose. Since the density of these cores was rather low compared to the cores taken from the blocks, the cutting into suitable samples could be made using a knife.

Figure 4-5. *The photo shows the uppermost part of the bentonite seal and the geotextile separating the bentonite from the filter section. The geotextile is folded over the filter and bentonite pellets were blown into this gap during installation.*

Figure 4-6. *Left: The central parts of the bentonite seal were sampled using a core drill. Right: The outermost parts, close to the rock wall were sampled with a special made "half pipe".*

Calculations

The base variables water content w (%), dry density r_d (kg/m^3), void ratio e (-) and degree of saturation S_r (%) were determined according to Equation 4-1 to 4-4.

$$w = 100 \cdot \frac{m_{tot} - m_s}{m_s} \quad (4\text{-}1)$$

$$\rho_d = \frac{\rho}{1 + w/100} \quad (4\text{-}2)$$

$$e = \frac{\rho_s}{\rho_d} - 1 \quad (4\text{-}3)$$

$$S_r = \frac{\rho_s \cdot w}{\rho_w \cdot e} \quad (4\text{-}4)$$

where

m_{tot} = total mass of the specimen (g)

m_s = dry mass of the specimen (g)

r = bulk density of the specimen (kg/m^3)

r_s = particle density (kg/m^3)

r_w = density of water (kg/m^3)

The dry mass of the specimen is obtained from drying the wet specimen at 105 °C for 24h. The bulk density is calculated from the total mass of the specimen and the volume determined by weighing the specimen above and submerged into paraffin oil.

The mass of the single specimens, both for determinations of water content and for density, have mainly been between 20 and 40 g.

Test matrix

An extensive sampling of the bentonite seal has been performed. The sampling of the vertical bentonite seal surface is shown in Figure 4-7 (left). This sampling was performed in five vertical sections, BS1 to BS5 (BS=Bentonite Seal), Figure 4-7 (right). Approximately ninety samples were taken from each vertical section i.e. in total 450 samples have been taken from the bentonite seal.

Results

The results from all measurements on the dry density in the bentonite seal are presented in Figure 4-8. The results are divided after measuring sections on the x-axis, but the individual position of each sample within the associated section has not been considered in the graph. The samples taken from the central parts (former block stack) are marked with black dots and the samples taken in the periphery (former pellet filled slot) are marked with blue cubes. As shown in the graph there is an evident difference in dry density between the central parts and the periphery parts in each section. The density in the central parts is clearly higher even though the spread is high.

The results from all measurements on the bentonite seal are also presented in contour plots provided in Figure 4-9 (water content distribution) and Figure 4-10 (dry density distribution).

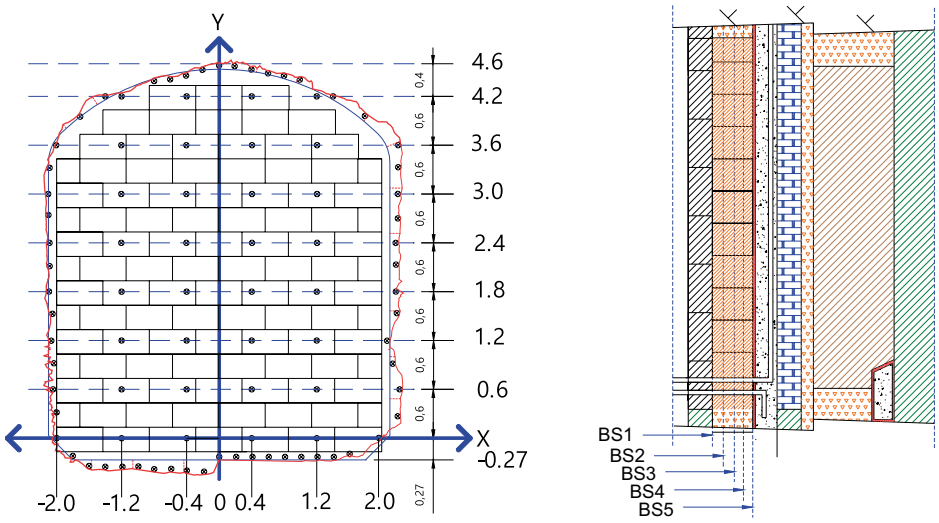

Figure 4-7. *Schematic showing the planned sampling of the bentonite seal. Left: The sampling of the vertical backfill surface. Right: The vertical sampling was performed in five different sections of the seal.*

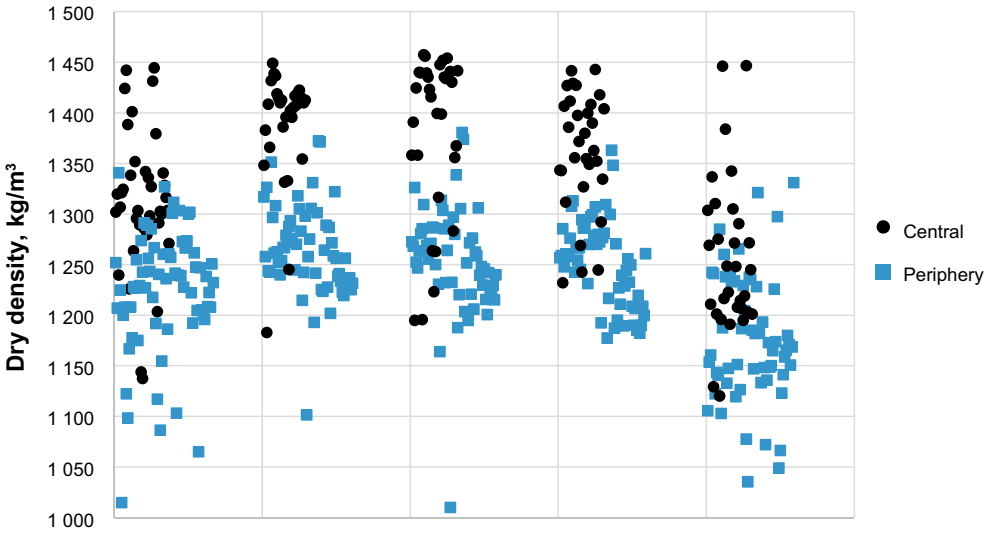

Figure 4-8. *Graph showing the results from all measurements on dry density in the bentonite seal. The results are divided after measuring section on the x-axis. The samples taken from the central parts (former block stack) are marked with black dots and the samples taken in the periphery (former pellet filled slot) are marked with blue cubes.*

The dry density in the bentonite seal varies roughly between 1 020 and 1 460 kg/m^3 (Figure 4-8 and Figure 4-10). The dry density in section 5 (closest to the filter) is clearly lower than in the other sections. This depends probably on that the bentonite seal has swelled and compressed the filter material. Depending on inner friction in the compacted bentonite, a complete homogenization after swelling will take long time. The density is also lower in section 1 (closest to the concrete beams) and this can be explained by the fact that during the water filling up of the filter section, water has been flowing into the initial gap between the concrete beams and the bentonite blocks which have resulted in an early swelling of the bentonite in this section.

The lowest density of the bentonite seal is in general found in the periphery i.e. in the former pellet filled slot. The dry density of the pellet filling was after installation approximately 900 kg/m^3. The determined density after termination shows that the density of the former pellet filling in general has increased to between 1 100 and 1 300 kg/m^3. This means that the central blocks with higher dry density (1 682 kg/m^3 at installation) have swelled and compressed the pellet filling which have resulted in a higher density. The dry density in the central areas of the former blocks, in section 2, 3 and 4, have been determined to be in general between 1 300 and 1 500 kg/m^3.

By using the measured density and water contents the degree of saturation can be calculated for every sampling position. The bentonite seal is in general completely saturated. The degree of saturation is calculated to between 96 and 102 % with only some minor exceptions. The determination of density and water content are not made on exactly the same sample, which is impossible, but on samples positioned very close to each other. This may lead to the fact that there will be a certain deviation in the calculated degree of saturation even if the samples are saturated. The range in the calculated degree of saturation represents thus only the accuracy in the measurements.

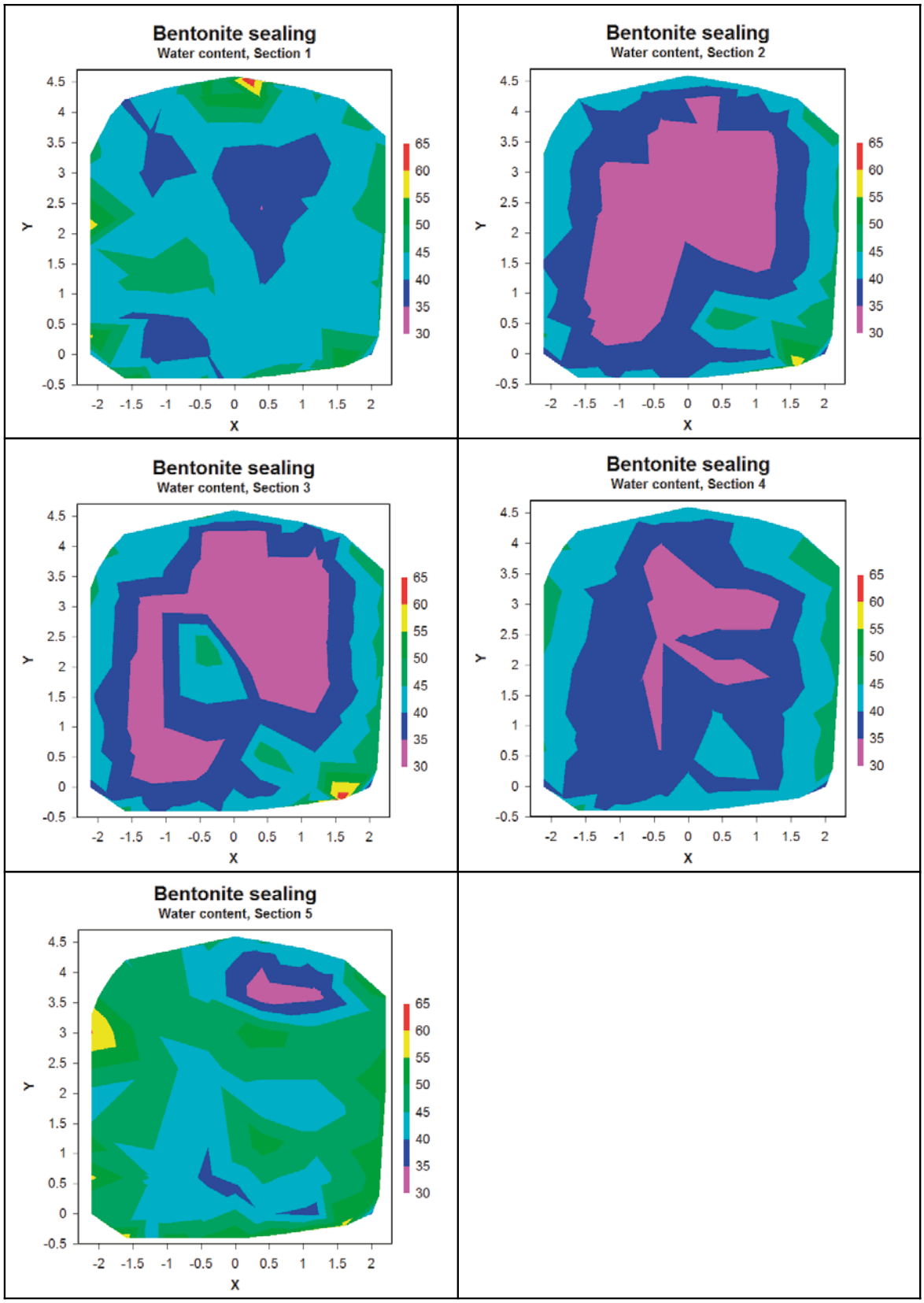

Figure 4-9. *Graphs showing the water content distribution in the bentonite seal in the five different sections sampled.*

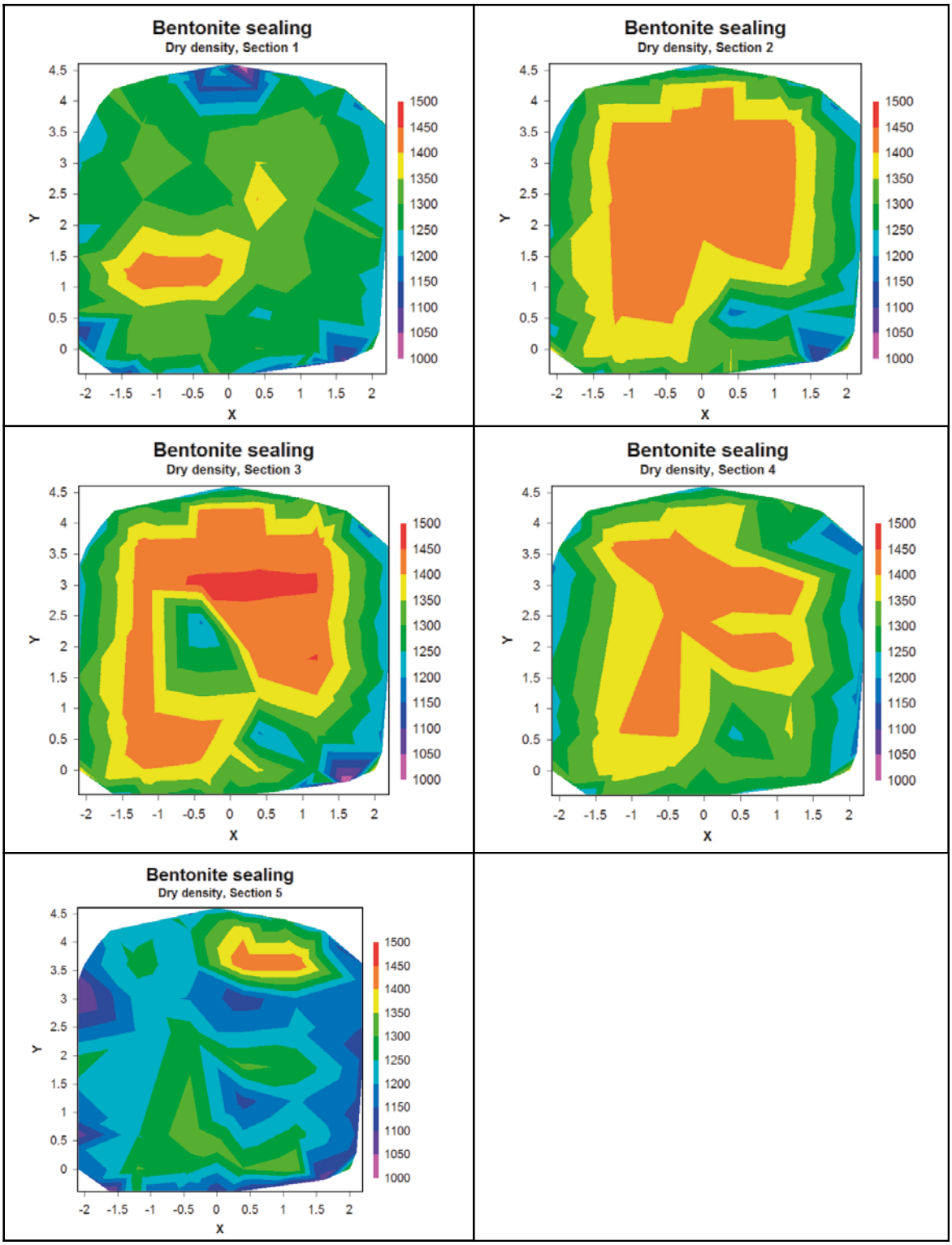

Figure 4-10. *Graphs showing the dry density distribution in the bentonite seal in the five different sections sampled.*

4.3.6 Determination of exchangeable cations (EC)

General

Determination of exchangeable cations (EC) of smectite has earlier been made within many SKB projects. The general description below together with the method description in next section has been taken from Sandén et al. (2014).

"The negative layer charge of smectite is balanced primarily by reversibly adsorbed, i.e. exchangeable, cations in the interlayer region. In natural bentonite the exchangeable cation pool is generally a mixture of mono- and divalent cations, mainly Na^+, K^+, Mg^{2+}, and Ca^{2+}. The valence of the charge compensating cations will affect properties such as swelling and dispersion behavior of the smectite, which motivates that a discrimination is made between, for instance, Na-dominated and Ca-/Mg-dominated bentonites in quality assessments of bentonites based on their hydro-mechanical properties ".

The bentonite seal in the Dome plug has been positioned between a concrete beam wall and a filter section. Äspö formation water has been pumped into the filter section to maintain the 4 MPa water pressure that has been kept for more than three years. The water has then been flowing from the filter through rock fractures or leaked through the plug, see description in Section 3.3, which means that there has been a continuously change of water in the filter. The formation water at Äspö contains almost similar amounts of Na and Ca (about 2.5 g/l). The experiment design has thus given an opportunity to investigate how the original cation pool in the bentonite (Na-dominated) has been influenced of the exposure to the formation water on one side and the contact with cement on the other side.

Method

The exchangeable cations were extracted by three successive displacements with ammonium in an alcoholic solution (0.15 M NH_4Cl in ~80 % ethanol) according to a procedure originally recommended for CEC determinations of gypsiferous/calcareous soils (e.g. Belyayeva 1967).

Using a modified procedure of Belyayeva (1967) 0.8 g of the ground sample was shaken for 30 minutes in approximately one third of a total volume of 50 ml of the extractant. After centrifugation, the supernatant was collected. This treatment was repeated three times. After evaporation of the alcohol and adjustment of the volume of the residual supernatant with deionized water, the concentration of Ca, Mg, Na, and K was determined by use of an ICP-AES equipment at the Department of Biology, Lund University. The water content of the bentonite was determined for a separate sample.

Test matrix

The composition of the exchangeable cation pool was determined on fifteen samples from a core drilled out from the bentonite seal. The core had the coordinates −1.2, 1.8 (see Figure 4-7).

The core had a total length of 560 mm and samples were taken at different distances from the gravel filter and from the concrete beam wall.

Results

The data on the exchangeable cations are compiled in Table 4-1. The table shows the concentration of the four determined cations (Ca, Mg, Na and K) and the total sum of cations for all samples. The concentration of cations was determined on duplicates for all fifteen positions.

The presented values of the reference sample are, however, not from the same batch. The blocks used in the seal were manufactured using material from a batch delivered in 2012 and the reference material is from a batch delivered in 2015 (Sandén et al. 2016).

Table 4-1. Exchangeable cations extracted by exchange with NH_4^+ in alcoholic solution.

Sample id	Distance from Concrete/Filter (cm)	Ca (meq/100 g)	Ca (%)	K (meq/100 g)	K (%)	Mg (meq/100 g)	Mg (%)	Na (meq/100 g)	Na (%)	Sum (meq/100 g)
Ref	na	26.4	29	1.8	2	12.2	13	51.2	56	92
C, 0–1	0–1	44.84	51.81	1.57	1.82	2.80	3.24	37.33	43.14	86.54
C, 0–1	0–1	44.44	51.53	1.57	1.82	2.76	3.20	37.47	43.45	86.25
C, 1–2	1–2	47.40	50.93	1.62	1.74	3.12	3.35	40.92	43.98	93.06
C, 1–2	1–2	45.12	50.69	1.60	1.80	2.92	3.28	39.37	44.23	89.01
C, 3–4	3–4	41.00	47.74	1.61	1.88	3.28	3.82	39.99	46.56	85.88
C, 3–4	3–4	42.66	47.98	1.57	1.77	3.38	3.80	41.31	46.46	88.91
C, 5–6	5–6	38.69	43.71	1.67	1.89	4.57	5.16	43.59	49.24	88.52
C, 5–6	5–6	36.82	43.36	1.61	1.90	4.28	5.04	42.22	49.71	84.93
C, 8–9	8–9	31.76	37.33	1.83	2.15	6.03	7.09	45.45	53.43	85.06
C, 8–9	8–9	31.30	37.36	1.80	2.14	6.13	7.32	44.57	53.18	83.80
C, 16–17	16–17	19.05	23.84	1.96	2.45	7.96	9.96	50.96	63.76	79.93
C, 16–17	16–17	19.04	23.23	1.96	2.39	7.94	9.69	53.04	64.69	81.98
C, 22–23	22–23	17.07	21.34	1.96	2.46	8.13	10.16	52.81	66.04	79.96
C, 22–23	22–23	16.33	20.90	1.92	2.46	6.74	8.63	53.14	68.01	78.13
C/F, middle	28	15.76	20.69	1.87	2.46	6.25	8.20	52.29	68.65	76.17
C/F, middle	28	15.96	20.94	1.90	2.50	6.57	8.62	51.76	67.94	76.19
F, 22–23	22–23	20.17	23.83	2.53	2.99	9.28	10.97	52.67	62.21	84.66
F, 22–23	22–23	19.52	23.54	2.14	2.58	8.97	10.81	52.31	63.07	82.93
F, 15–16	15–16	23.52	28.43	1.94	2.34	8.60	10.39	48.68	58.83	82.74
F, 15–16	15–16	24.21	29.23	2.01	2.42	8.83	10.66	47.77	57.69	82.82
F, 8–9	8–9	41.51	47.49	1.56	1.79	7.69	8.80	36.65	41.93	87.41
F, 8–9	8–9	42.97	47.53	1.50	1.66	7.53	8.33	38.41	42.48	90.41
F, 5–6	5–6	50.24	57.75	1.26	1.45	4.89	5.62	30.61	35.18	86.99
F, 5–6	5–6	51.58	57.66	1.27	1.42	5.36	5.99	31.24	34.93	89.45
F, 3–4	3–4	56.80	62.48	1.13	1.25	4.46	4.90	28.51	31.37	90.90
F, 3–4	3–4	55.76	63.36	1.09	1.24	3.66	4.16	27.49	31.24	87.99
F, 1–2	1–2	60.09	68.21	1.03	1.17	2.85	3.23	24.13	27.38	88.10
F, 1–2	1–2	61.27	66.48	1.05	1.14	3.71	4.02	26.13	28.35	92.16
F, 0–1	0–1	60.45	66.23	1.02	1.12	4.09	4.48	25.71	28.17	91.27
F, 0–1	0–1	57.92	66.43	0.98	1.12	3.09	3.54	25.21	28.91	87.19

In Figure 4-11 the cation pool distribution at different distances from the concrete beam wall is presented. Every presented value is an average from the two duplicate samples taken for every position.

As shown in the graph, there had been an evident influence from both sides of the bentonite seal i.e. the filter section and the concrete beam wall, on the cation pool distribution in the bentonite. The greatest effect could be seen on the distribution of Ca and Na. The content of Ca-ions has increased significantly in the bentonite facing the filter section and at the same time the concentration of Na-ions has decreased correspondingly. The same redistribution could be seen on the bentonite facing the concrete beam wall albeit to a lesser content. The effect of the contact with the filter section and the concrete beams respectively, decreased significantly towards the central parts of the bentonite block and the cation pool distribution appeared to be largely unaffected within 15 cm from the boundaries. These values fit well with investigations made on the same bentonite batch within other projects, see e.g. Börgesson et al. (2015b). The results indicated that the bentonite seal have had access to formation water from both sides i.e. not only from the filter section but also from the concrete beam side.

The cation concentrations in the filter should have been fairly constant during the pressurization of the filter due to the continuous leakage into the rock. This data set should therefore be useful for testing the ability to model the diffusion and exchange of cations in the bentonite. No chemical modelling was however performed in this project.

Non-reactive solutes and easily soluble salts, such as chlorides and carbonates of alkali metals, will necessarily contribute to the extracted cation pool, which is an inherent problem in extraction methods for exchangeable cations. The saturation of the bentonite seal has thus resulted in a certain excess of chlorides and this is probably the explanation for the increase of the total sum of cations at both ends of the bentonite core.

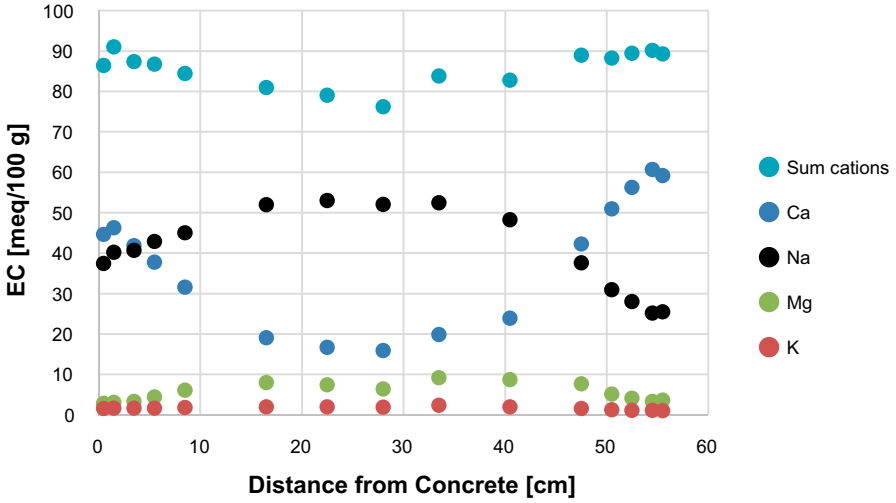

Figure 4-11. *The cation pool distribution determined at different distances from the concrete beam wall. The presented values are an average of duplicate samples.*

4.4 Filter sections consisting of gravel filling and LECA

4.4.1 General

The filter section is positioned behind the bentonite seal and consists of two material layers, a stiff draining material made of 300 mm thick LECA beams and a 300 mm thick layer of a geological draining material (gravel 2–4 mm). In addition, a geotextile is positioned between the gravel filling and the bentonite seal in order to prevent the bentonite from swelling into the voids of the filter.

During excavation of the filter section, the following have been checked/measured:

1. The filter material i.e. the gravel filling was checked regarding any signs for bentonite that has leaked into the filter.
2. The drainage tube and the de-airing tube were checked visually, especially the nets covering the inlets/outlets.
3. The thickness of the section filled with drainage material and the position of the LECA wall in relation to the concrete beam wall was measured at different positions.

4.4.2 Filter material

After visual inspection of the filter sections made during the excavation, the assessment was that it consisted only of the pure gravel filling. No bentonite had eroded or been extruded into the voids of the filter i.e. the separating geotextile against the bentonite seal and the LECA wall against the backfill had prevented bentonite from eroding or being extruded into the gravel filling.

4.4.3 Status of drainage and de-airing tubes

Two steel pipes were installed in the gravel filled filter (43.6 x 3.2 mm). The pipes pass through the bentonite seal, the concrete beams and the concrete dome. The main purposes with the tubes were to drainage and de-air the filter section during the construction. Another purpose was to saturate the bentonite seal in a controlled way i.e. without causing piping and erosion of bentonite seal. This was made by filling the filter with water but not letting the pressure increase to high.

In conjunction with these activities it was discovered that the function of the pipes not was completely as intended regarding the drainage capacity. This was assessed to partly depend on the fine meshed copper nets that were positioned on the inlets of the pipes as a filter with the purpose to prevent the surrounding gravel to fall into the tubes. Several stops in the water flow occurred and the problems was believed to depend on the copper nets that were clogged by finer materials.

The pipes and the nets were found during the excavation and the copper filters were visually inspected, Figure 4-12. The filters were partly clogged but it was although assessed that it still was possible for water to flow through them.

Figure 4-12. *Left: Close-up of the upper de-airing tube with copper net and a broken hose clamp. Right: Close-up of the removed copper net placed beside the de-airing tube.*

4.5 Thickness and movements of the filter section

Thickness of filter section consisting of gravel filling

The target width of the section filled with gravel was in conjunction with the installation set to 300 mm. During excavation the width was measured several times, at different levels. The results from the measurements gave that the width varied between 210 and 250 mm, see photo from one measurement provided in Figure 4-13.

A measurement on the displacement sensor that had been in contact with the bentonite seal, was also made, see photo provided in Figure 4-14. The displacement sensor to the left in the photo was measuring the displacement of the bentonite seal and the displacement sensor to the right was measuring the displacement of the LECA wall. By measuring the distance between the LECA wall and the end of the sensor that has been positioned against the bentonite seal, the thickness of the filter section could be determined to 220 mm.

Movements of the LECA wall

The data registered during test time have indicated that the LECA wall has moved upstream approximately 30 mm, see graph provided in Figure 3-7. This distance should, however, be seen as a minimum movement since it was judged that the sensor had exceeded its range and then failed. Measurements during excavation and sampling showed that the distance between the inside of the concrete beam wall (fixed) and the LECA wall varied between 810 and 840 mm. This means that the LECA wall has moved between 10 and 40 mm upstream during the test time (At installation the bentonite seal had a thickness of 500 mm and the gravel filling a thickness of 300 mm).

4.5.1 Removal of filter material

After having removed the uppermost bentonite of the seal the geotextile separating the bentonite from the gravel filling was exposed. The gravel filling was removed from the gap by using a special vacuum truck that sucked up the gravel filling from the gap, Figure 4-15. This procedure was done at three different occasions during the dismantling.

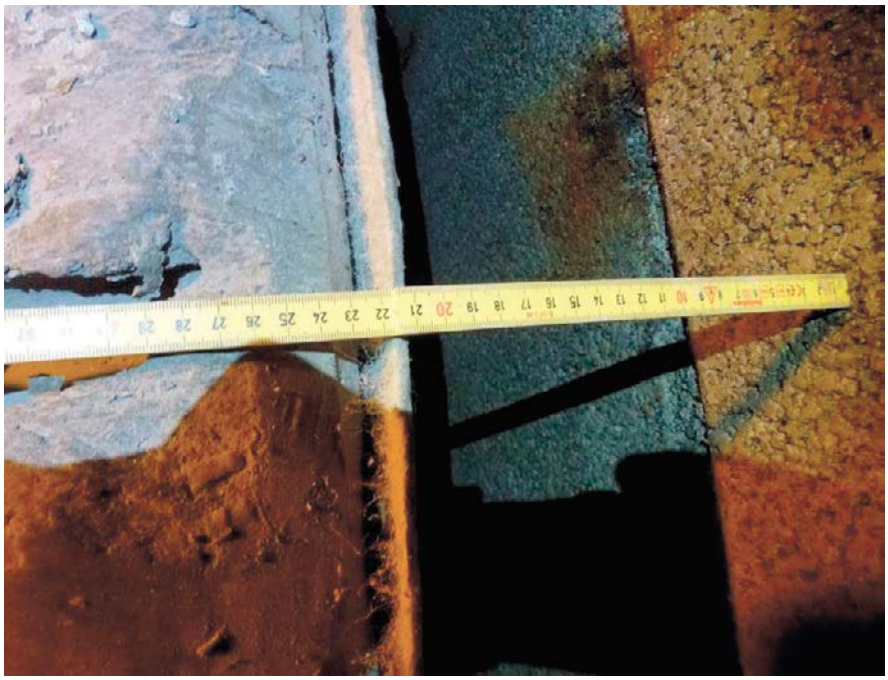

Figure 4-13. *Measuring the filter section thickness at the upper level of concrete beam 5.*

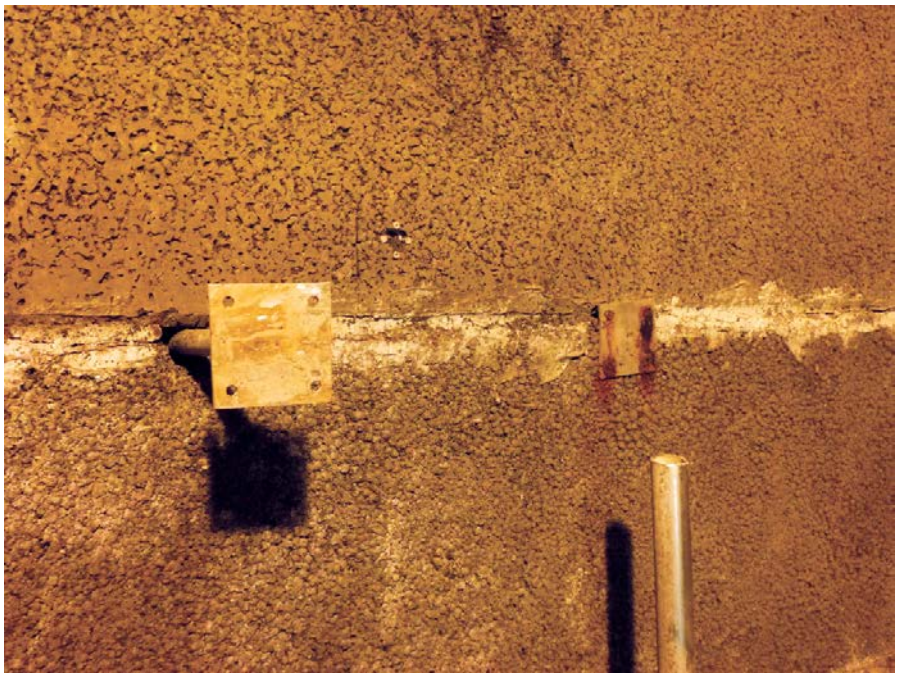

Figure 4-14. *Photo showing two of the displacement sensors (the vertical steel tube was used for de-airing of the filter and has been cut off).*

Figure 4-15. *A vacuum truck was used to remove the filter material.*

4.6 Backfill section

4.6.1 General

The backfill section is positioned behind the filter section and has a length of 1 100 mm. The central parts consist of a block stack (brick size blocks) and the gaps between blocks and rock walls were filled with bentonite pellets. The bentonite pellets were also used to even out the floor to achieve a foundation for the block stack. In addition, two vertical sections, one positioned just behind the LECA wall (thickness of 150 mm) and another positioned between the block stack and the tunnel end (thickness of 50 mm) were filled with bentonite pellets.

During excavation of the backfill section, the following have been checked/measured:

1. The contact between bentonite and rock have been checked. Any signs for channels, missing bentonite due to erosion etc have been checked.
2. The thickness of the backfill has been measured. The backfill section had at installation a thickness of 1 100 mm. According to displacement measurements during test time, the LECA wall has been pushed upstream by the swelling bentonite seal and compacted the backfill section.
3. The water content and density distribution have been determined in approximately 360 points in the backfill.

4.6.2 Removal of LECA beams

The uppermost part of the LECA wall was installed as a masonry with smaller blocks instead of a beam as for the concrete beam wall. This upper part was rather easily crushed and removed by an excavator. The photo provided in Figure 4-16 shows the exposed backfill behind the top of the LECA wall after removal of the masonry.

The LECA beams were casted against each other with a thin concrete layer but they were not fastened against the rock wall i.e. the whole LECA wall could move freely in relation to the rock. This means that the individual beams could be removed one by one by use of a wheel loader that pushed them loose from each other and then could lift them away, Figure 4-17. After removal of one LECA beam the bentonite behind was sampled and removed before the work with removal of the next concrete beam was started.

Figure 4-16. *The uppermost part of the LECA wall has been removed and the backfill behind exposed.*

During the sampling of the backfill, see description in Section 4.6.5, the remaining LECA beams were fixed against the rock wall by steel beams to prevent them from moving during the excavation of the bentonite behind.

4.6.3 Contact between backfill and rock

The backfill bentonite was in tight contact with the rock surface all around the tunnel contour. It was obvious that the backfill blocks had swelled and compacted the pellet filling against the rock, see also results from the density determinations in Section 4.6.5.

The photo provided in Figure 4-18 shows the contact between bentonite and the rock surface at the ceiling. The green dots marks where samples were planned to be taken.

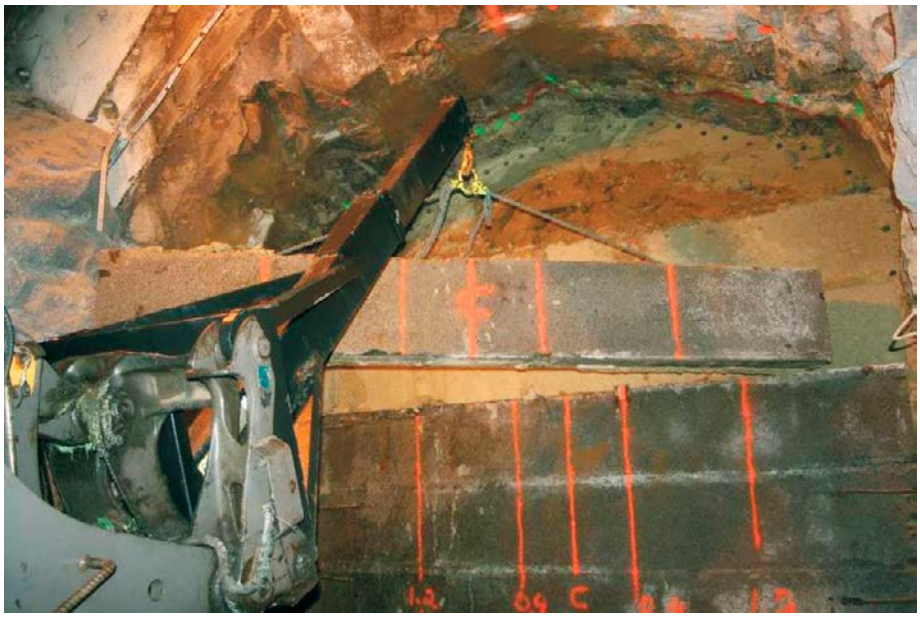

Figure 4-17. *Removal of a LECA beam.*

Figure 4-18. *Photo showing a close-up of the contact between backfill bentonite and ceiling. The green dots shows the sampling points around the bentonite-rock contour at the ceiling.*

4.6.4 Thickness of backfill section

The backfill section has a total depth of 1 100 mm whereas the first 150 mm thick gap behind the LECA wall was filled with pellets (Cebogel). The displacements measurements of the LECA wall indicated that the LECA wall has moved upstream approximately 30 mm, see graph provided in Figure 3-7. Measurements made during excavation of the filter section resulted in an estimated movement of the LECA wall between 10 and 40 mm, see also Section 4.5.

The sampling of the backfill showed that the pellet filled gap behind the LECA wall had been compressed to a clearly higher density than the density reached during installation. The photo provided in Figure 4-19 shows the former pellet layer behind the LECA wall. In the photo a sample has been excavated from the pellet filling (Cebogel) and the backfill blocks (Asha) can be seen in the bottom of the hole. Depending on the large difference in color between the Asha blocks and the Cebogel pellets, which not was intentional, it was possible to clearly identify the boundary between the two materials. The thickness of the former pellet filled gap varied somewhat but was estimated to be approximately 100 mm.

4.6.5 Water content and density distribution

Sampling techniques

The sampling techniques used for the backfill has been like the ones used for the bentonite seal, see Section 4.3.5. The photos provided in Figure 4-20 shows the two different sampling techniques used. The photo to the left shows the core drilling technique used for the central area of the backfill i.e. where the backfill blocks were stacked. The photo to the right shows the simpler method with a half-pipe that was pushed into the material by help of a hammer that was used for the former pellet filled slots.

Figure 4-19. *Photo showing the former pellet layer behind the LECA wall. In the photo a sample has been excavated from the pellet filling (Cebogel) and the backfill blocks (Asha) can be seen in the bottom of the hole.*

After removal of a LECA beam the outermost surface i.e. the former pellet filled gap was sampled manually with the pipe technique, see the right photo in Figure 4-20. This sampling technique was used both along the rock periphery and on the central parts. The next step was to drill out the cores from the parts of the backfill where backfill blocks had been stacked. The photo provided in Figure 4-21 shows the upper part of the backfill after removal of the uppermost masonry and the first LECA beam.

Figure 4-20. *Left: The central parts of the backfill were sampled using a core drill. Right: The outermost parts, close to the rock wall were sampled with a special made "half pipe".*

Figure 4-21. *Photo showing the upper part of the backfill section after sampling. The core drilled holes in the central area can be seen and also the sampling of the backfill rock contour.*

Calculations

See description in Section 4.3.5.

Test matrix

An extensive sampling of the backfill section have been performed. The sampling of the vertical backfill surface is shown in Figure 4-22 (left). This sampling was performed in five vertical sections BF1 to BF5 (BF=BackFill), Figure 4-22 (right). Approximately ninety samples were taken from the vertical sections BF1-BF4. In addition, about seventeen samples were taken from the innermost part of backfill section BF5 in the central parts. In total 380 samples were taken from the backfill section.

Results

The results from all measurements on the dry density of the backfill are presented in Figure 4-23. The results are divided after measuring sections on the x-axis, but the individual position of each sample within the associated section has not been considered in the graph. The samples taken from the central parts (former block stack) are marked with black dots and the samples taken in the periphery (former pellet filled slot) are marked with blue cubes. As shown in the graph there is an evident difference in dry density between the central parts and the periphery parts in each section. The density in the central parts is clearly higher even though the spread is high.

The samples in section 1 are all from the pellet filled gap just behind the LECA wall (note that the black dots presented in this section are from the central parts, not from block parts). The dry density is for all these samples low, between 875 and 1 225 kg/m^3, even if most of the samples have a dry density that is higher than of the pellet filling after installation.

The samples in section 5 are from the innermost parts of the backfill where there also was a thin pellet filled gap (thickness of about 50 mm), Figure 1-1. Since the samples were drilled out, see photos provided in Figure 5-20, it was difficult to take the samples closest to the rock. The results from these samples are assessed to be a mixture of more or less homogenized blocks and pellets.

The results from all measurements on the backfill are also presented in contour plots provided in Figure 4-24 (water content distribution), Figure 4-25 (dry density distribution) and Figure 4-26 (degree of saturation distribution).

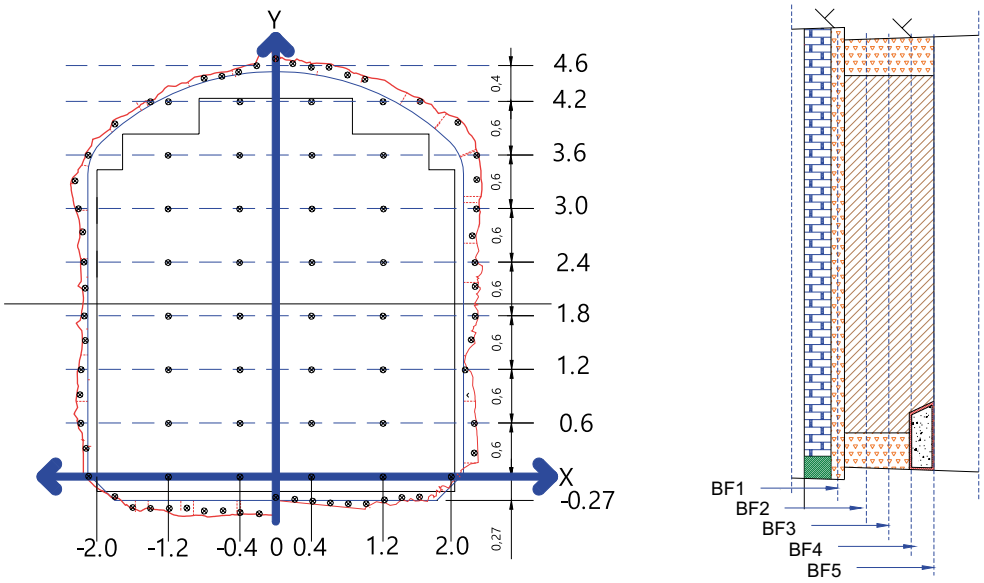

Figure 4-22. *Schematic showing the planned sampling of the backfill section. Left: The sampling of the vertical backfill surface. Right: The vertical sampling was performed in four different sections of the seal. In addition, extra samples were also taken from the innermost part of the backfill section.*

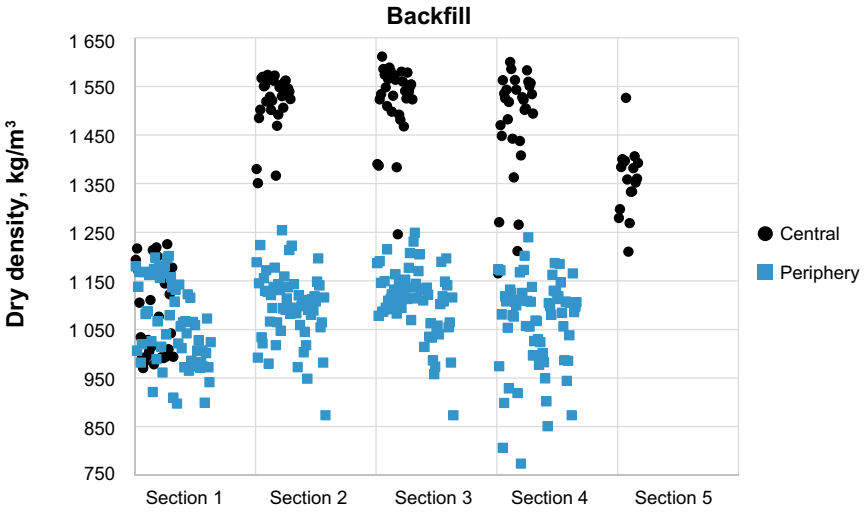

Figure 4-23. *Graph showing the results from all measurements on dry density in the backfill. The results are divided after measuring section on the x-axis. The samples taken from the central parts (former block stack) are marked with black dots and the samples taken in the periphery (former pellet filled slot) are marked with blue cubes.*

The dry density in the backfill varies in general between 900 and 1 600 kg/m^3 (Figure 4-25). As also seen in Figure 4-23, the dry density in backfill section 1 (closest to the filter) is clearly lower than in the other sections. This section was originally filled with pellets with a dry density of approximately 900 kg/m^3. The section had at time for installation a width of 150 mm, see schematic drawing in Figure 1-1. The density determined during the excavation varies between 875 and 1 225 kg/m^3 i.e. the pellet filling has been compressed by the swelling backfill but also by the movement of the LECA wall that according to measurements has been pushed upstream about forty mm by the swelling bentonite seal.

The density in the central parts of the backfill i.e. the former block stack in section 2, 3 and 4, is clearly higher than the periphery. The dry density in the central regions is between 1 500–1 600 kg/m^3 (1 750 kg/m^3 at installation) which can be compared with the density determined in the periphery which in general is between 1 000–1 200 kg/m^3. The large differences in density shows that the backfill has not homogenized completely, which was also not expected according to the modelling, see modelling results provided in Chapter 6. Differences in density are, however, expected also after long time when homogenization has occurred, depending on inner friction in the bentonite.

The density determined in the innermost part (section 5, extra samples) is lower than the rest of the backfill, between 1 200 and 1 500 kg/m^3. This depends, on the fact that a thin pellet layer, thickness of 50 mm, was installed between the block stack and the inner concrete wall, see also drawing provided in Figure 1-1.

By using the measured density and water contents the degree of saturation can be calculated for every sampling position. As shown in the graphs, Figure 4-26, the backfill is largely saturated but there are some inner parts in the former block stack in especially section 3 and 4 that have a somewhat lower degree of saturation, between 85 and 95 %. This is well in conformity with the pre-modelling of the saturation process, see Chapter 5.

The determination of density and water content are not made on exactly the same sample, which is impossible, but on samples positioned very close to each other. This may lead to the fact that there will be a certain deviation in the calculated degree of saturation even if the samples are saturated.

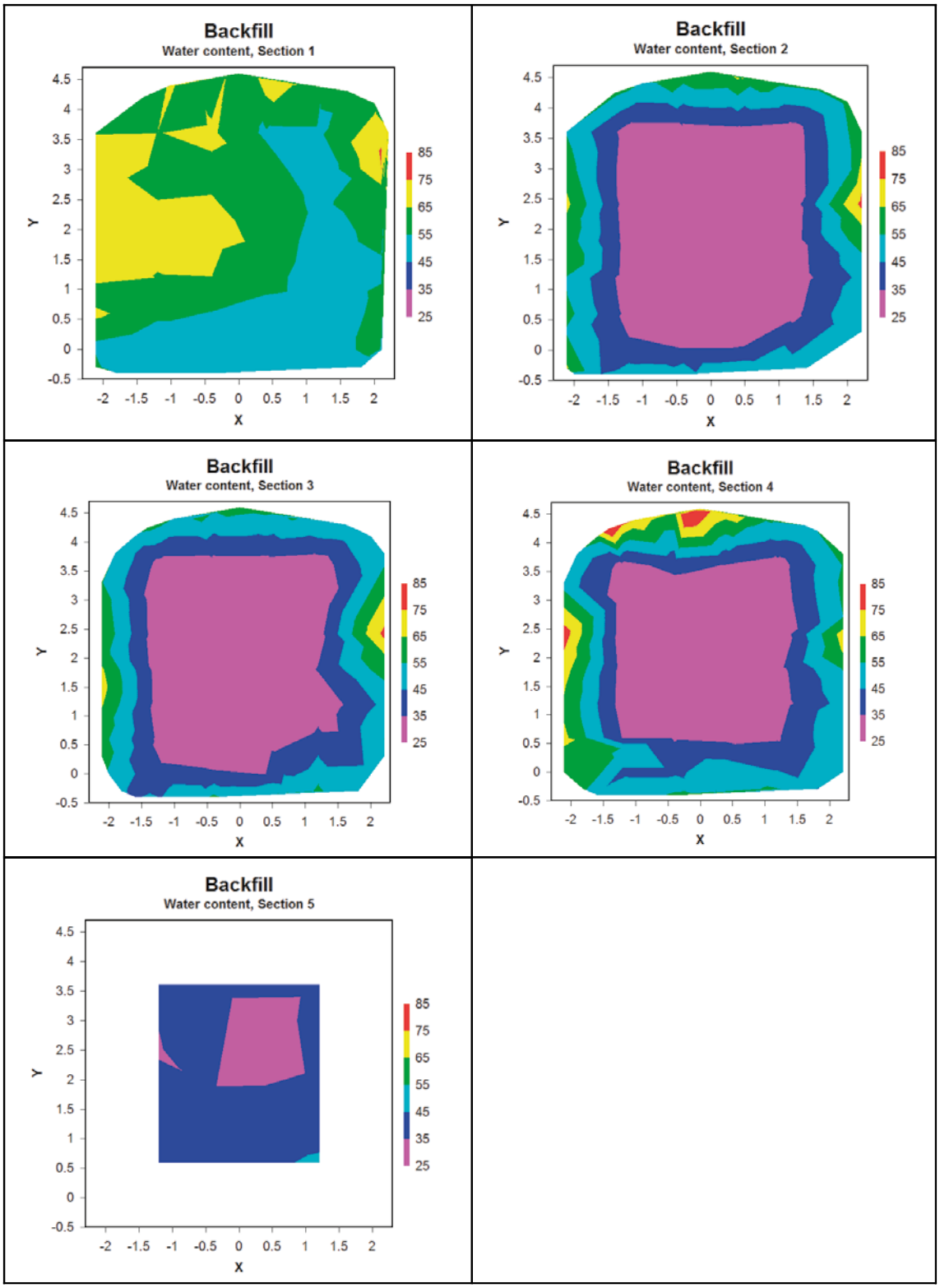

Figure 4-24. *Graphs showing the water content distribution in the backfill in the five different sections sampled.*

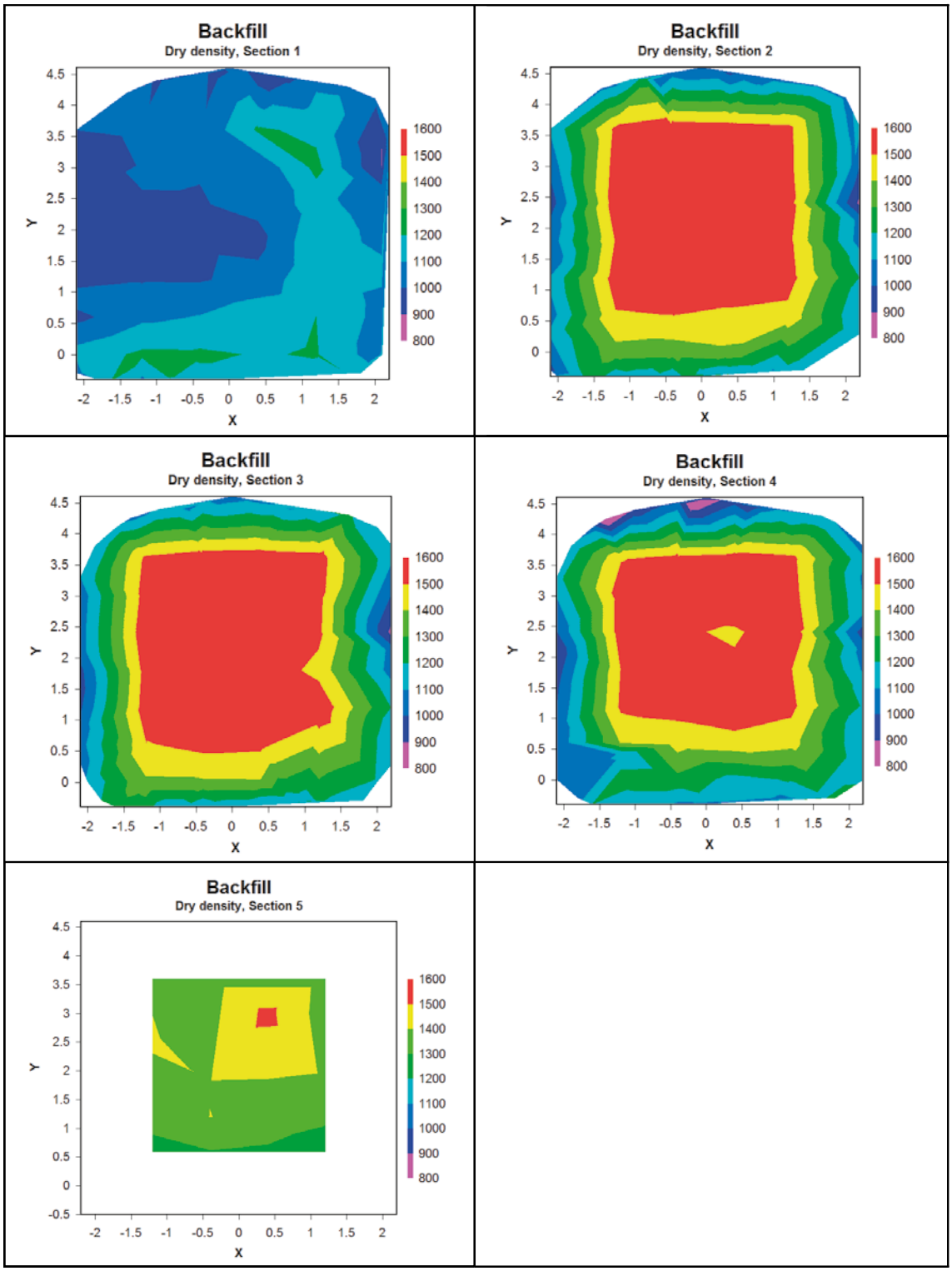

Figure 4-25. *Graphs showing the dry density distribution in the backfill in the five different sections sampled.*

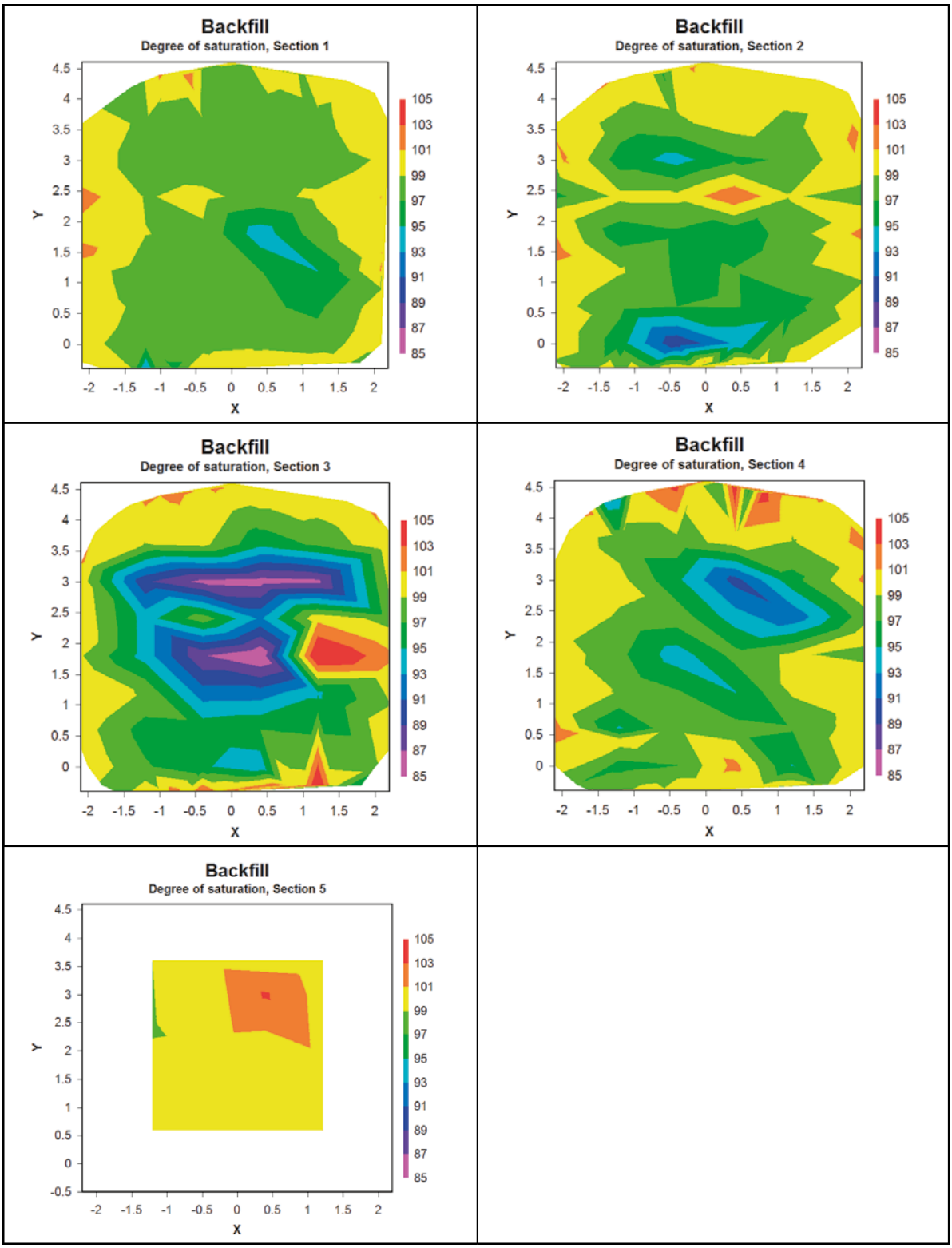

Figure 4-26. *Graphs showing the degree of saturation distribution of the backfill in the five different sections sampled.*

The backfill had in general a high degree of saturation, see Section 4.6.5. Although the backfill blocks had taken up water and swelled it was still possible to see the contours of the former blocks, Figure 4-27. The former gaps between the blocks had, however, healed and the blocks were more or less acting as a unit.

Figure 4-27. *Photo showing a section of the former block stack during excavation.*

5 Modelling

The purpose of the numerical modelling of the dome plug was to predict how far the hydration and the homogenization of the bentonite seal and the backfill had proceeded at the time of the excavation. In order to do that some modifications had to be done as compared to the models presented in Börgesson et al. (2015a). For example, the geometry was slightly updated, so as to include the pellets slot near the back wall and the applied water pressure used in the field experiment was included in the models.

The field test has provided sensors data throughout the test period which models could be compared with, and during the development of the models presented below only sensors data were available. In contrast, the dismantling operation provided information about the extent of hydration and the dry density distribution which enabled a more extensive comparison. Moreover, the dismantling data made it possible to perform other types of evaluations by which the consistency of different data sets could be assessed, for instance regarding the total bentonite mass and the relation between the measured effective stresses and dry density at the sensor positions.

This chapter is divided in the following parts: i) the model setup; ii) model results and comparisons with sensors data; iii) model results and comparisons with dismantling data; iv) an assessment of the consistency of different data sets; and v) a discussion on the validity of the material models.

5.1 Model setup

The first approach to predict the hydration and the homogenization was to create a hydro-mechanical (HM) model in which the hydraulic boundary condition in the filter section was set to the correct level of 4 MPa. However, it was found that it was not possible to get this model to converge. Instead three models were constructed: on one hand a HM model with a hydraulic boundary condition with atmospheric pressure (0.1 MPa); on the other hand two hydraulic (H) models with correct boundary pressure (4 MPa) and with different approaches regarding the dry density distribution, either as the dry densities at installation (denoted initial state) or for a dry density level in which the different bentonite fillings have reached complete homogenization (denoted homogenized state). The HM model was motivated by the goal to predict the homogenization of the bentonite fillings, even though the accuracy of the time scale for this would be limited. The motive for pursuing the approach with two different H models was to predict the time scale of bentonite hydration under the assumption that this can be bounded by the two defined extreme cases.

The model setup can be divided into three categories: 1) the geometry and mesh, 2) the boundary and initial conditions and 3) the material parameterization. These are described in three separate sections below.

5.1.1 Model geometries

The geometry of the models was based on the real tunnel section measurements and the actual design of the field experiment. The two-dimensional geometry and the mesh used are shown in Figure 5-1. The model assumes rotational symmetry around the tunnel axis. The actual dome plug is not included in the model and is instead included as a boundary condition (see next section). In Figure 5-1 the materials used to simulate the experiment is shown. This figure illustrates what will later be termed the initial state. In one model a homogenized state was assumed at installation. In this state the backfill and seal blocks, as well as the pellets in Figure 5-1 was replaced by a single material called “Homogenized bentonite”.

5.1.2 Boundary and initial conditions

The same initial liquid pressure (−45.9 MPa) was used for all materials in the analyzed models, except for the backfill blocks, which was given an initial liquid pressure equal to −57.9 MPa (which better corresponds with the initial relative humidity in these blocks). The initial total principal stresses

were set to −0.11 MPa in all directions in all models including mechanical processes. A constant temperature and gas pressure of 20 °C and 0.1 MPa, respectively, was defined in the models while gravity was neglected. The defined initial stresses correspond to a net mean stress of 0.01 MPa in the models.

The water was supplied to the bentonite through a hydraulic surface boundary in the model. The liquid pressure in this boundary was increased from −45.9 MPa to 0.1 MPa during the first 243 days of the model. After that time the boundary condition varied between the different models, as is illustrated in Figure 5-2. The mechanical boundary conditions along the concrete dome plug and the rock wall were fixed while roller supports were used at the symmetry axis as well as at the back of geometry, an illustration of this is shown in Figure 5-2.

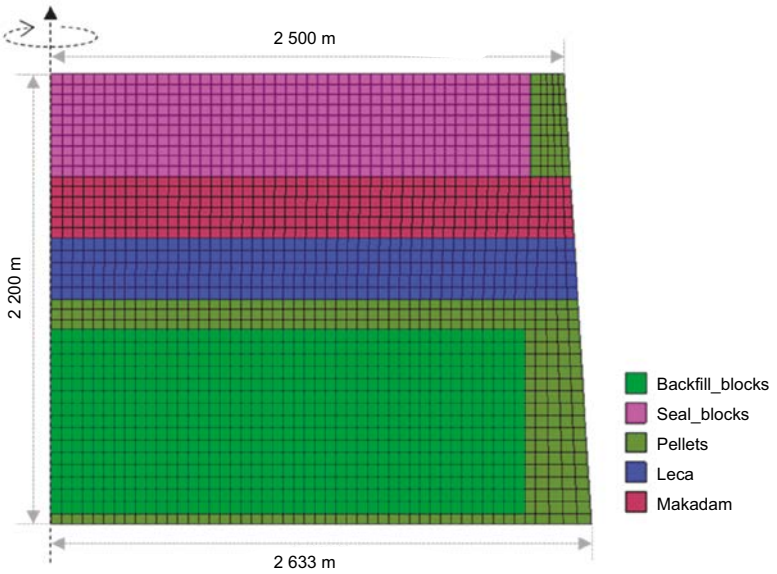

Figure 5-1. *Geometry, materials and mesh used in the modelling of the dome plug experiment. The model is 2D-axisymmetric, with the symmetry axis parallel to the tunnel axis.*

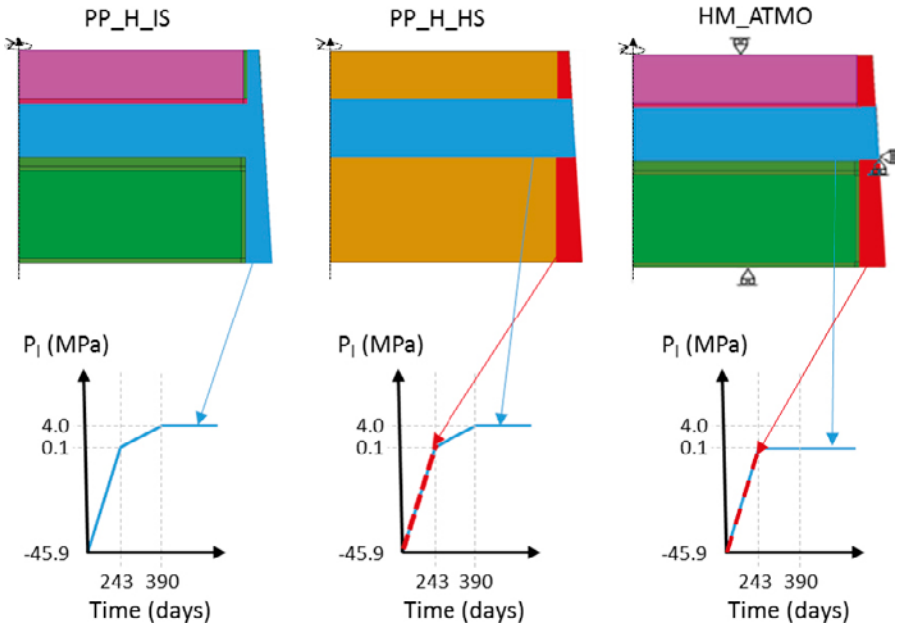

Figure 5-2. *Applied boundary conditions (hydraulic and mechanical) in the three reported models (see Table 5-3). No liquid flow is allowed over the outer boundaries, and along the symmetry axis roller boundary conditions are set by definition.*

5.1.3 Material parametrization

The hydro-mechanical material parameterization of the bentonite constituents (backfill blocks, seal blocks and pellets) was derived using the algorithms described in Åkesson et al. (2010a). The parameters of the bentonite constituents are shown in Table 5-1. Also included are the material parameters used for the" Homogenized bentonite" material.

To put bounds on the influence of mechanical processes on the hydration process two models needs to be simulated – an initial state model and a fully homogenized model. Constructing the initial state model is straight forward – it assumes that no changes in dry density takes place during the hydration. The homogenized state is somewhat more complicated, and some assumptions had to be made:

- The homogenized void ratio was assumed equal to 0.92 – this value comes from the evaluation in Börgesson et al. (2015a) and does not consider the pellets column at the back wall.
- No displacements of the filter material were considered.

As for the filter materials the HM material parameters are shown in Table 5-2 below.

Table 5-1. Hydro-mechanical parameterization of the buffer components.

Parameter			Backfill blocks	Seal blocks	Pellets	Homogenized buffer
Initial void ratio	e_0	(–)	0.62	0.686	2.09	0.92
Water content	w_0	(%)	17	17	17	17
Initial porosity	ϕ_0	(−)	0.383	0.407	0.676	0.48
Intrinsic permeability	k_0	(m^2)	1.9×10^{-21}	3.2×10^{-21}	5.2×10^{-19}	1.54×10^{-20}
	n_0	(−)	0.383	0.407	0.64	0.48
Relative permeability	k_{rl}	(−)	S_l^3	S_l^3	S_l^3	S_l^4*
Water retention curve	P_0	(MPa)	18.9	10.0	0.162	3.024
	λ	(−)	0.195	0.185	0.190	0.195
Target void ratio	e_T	(−)	0.92	0.92	0.92	
Porous elasticity	κ_{l0}	(−)	0.12	0.12	0.15	
	α_i	(−)	−0.021	−0.021	−0.021	
	α_{ils}	(−)	0	0	0	
	K_{min}	(MPa)	20	20	1	
Swelling modulus	κ_{s0}	(−)	0.3	0.3	0.3	
	α_{ss}	(−)	0	0	0	
	α_{sp}	(−)	[1)]	[1)]	[1)]	
	p_{ref}	(MPa)	0.5	0.5	0.025	
Poisson's ratio	v	(−)	0.2	0.2	0.4	
Plastic stress strain modulus	λ_0	(−)	0.194	0.194	0.286	
	r	(−)	0	0	0	
	β	(MPa^{-1})	0	0	0	
Critical state line parameter	M	(−)	0.262	0.262	0.743	
Tensile strength	p_{s0}	(MPa)	1.41	1.41	0.02	
	k	(MPa^{-1})	0	0	0	
Non-associativity parameter	α	(−)	0.5	0.5	0.5	
Pre-consolidation stress	p_0*	(MPa)	6.37	6.37	0.11	
	p_c	(MPa)	1	1	1	

* The exponent was increased to 4 in the relative permeability of the homogenized buffer in order to keep the evaluated diffusivity realistic.

[1)] Inbuilt α_{sp}-relation.

Table 5-2. Parameter values used for filter materials.

			Macadam	Leca
Initial porosity	n	(−)	0.35	0.35
Intrinsic permeability	k_0	(m^2)	10^{-18}	10^{-18}
Relative permeability	k_r	(−)	S_r^3	S_r^3
Water retention curve	P_0	(MPa)	0.003	0.003
	λ	(−)	0.9	0.9
Young modulus	E	(MPa)	20	90
Poisson's ratio	v	(−)	0.25	0.2

5.2 Model results and sensors data

An overview of the models is shown in Table 5-3. Due to convergence problems, no mechanical model with correctly applied water pressure in the filter materials could be completed. Instead a hydro-mechanical model with atmospheric pressure in the filters was simulated, and two hydraulic models which studied the effects of the applied water pressure in the filter on the hydration evolution were constructed and simulated.

5.2.1 Hydraulic models

Two purely hydraulic models were simulated – aimed at better understanding the hydration evolution in the seal and backfill blocks.

An overview of the relative-humidity evolution in the two hydraulic models are shown in Figure 5-4 to Figure 5-5 together with experimental data for comparison. In Figure 5-3 the placement of the relative humidity sensors in the field experiment is shown; the colors of the arrows is set the same as the corresponding lines in the result plots below.

Table 5-3. Overview of reported models.

Model ID	Model name	Processes	Description
PP_H_IS	PM_DM_PP_H_BBS.gid	H	Water pressure prescribed according to Figure 5-2, all materials in the initial state
PP_H_HS	PM_DM_PP_H_HOMO_WET.gid	H	Water pressure prescribed according to Figure 5-2, all materials in the homogenized state
HM_ATMO	PM_DM_ATMO.gid	HM	Atmospheric pressure prescribed on the filter and pellets (after day 243). All materials initially in the initial state

In Figure 5-4 and Figure 5-5 the evolution in the initial state hydraulic model is shown in the bentonite seal blocks and backfill blocks respectively. As is seen the relative humidity in the numerical model falls behind the relative humidity in the field experiment quite significantly. Only in the points nearest the filter in the seal blocks (Figure 5-4, right panel) is the hydration history relatively close to that seen in the field.

In the model with an initially homogenized buffer (Figure 5-6 and Figure 5-7), however, the hydraulic evolution is considerably closer to the measured relative humidity.

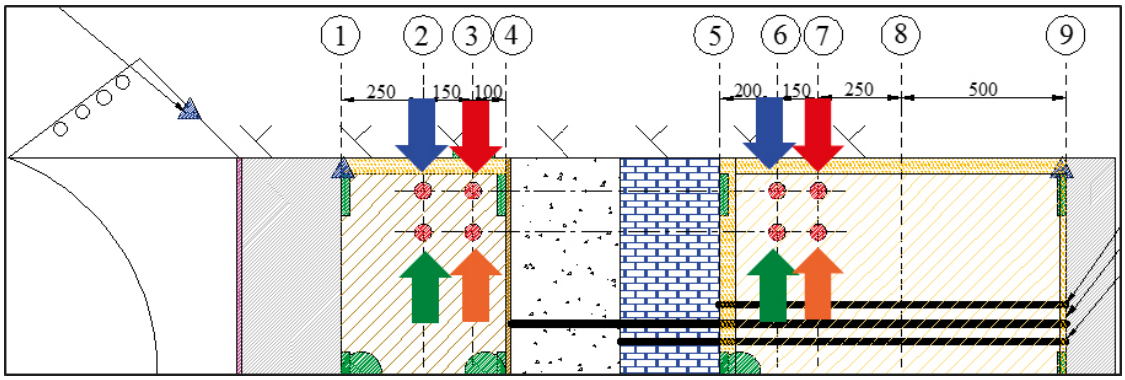

Figure 5-3. *Placement of relative humidity sensors in the field experiment.*

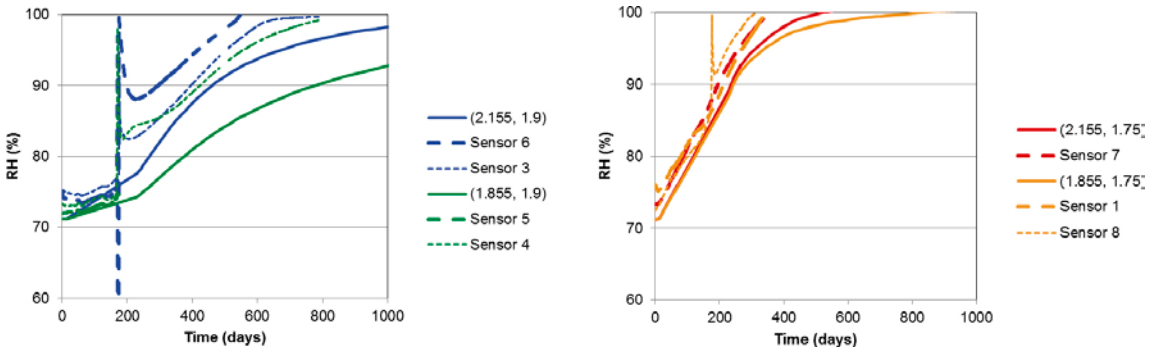

Figure 5-4. *Comparison of the relative-humidity evolution in the bentonite seal blocks from the model PP_H_IS.*

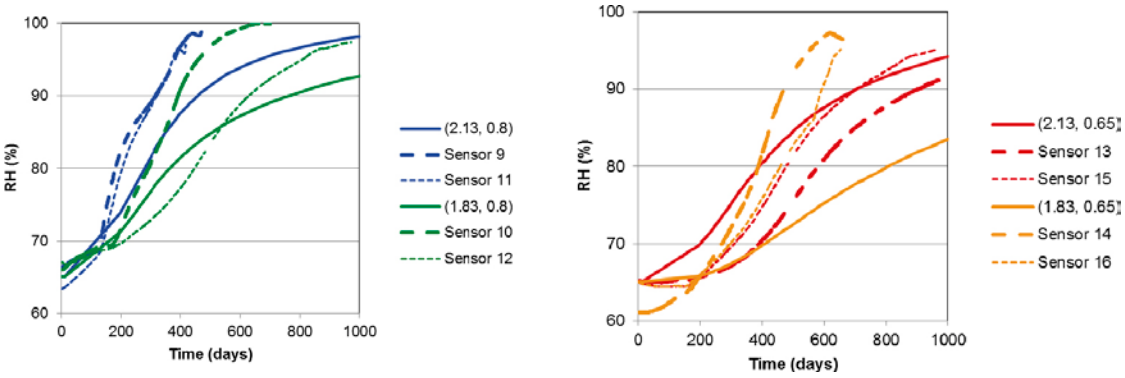

Figure 5-5. *Comparison of the relative-humidity evolution in the bentonite backfill blocks from the model PP_H_IS.*

Finally, a comparison of the degree of saturation in the two hydraulic models at the time of dismantling (i.e. on day 1 768) is shown in Figure 5-8.

As is seen the degree of saturation in the seal blocks is rather similar, however in the backfill blocks the degree of saturation in the homogenized model is slightly lower; this is an effect of the pellets column (which remains rather dry in the initial state model). These models therefore indicated that the seal would not be fully water saturated at the time of the dismantling

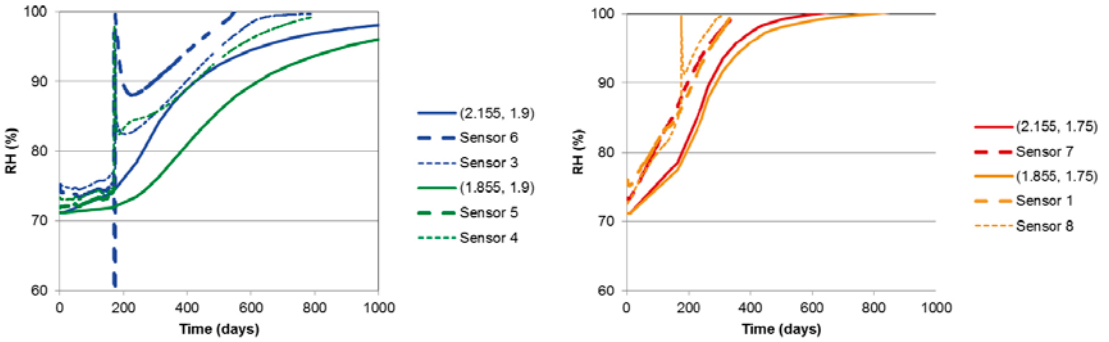

Figure 5-6. *Comparison of the relative-humidity evolution in the bentonite seal blocks from the model PP_H_HS.*

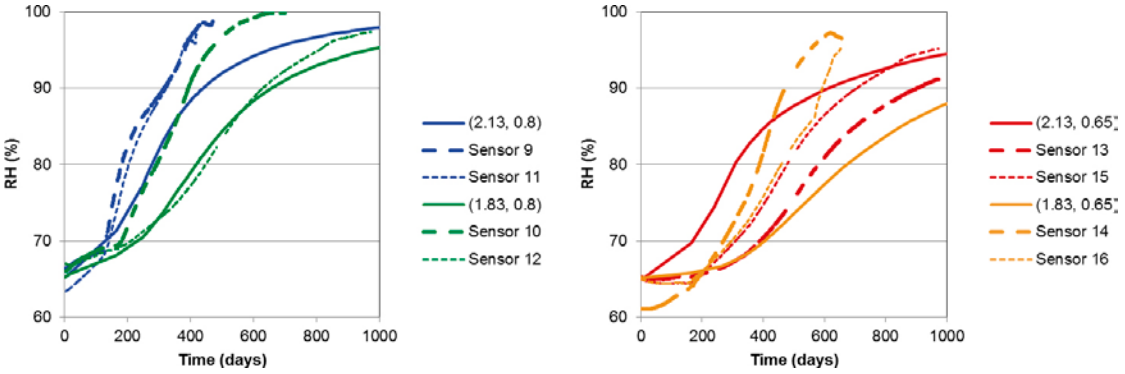

Figure 5-7. *Comparison of the relative-humidity evolution in the bentonite backfill blocks from the model PP_H_HS.*

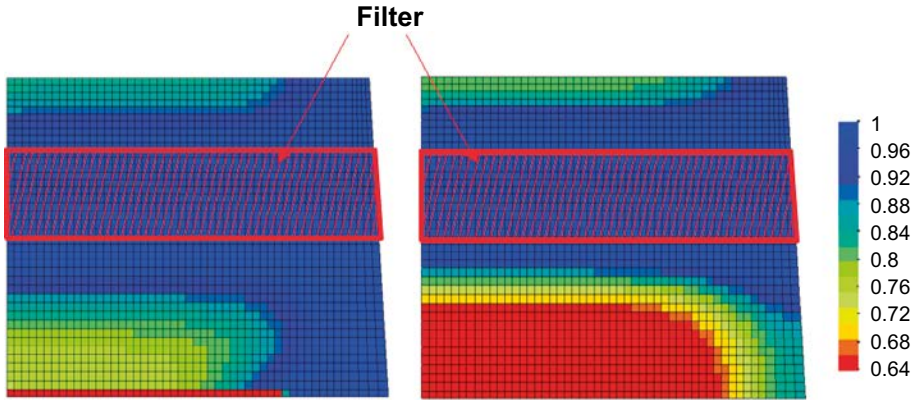

Figure 5-8. *Degree of saturation at time of dismantling in the two hydraulic models: PP_H_IS (left) and PP_H_HS (right).*

5.2.2 Hydromechanical model

The hydraulic evolution in the HM model is shown in Figure 5-9 and Figure 5-10. As can be seen the relative humidity increases at a slower rate in the model as compared to in the field experiment. This is not surprising, as the applied water pressures in the field could not be included in the model.

A comparison of the degree of water content time-evolution from the models PP_H_IS, PP_H_HS and HM_ATMO is shown in Figure 5-11. The water content is here shown in a point on the symmetry axis at the inner wall of the plug, which is the last point in the seal blocks to be saturated. Also included is the time at which the plug is assumed to be dismantled (December 4th, 2017 – dashed grey line). As can be seen none of the models are fully saturated at this point in time.

In Figure 5-12 the placement of the radial stress sensors in the field experiment is shown; the colors of the arrows are set the same as the corresponding lines in the result plots below.

In Figure 5-13 the radial stresses in the seal blocks are shown and compared to experimental data. These results were evaluated as the measured total pressures minus the water pressure in the filter. As is seen the radial stress is significantly higher than what was registered, in particular in the outer point on the tunnel plug wall (Figure 5-13, left).

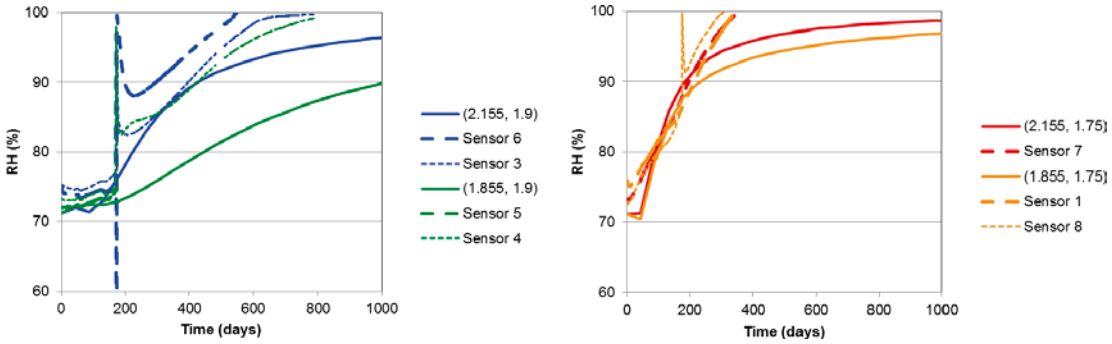

Figure 5-9. *Comparison of the relative-humidity evolution in the bentonite seal blocks from the model HM_ATMO.*

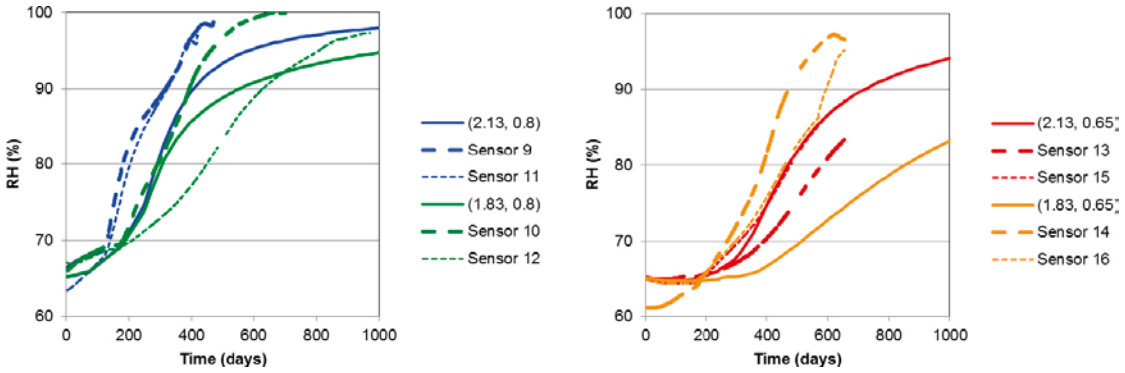

Figure 5-10. *Comparison of the relative-humidity evolution in the bentonite backfill blocks from the model HM_ATMO.*

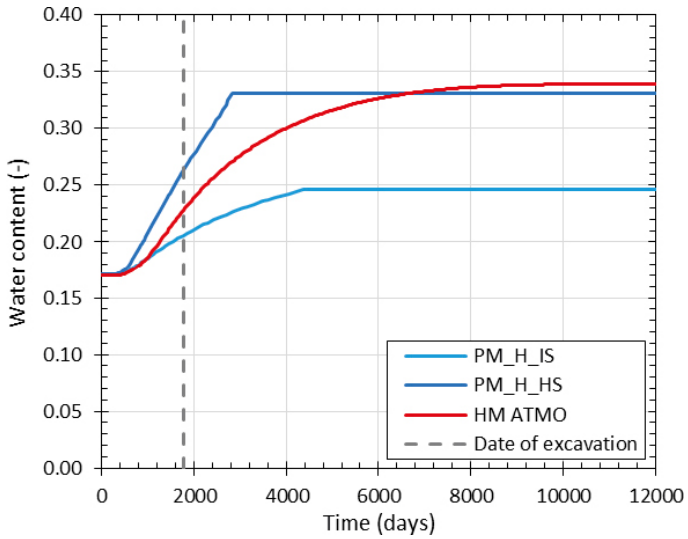

Figure 5-11. *Water content as function of time in the last saturated point in the bentonite seal point. In all three models shown this point is on the symmetry axis at the position of the plug inner wall.*

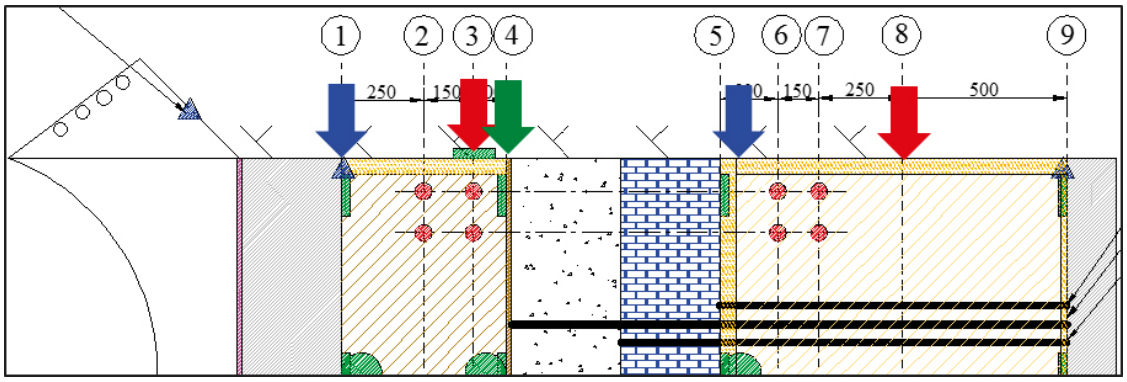

Figure 5-12. *Placement of radial stress sensors in the field experiment.*

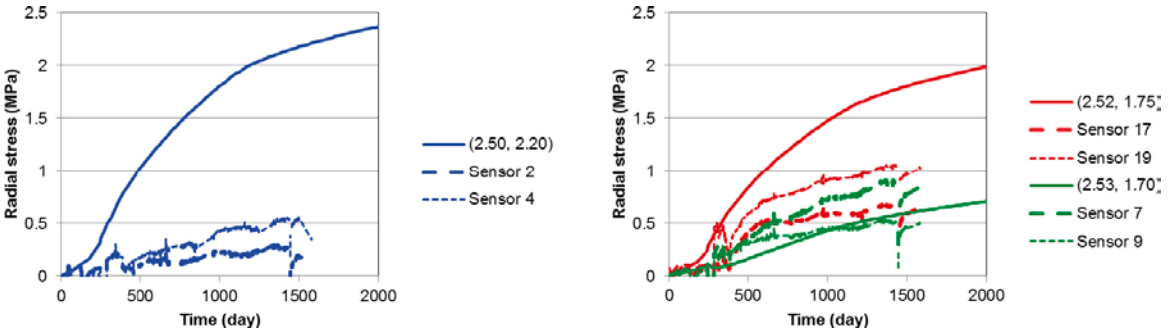

Figure 5-13. *Comparison of the radial stress in the bentonite seal blocks from the model HM_ATMO.*

In Figure 5-14 the stress evolution in the backfill blocks is shown. The agreement here is quite good for sensor 18, while sensor 12 and 14 shows almost no signal. The lack of a signal in the field experiment in sensors 2, 4, 12 and 14 is probably due to effects which are not included in the model (erosion, sensors accuracy, gaps between blocks, natural inflow during the first 117 days, etc.).

In Figure 5-15 the positions of the axial stress sensors are shown. Again, the colors of the arrows showing the sensor positions can be used to identify the corresponding sensors in the plots below.

In Figure 5-16 the axial stress evolution in the seal blocks is shown. The modelled values are in general higher than those measured in the field experiment, in particular at the interface with the filter material (Figure 5-16, right).

In Figure 5-17 the axial stress evolution in the backfill blocks is shown. The sensors near the filter shows similar values to the modelled results, while one of the sensors near the back wall shows significantly lower values than those modelled. However, one sensor (no 20) showed significantly higher values than in the model. One reason for this discrepancy may be that it was not possible to obtain convergence if the pellets-filled slot at the back was supplied with water, as was the case in the field test.

In Figure 5-18 the displacement sensors placements are shown. The colors of the arrows can be used to identify the sensors in the results graph in Figure 5-19. As can be seen the modelled displacements agree reasonably well during the first 400 days, although the response was faster than in the experiment, where after sensors 2 and 3 gave no data, and sensor 1 indicated no further displacements, which is not the case in the model.

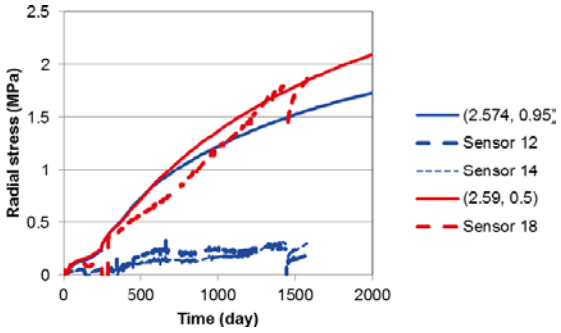

Figure 5-14. *Comparison of the radial stress in the bentonite backfill blocks from the model HM_ATMO.*

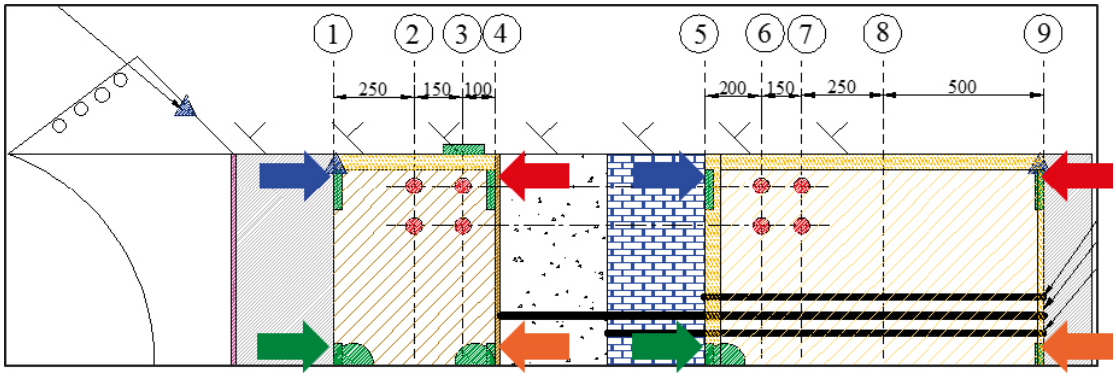

Figure 5-15. *Placement of axial stress sensors in the field experiment.*

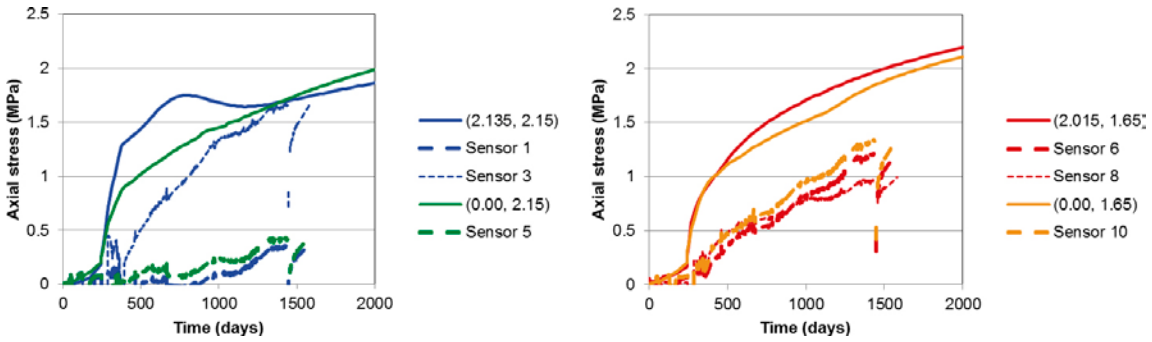

Figure 5-16. *Comparison of the axial stress in the bentonite seal blocks from the model HM_ATMO.*

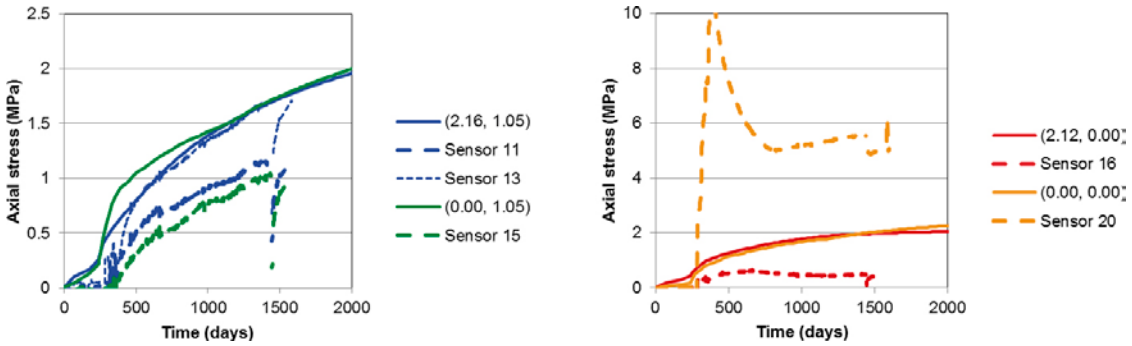

Figure 5-17. *Comparison of the axial stress in the bentonite backfill blocks from the model HM_ATMO.*

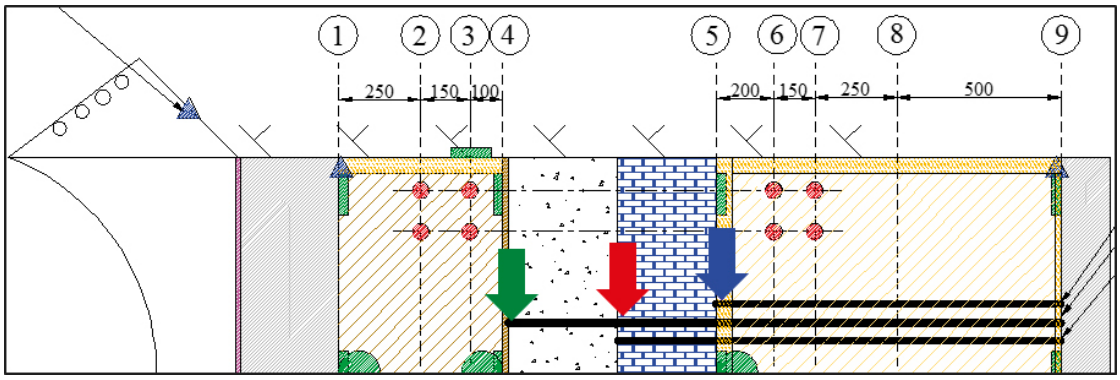

Figure 5-18. *Placement of axial displacement sensors in the field experiment.*

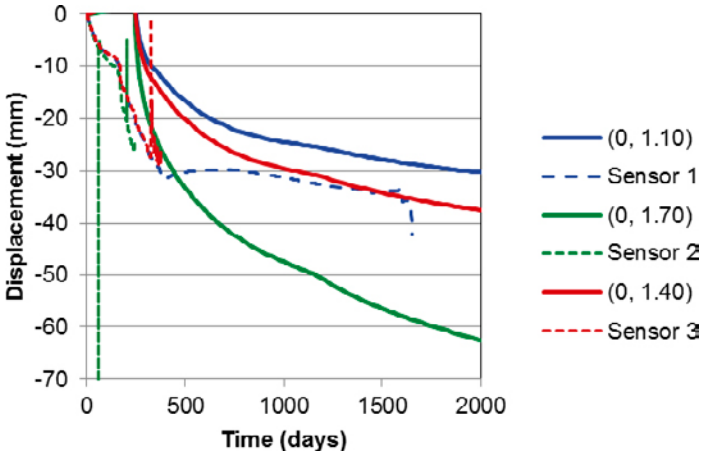

Figure 5-19. *Axial displacements as measured (dashed lines) and modelled (solid lines).*

5.3 Model results and dismantling data

The presented numerical models were designed for a 2D axisymmetric geometry. In order to enable a comparison of the model results with dismantling data with respect to degree of saturation and dry density (Section 4.3.5 and 4.6.5) the experimental data were converted in the following way:

- For each sample, the distance for the sample position (see X, Y coordinates in Figure 4-7) to a mid-point (X=0; Y=2.1) was calculated.
- For each sampling section, an axial distance from the tunnel ending was calculated. For the sections in the bentonite seal these were: 2.20, 2.08, 1.95, 1.83 and 1.70 m, and for the backfill the corresponding distances were 1.10, 0.83, 0.55, 0.28 and 0 m.
- The samples from the *former block stack from each sampling section* was arranged in groups defined for the following intervals of distances: 0 to 1.0 m; 1.0 to 1.6 m; 1.6 to 2.0 m; and 2.0 to 2.6 m.
- The mean value of the dry density and the degree of saturation was calculated for all samples in each group, and a radius representative for each interval (0.5, 1.3, 1.8 and 2.3 m, respectively) was assigned to each mean value.
- The mean value of the dry density and the degree of saturation was calculated for all samples from the *former pellets-filled slot from each sampling section,* and a radius corresponding to the outer radius in the model geometry for the axial distance for each section was assigned for each mean value.

These sets of mean values and axial and “radial” distances were used to generate contour plots similar in shape to the modelled contour plots.

The contour plot for the measured degree of saturation is shown in Figure 5-20, and it can clearly be seen that the rate of bentonite hydration was significantly underestimated with the numerical models, both for hydraulic models presented in Figure 5-8 as well as the HM model presented in Figure 5-20 (lower left). It can be noted that the saturation degree of the bentonite seal generally exceeded 98 %, whereas the backfill generally exceeded 94 %. This means that the extent of homogenization in the presented HM model could also be expected to be underestimated. The experimental data was therefore also compared with a later date (10 000 days) in the HM model when the hydration and homogenization has progressed further. It can be seen that the modeled seal and large part of the backfill had saturated at that time Figure 5-20 (lower right).

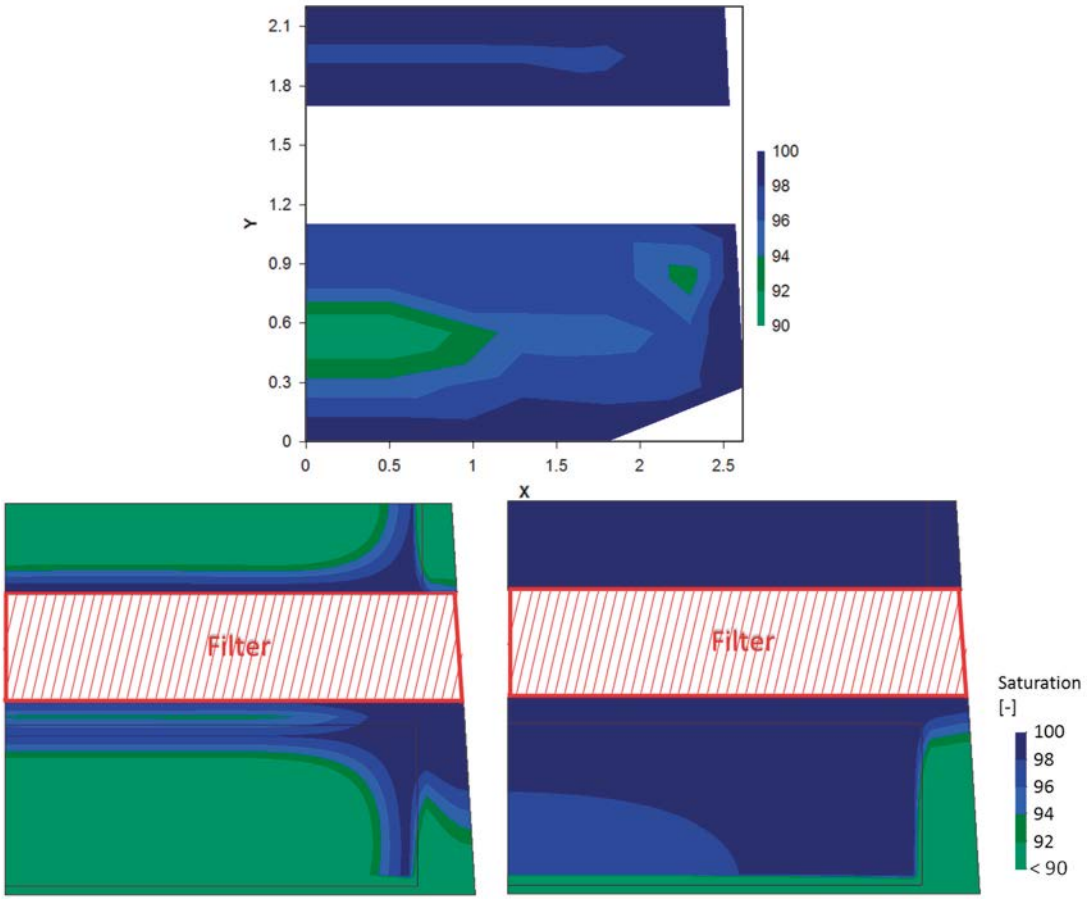

Figure 5-20. *Contour plots of degree of saturation: evaluated from experimental results (upper), and for HM model for the time of dismantling (day 1 768, lower left) and for HM model for day 10 000 (lower right).*

The contour plot for the measured dry density is shown in Figure 5-21 together with the model results, both for the day of dismantling and for 10 000 days. For the dismantling date, the highest dry densities in the HM model exceeded the highest values observed in the experimental data, both for the seal and the backfill, and this appears to reflect the underestimated extent of homogenization foreseen above. At 10 000 days the highest dry density in the model was also slightly higher than in the experiment, and this appears to be due to an underestimation of the compressibility of the filter and the pellets filling at the back. However, the lowest dry densities in the HM model (especially at 10 000 days) were clearly higher than the lowest values observed in the in experimental data, and this may be a consequence of the absence of friction along the boundaries towards the concrete beams, the filter, and the concrete wall at the end of the tunnel. In addition, there was a quite distinct measured dry density gradient in the backfill towards the filter; from 1 000 kg/m^3 to above 1 500 kg/m^3 within approximately 0.3 meter. This was a quite extensive remaining heterogeneity which may have been caused by: i) remaining unsaturated condition (although the degree of saturation generally exceeded 96 %), ii) the difference in material (although the properties of Asha and Cebogel can probably not explain this difference), and iii) displacements caused by the pressurization scheme and/or the dismantling operation. A similar gradient, although much less distinct, was found in the bentonite seal towards the filter; from slightly above 1 200 kg/m^3 to slightly below 1 400 kg/m^3 within approximately 0.1 meter. This heterogeneity could not be caused by any unsaturated conditions or material differences, so this was either consistent with the hysteretic behavior of MX-80, or it was a remnant of the pressurization scheme and/or the dismantling operation.

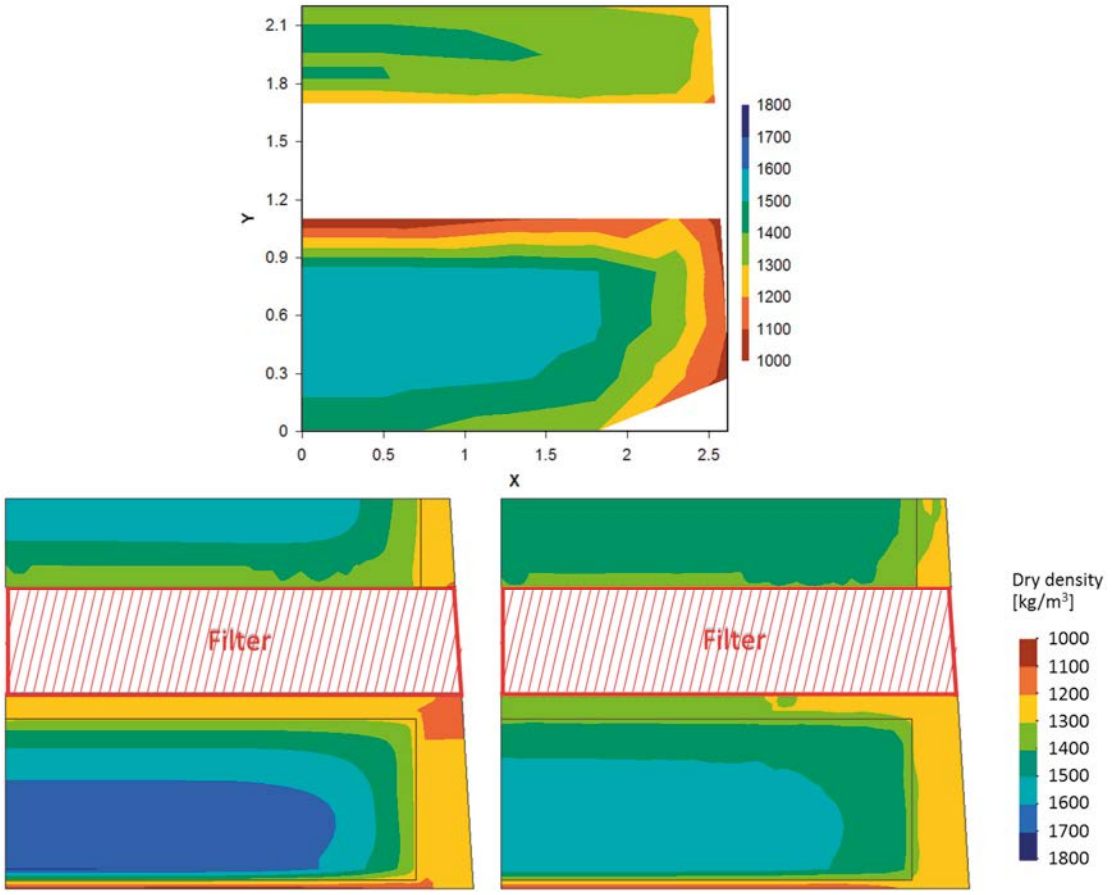

Figure 5-21. *Contour plots of bentonite dry density: evaluated from experimental results (upper), for HM model for the time of dismantling (day 1 768, lower left) and for HM model for day 10 000 (lower right).*

A comparison of calculated displacements in the model and experimental data registered with displacement sensors is shown in Figure 5-19 and demonstrates that the agreement was reasonable good during the first 400 days although the response in the model was slower than in the experiment. The dismantling has provided additional data on the displacement fields: the interface between the bentonite seal and the gravel moved 60–120 mm upstream, and the corresponding interface between the Leca wall and the backfill moved 10–40 mm upstream. The last result from the sensor at the Leca/backfill interface (i.e. −43 mm) was quite consistent with the dismantling data. This can be compared with the results from the HM model for a time corresponding to the start of the dismantling (day 1 768) in which the displacements were 60 mm (seal/gravel) and 30 mm (Leca/backfill), respectively. The modelled displacements at day 10 000, with almost saturated conditions, were approximately 70 and 20 mm, respectively (Figure 5-22).

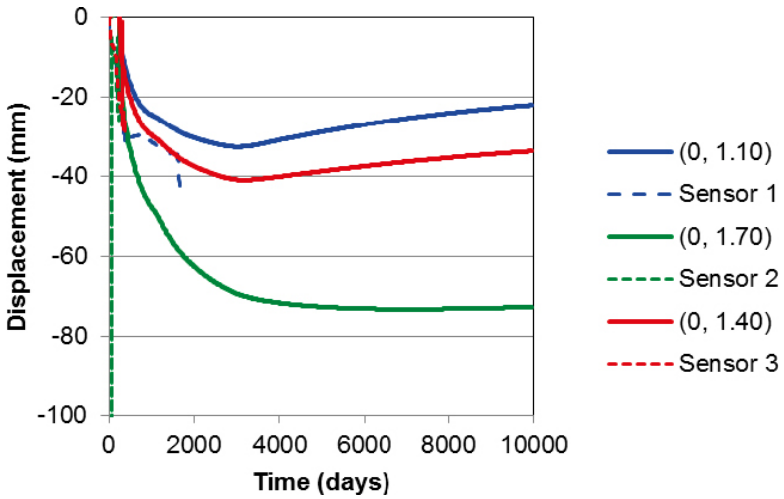

Figure 5-22. *Long-term evolution of modelled axial displacements together with sensors data.*

6 Evaluations

6.1 Compliance of requirements and design premises

6.1.1 Bentonite seal

The bentonite seal was designed with the premise that the swelling pressure on the concrete plug should not exceed 2 MPa. For MX-80 bentonite, such a swelling pressure level can be reached at a dry density level of approximately 1 400 kg/m^3. Bentonite blocks with a relatively low dry density was therefore specially manufactured. The average installed dry density of the bentonite seal in Domplu was 1 560 kg/m^3 (Table 2-1), and in order to reduce the swelling pressure, a pellets-filled slot behind the filter section was installed and dimensioned to a thickness of 150 mm. In addition, the gravel filling in the filter section was assessed to exhibit a specific compressibility. By taking these compressible components into account, a theoretical final swelling pressure on the Domplu concrete plug was calculated to 2.48 MPa (Grahm et al. 2015), which corresponds to a dry density of ~1 450 kg/m^3.

The weighed mean value of the dry density measurements in the seal during the dismantling was found to be 1 342 kg/m^3. This means that design premise of limiting the swelling pressure on the concrete plug to 2 MPa could be fulfilled. It can be noted that the main reason for the difference between the expected and the implemented dry density levels, appears to be that the gravel filling was more compressible than first anticipated.

Remark

Several conditions call for a revision of the design premises for the bentonite seal: i) the use of conventional backfill blocks instead of specially manufactured seal blocks would simplify the logistics associated with the installation; ii) an increase of the allowed swelling pressure on the concrete plug would make the design more robust (i.e. less dependent on wall friction), and should also improve the seal healing ability due to higher dry density; and iii) a procedure in which the rock wall at the section of the seal is made smooth (e.g. by sawing) and no pellets-filling is installed (or minimized) would result in a higher dry density level close to the rock wall, and (possibly) in an ability to raise the water level in the filter at a faster rate (see below).

6.1.2 Filter section

The filter section was designed with the intention to obtain a sufficient drainage capacity. More specifically, the goal was to be able to *drain a flow rate of 5 liters per minute* with only a *minor raising of the water level* in the filter. An additional goal was *to raise the water level of the filter* in such a way that the pellets-filling of the seal could be water saturated so that this could withstand the hydraulic gradient caused by the water-filled filter. This operation was planned to be performed *during a period of six days*.

The three draining tests and filter fill-up performed during the early stage of the Domplu test showed that it was not possible to drain a flow rate of 1.4 liter per minute without raising the water level to the level of the de-airing pipe (day 167), which means the first goal could not be fulfilled. An equipment for slowly raising the water table in the filter section was developed and a test was performed in which hoses attached to the drainage and deairing pipes were slowly raised (day 188), although this was performed without draining any excess flow. This means that the second goal could have been fulfilled if the drainage capacity had been sufficient.

In addition to sealing ability, the dimensioning of the pellets-filled slot behind the filter section was influenced by the compressibility of the filter material used in the filter section (see above).

Remark

The design of the filter should be updated so that the goals can be fulfilled. Two improvements can be identified in order to increase the drainage capacity: i) multiplication of the number of drainage tubes at the bottom of the filter; and ii) employment of wider nets to cover the endings of the drainage tubes and deairing tube.

In addition, the deformation properties of gravel filling (in combination with varying pore pressure) should be further analyzed.

6.1.3 Water tightness

Grahm et al. (2015) suggested a water tightness requirement for the deposition tunnel plug according to which the leakage past the plug would be lower than 0.1 l/min (corresponding to *6 liters per hour)*. The current technical design requirement regarding the tightness of the plug was defined by Posiva and SKB (2017; Section 6.5.3) after the installation of Domplu, and was formulated as: "*200 m^3 total outflow before the backfill is saturated*". Some comments can be made regarding this requitement. The time to reach water saturated conditions in the backfill is at least 80 years according to hydraulic models presented by Åkesson et al. (2010b). Together with the tightness requirement, this would imply that the flow rate past the plug should not exceed *0.3 liters per hour*. It can be noted that this is a factor 20 lower than the limit suggested by Grahm et al. (2015). The saturation time of the backfill in some tunnels is expected to be orders of magnitude longer (Sellin et al. 2017), which would imply that a corresponding flow rate requirement would be orders of magnitude lower.

Experimental results from the Dome plug showed that the part of the total leakage which represented the leakage past the plug (quantified with a weir in front of the plug) levelled off to *1–3 liters per hour* after approximately one year of pressurization. On the other hand, the total flowrate injected into the filter, and which has largely migrated out into the rock, leveled off to *20–25 liters per hour*. The samples taken from the bentonite seal during the dismantling operation showed that this component was water saturated and quite homogenized with dry density levels in the approximate interval 1 100–1 450 kg/m^3 which therefore should imply that it exhibited a high tightness to water. The flowrate through the *entire* seal section can be estimated for a hydraulic conductivity of 10^{-12} m/s (representative for MX-80 with a dry density of 1 200 kg/m^3, Åkesson et al. 2010a) and a pressure difference of 4 MPa (20 $m^2 \cdot 10^{-12}$ m/s · 400/0.5 m/m) which gives *0.06 liter per hour*. This indicates that the quantified leakage should have passed through the rock rather than through the bentonite/concrete. In fact, the tunnel mapping performed in the tunnel prior to the wire-sawing of the slot abutment revealed the presence of water-bearing fractures which intersected the rock sections in which the filter and bentonite seal subsequently were installed, and this appears to have enabled water to circumvent the bentonite seal. In addition, the pressurization of the filter with 4 MPa can be regarded as high in comparison to hydrostatic pressure in the rock. When the pumps were turned off in June 2017, the pressure in the filter decreased rapidly to a level of 13 bar. If this difference in pressure caused an opening of intersecting fractures during pressurization, then this may have implied an exaggerated overall permeability of the plug-rock construction.

The results from the Domplu field tests indicate that the *bentonite/concrete construction* can meet the requirement on the limited permeability of the plug. The quantified leakage past the plug (1–3 l/h) exceeded the flow rate limit implied from the tightness requirement (0.3 l/h), but according to the available information this was likely to be caused by *water-bearing fractures in the rock*.

Remark

The objective for restricting the water flow past the tunnel plug is to limit the erosion of bentonite from the deposition holes. The occurrence of water-bearing fractures *and* the drawdown profile (Figure 6-1) during the operational phase may both have a significant influence on the bentonite erosion. The time to restore the hydrostatic pressure distribution therefore appears to be a more relevant time frame than the time to reach water saturated conditions in the backfill, since such a condition would imply that the driving force for water flow past the plug would cease to exist.

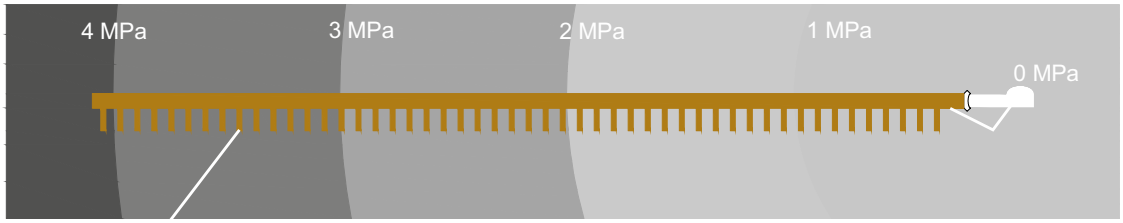

Figure 6-1. *Schematic illustration of draw down along a deposition tunnel intersected by water bearing fractures at different pressure levels.*

Finally, no traces of any erosion channels could be found during the dismantling of the bentonite seal in the Domplu experiment, and this support the notion that the seal exhibited a low permeability. However, *if* an erosion channel would have been formed, for instance during the filling of the filter and a concurrent leakage past the concrete plug, then this channel may still have been present after a long time. Laboratory tests of seal healing (in which specimen through which a ∅5 mm hole was drilled and subsequently left to self-heal for 3 weeks) have indicated that the dry density should exceed 1 400 kg/m^3 to ensure that the hydraulic conductivity for the intact specimen is maintained (Johannesson et al. 2010). Since all samples from the peripheral part of the bentonite seal in Domplu was lower than this level, this may have implied a limited ability for potential erosion channels to self-heal, and this motivates the increase of the overall dry density level of the bentonite seal.

6.1.4 Gas tightness

A gas tightness requirement was first addressed in a request from SSM in which SKB was asked to present a calculation of the extent of leakage of oxygen through the tunnel plug and how this will influence the degradation processes on the copper canister. In SKB's reply (SKB 2014) it was stated that: "*SKB defines gas tight as a situation where no gas phase is present in the hydraulically sealing part of the plug*" and that the "*requirement for gas tightness … can be assumed to be fulfilled if a water column is maintained … in the filter section of the plug … throughout the operational period of the entire repository*". SSM (2016, page 163) has subsequently observed that the requirement regarding the gas tightness implies a need for a continuous monitoring of the water level in the filter during the entire operation period in order to ensure the safety function of the plug.

The reference design of the plug consists of drainage pipes which "shall drain the water collected in the filter and transport it out from the deposition tunnel to prevent water pressure to be applied on the concrete plug before it has cured and gained full strength" (SKB 2010). These drainage pipes can be equipped with pressure sensors which will enable the monitoring of the water level as well as the water pressure in the filter. This can either be performed through manual readings or by using a data logger system. The fulfillment of the gas tightness requirement is thus question of keeping the filter waterfilled and to monitor this state.

A gas tightness test was performed within the Domplu field test. This was implemented by draining the water from the filter; pressurization of the filter with helium gas to 0.4 bar gauge and by monitoring the gas pressure evolution. During a period of 18 hours it was found that the gas pressure increased with 3 kPa, which indicated that a noticeable inflow of water occurred during this measurement. The monitoring was also complemented with a sniffer leak search along the entire front surface of the concrete plug. No detectable concentrations were however found. The test therefore verified that the seal was gas tight.

Remark

Posiva and SKB (2017) has stated that "the plug also needs to be reasonably gas tight to *stop convection of air* during the operational phase". However, SKB (2014) pointed out that if all the oxygen in the trapped air in a deposition tunnel is assumed to be consumed immediately after installation then this would lead to a reduction of the gas pressure to approximately 80 % of the initial level. This could therefore imply an *advective* inflow of oxygen which would amount to 25 % of the original oxygen amount which would be a fairly marginally addition. Due to this discrepancy it is recommended that the statement about convection of air is reformulated.

6.2 Consistency evaluation

Three evaluations of the consistency of different data sets are presented below regarding: i) the total mass of bentonite; ii) the relation between dry density and the effective stress at the sensor positions; and iii) the relation between the displacement of the Leca/backfill interface and the filter pressure.

Total mass

The mean dry density values illustrated in Figure 5-21 (upper) were used to calculate weighted mean values for the seal and backfill respectively. These values were in turn adjusted for the observed displacements and could therefore be compared with the mean dry density at the installation. The weighted mean dry density was calculated as:

$$\overline{\rho_d} = \frac{\sum V_{ij} \cdot \rho_{d\,ij}}{\sum V_{ij}} \qquad (5\text{-}1)$$

where V_{ij} represented the volume of cylinders (generally hollow) and with indices i (= 1..4) and j (=1..5) indicated the axial and radial position, respectively. The axial positions coincided with the geometry at installation and so that the depths of the fillings were divided in four sections with bounding axial coordinates for the seal: 2.20, 2.08, 1.95, 1.83 and 1.70 m, and for the backfill: 1.10, 0.83, 0.55, 0.28 and 0 m. The cylinders were defined with bounding radial coordinates coinciding with the coordinates adopted for the contour plots, i.e. 0, 0.5, 1.3, 1.8, 2.3 m and varying with depth between 2.50 and 2.63 m. The dry density for each cylinder ($\rho_{d_{ij}}$) was calculated as the mean value of the dry density at the four bounding coordinates. These weighted mean values were found to be 1 342 and 1 367 kg/m^3 for the seal and backfill, respectively. These values should correspond to the ratio between the total dry mass and the final total volume: $\overline{\rho_d} = m_T/V_f$. If this is adjusted for the ratio between the final and the initial total volume, then this should be equal to the initial mean dry density:

$$\overline{\rho_d} \cdot \frac{V_f}{V_i} = \frac{m_T}{V_i} \qquad (5\text{-}2)$$

For an 80 mm extension of the seal (within the interval 60–120 mm) and a 25 mm shortening of the backfill (midpoint in interval 10–40 mm) this gives V_f/V_i-ratios of 580/500 and 1 075/1 100, respectively, which in turn gives equivalent dry density values of 1 556 and 1 336 kg/m^3 for the seal and backfill, respectively. These values can be compared with the mean dry density at the installation (in Table 2-1) which were found to be 1 560 and 1 440 kg/m^3, for the seal and backfill, respectively. This means that the dismantling data for the seal is quite consistent with the installation data. On the other hand, the evaluation shows that the equivalent dry density of the backfill at dismantling was approximately 7 % lower than the installation data. The main cause for this deviation appears to be the low dry density values found in the pellets filled slot adjacent to the Leca wall.

Dry density vs. effective stresses

The total pressure values increased successively during the test period and ranged between 4.1 and 5.8 MPa prior to the relief of the pressurization in June 2017 (Figure 3-4 and Figure 3-5). The sensor at the center of the concrete wall at the back of the backfill showed 9.2 MPa. In order to analyze the swelling pressure this can be evaluated as an effective stress so that the water pressure is subtracted from the total pressure. A compilation of such evaluated swelling pressures is shown in Figure 6-2. These values were for each swelling pressure related to the dry density of the four bentonite samples taken at positions most immediate to the position for the sensor (Figure 6-3). Each swelling pressure was illustrated against a dry density interval representing the extreme values for each such set. For simplicity, only data from measuring sections 1, 4 and 5 were included in this evaluation. The test data was compared with an interval with two bounding line, adopted for MX-80 (Börgesson et al. 2018), for which the lower and upper line represents swelling and consolidation paths, respectively.

It can be noted that eight out of the 15 measurements generally fall within this interval. However, four of the sensors located in section 1 displayed stresses below the interval, while the three axially directed sensors in section 5 showed stresses above the interval. The reason for these deviations are not known. For the Section 1 data it could possibly be caused by uncertainties in the pressure measurements, either the actual total pressure measurement or the assumption that the filter pressure is representative as a pore pressure at the concrete beams. For the Section 5 data it could possibly be caused by displacements which in turn were caused by the pressurization scheme and/or the dismantling operation.

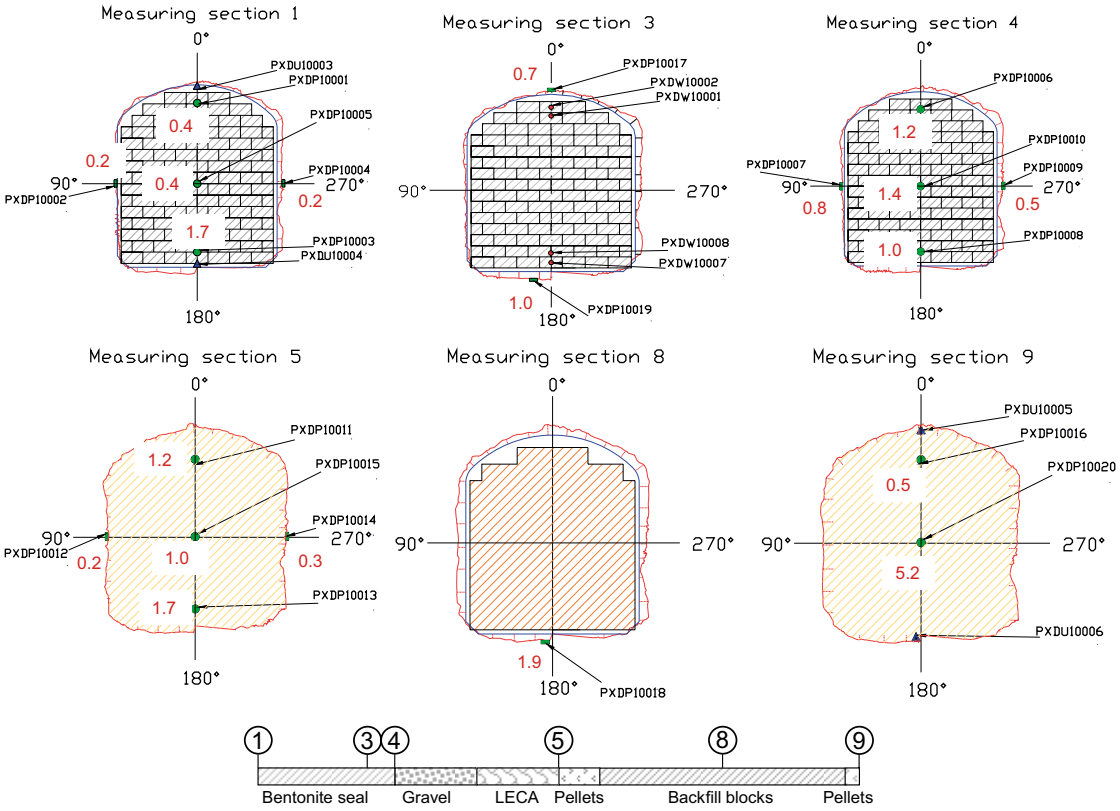

Figure 6-2. *Evaluated swelling pressure (in MPa) at total pressure sensor positions at day 1 583. Positions of measuring sections illustrated at the bottom.*

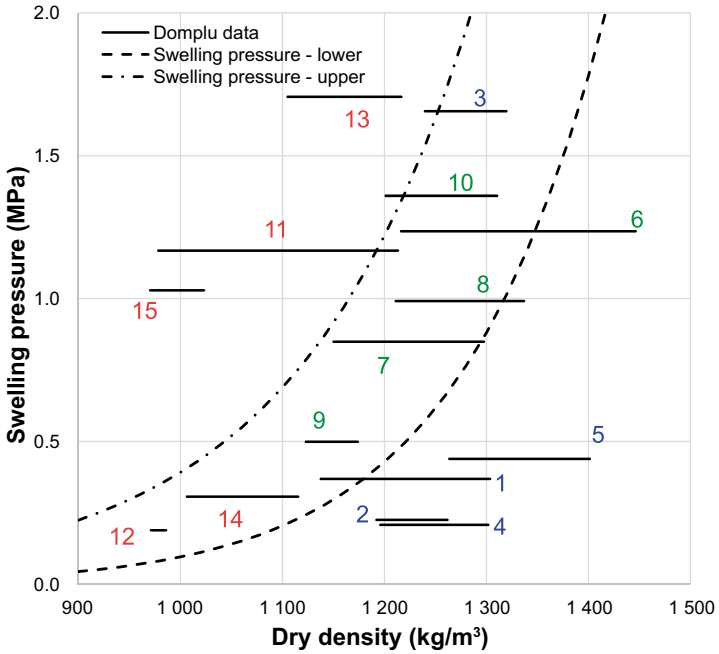

Figure 6-3. *Evaluated swelling pressure at the end of the monitoring period versus dry density ranges in bentonite samples taken close to the pressure sensors during dismantling. Numbers and colors indicate pressure sensors numbers and measuring sections, respectively; section 1 = blue; 4 = green; and 5 = red. An upper and lower swelling pressure curve derived by Börgesson et al. (2018) from independent tests with MX-80 is shown for comparison.*

Even if it isn't marked in Figure 6-3, it should be noted that the swelling pressure at sensor PXDP10020 (5.2 MPa) corresponded to a dry density interval of 1 384–1 527 kg/m^3 and that this range was fairly consistent with the two bounding lines.

Filter pressure – displacement correlation

The compression and the movement of the filter have impact on the final dry density distribution in the bentonite seal. It is therefore of interest to learn how the displacement of the filter was influenced by the pressurization of the filter. Even if two of the displacement sensors failed at a quite early stage of the test, there was apparently one (PXDD10001) which remained functional until the end of the test. Figure 6-4 shows a compilation of displacement and filter pressure data for four different periods: i) the initial evolution up to a pressurization of 4 MPa; ii) the involuntary pressure drops in January 2017; iii) the emptying and refilling of the filter in conjunction with the gas tightness test in June 2017; and iv) the strength test in August 2017. These trends demonstrate some systematic correlations:

- Increasing displacement have coincided with increasing filter pressure on at least seven occasions.
- Decreasing displacement (although minor) have coincided with filter pressures decreases at three occasions.
- Stable pressure levels subsequent to rapid changes have led to slow, counter-directed, displacements at four occasions.

Some general observations can be made even if it hasn't been possible to make a model which can mimic this behavior: the displacements at the Leca/Backfill interface appears to be "driven" by displacements at the seal/gravel interface, which are caused by swelling of the seal blocks. This was evident during the first 250 days when the displacement at the seal/gravel interface exceeded the displacements at the Leca/backfill interface (Figure 3-7). This data set therefore supports the notion that the pressurization of the filter contributed to the compression of the gravel filling.

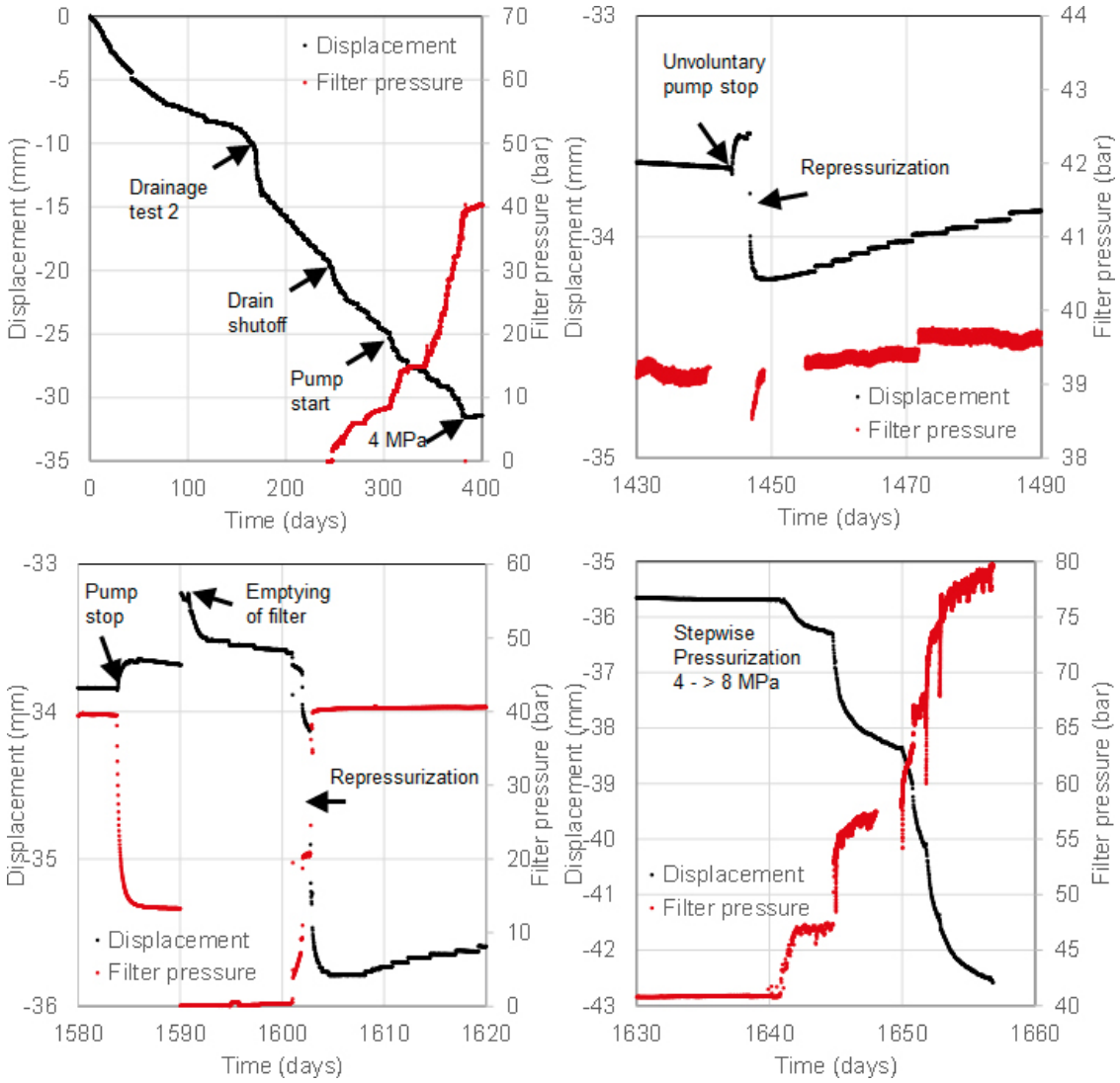

Figure 6-4. *Displacement and filter pressure evolution during four periods.*

6.3 Discussion on model validity

Three parts of the used material models is discussed below: the hydraulic model for bentonite, the mechanical model for bentonite and the mechanical model for the gravel.

Hydraulic model

The time-scale of hydration was clearly overestimated by the presented models. This was apparent by the high degree of saturation observed in the experimental data; especially for the bentonite seal. The precise time when saturated conditions were reach in the experiment is however unknown, which means that size of the deviation cannot be quantified. With the information at hand (i.e. the registered RH evolution and the dismantling data) and the saturation time for the hydraulic models, the difference in hydration rate appears to be in the order of a factor 2–3.

It should be observed that this hydration problem was complicated in at least three ways in comparison to a simple water-uptake problem: i) *the homogenization problem*, caused by the pellets-filled slot along the circumference of the block-stack and the deformable filter, which means that the dry density of the seal decreased significantly with time; ii) *the high filter pressure*, which means that the hydration didn't only follow the diffusion-like suction-driven water uptake, but also as an external pore-pressure-driven saturation front; and iii) *the potential circumventing* of the hydration problem by supplying water to the seal on the "backside" along the concrete beams.

The relevance of the first two explanations are illustrated by the result from the three different modelling approaches which showed that the hydraulic model with the homogenized dry density and the high filter pressure also displayed the fastest hydration. And unfortunately, it was not possible to make the hydro-mechanical model to converge together with a high filter pressure. The third explanation was supported by the lower dry density levels observed in section 1, and also the rapid pore pressure evolution observed for all pore pressure sensors, including two sensors located in section 1. Even if the hydraulic boundary condition extended into the pellets-filled slots in all presented modelling approach, there was no mechanism which enabled a rapid water transport between the seal blocks and the concrete beams in the models.

Mechanical model – bentonite

An attempt was made to predict the homogenization and the hydromechanical evolution of the bentonite-based components. However, the hydro-mechanical model could not converge if a boundary condition with 4 MPa water pressure was applied, and it was therefore necessary to use an atmospheric pressure boundary in order to obtain a solution. Even for a case with such a simplification, it was found to be very difficult to obtain convergence. Both the specific Domplu problem, and the high boundary water pressure, therefore appears to be difficult to solve with the used constitutive laws and numerical tool. It may nevertheless be valuable to comment on the validity of the hydro-mechanical model. This is illustrated in Figure 6-5 as stress paths for different nodes along the symmetry axis of the model in which the void ratio is plotted against the net mean stress. Some general observations can be made: the inner part of the seal and backfill blocks expands and end up precisely on the swelling pressure curve implemented in the swelling-modulus (κ_s). The pellets material also reaches the swelling pressure curve when it gets water saturated. But then it gets compressed from the adjacent bentonite blocks: first elastically and subsequently plastically. The adoption of an initial p_0^* value approximately twice as high as the swelling pressure implies that the stress path apparently overshoots the lower swelling pressure curve. A similar behavior can be observed for the outer part of the seal blocks, which initially expands, but which thereafter is compressed from the adjacent blocks. These stress paths are consistent with the hysteretic behavior generally observed for bentonite and this means that the material model is quite capable for prediction of the mechanical evolution of *unsaturated* bentonite.

Nevertheless, it has earlier been shown that this material models exhibits some inconvenient limitations; e.g. there are generally no defined void ratio dependences for the model parameters; there is no mechanism for the yield surface to contract during isotropic swelling; and suction (>0) cannot be represented for water saturated conditions (Börgesson et al. 2018). This has motivated the development of a new hydro-mechanical material model which is currently ongoing. This model is based on a description for which the swelling pressure (or the sum of the stress and suction, denoted the clay potential) for a specific void ratio is assigned in an allowed interval bounded by two lines for swelling and consolidation, respectively, and that the actual state between these lines is largely governed by the strain history. The lower curve in Figure 6-5 is identical with the line implemented in the swelling-modulus. The upper curve was derived from independent tests, see Börgesson et al. (2018).

In both the analytical dimensioning calculations of the field test, as well as in the numerical models, there was no specific description of Asha bentonite, which instead was treated as MX-80 bentonite. Since the installation, information on swelling pressure for Asha bentonite have been presented by Sandén et al. (2014). Swelling pressures measured for Asha 2010 and a salinity of 1 % is shown together with the two bounding swelling pressure lines (mentioned above) in Figure 6-6. It can be noted that the data set for Asha is fairly consistent with the swelling pressure lines, at least for a dry density level around 1 300–1 400 kg/m^3.

Mechanical model – gravel

The mechanical properties of the gravel filling have a significant impact on the hydro-mechanical evolution of the bentonite-based components. The displacements measured during the dismantling operation showed that the entire filter construction was compressed with approximately 65 mm (average displacement seal/filter 90 mm minus average displacement filter/backfill 25 mm). This is twice as high as the original analytical compression calculation in which the oedometer modulus of the gravel and Leca blocks were set to 24 and 100 MPa, respectively. With the initial thickness of

0.3 m for both the gravel layer and the Leca blocks, this meant that the expected compression for a swelling pressure of 2 MPa would be 31 mm. In hindsight, this discrepancy can to some extent be explained by the assumed absence of wall friction in the oedometer tests which may lead to an overestimation of the oedometer modulus. Guidelines for compression properties of coarse soils ("friktionsjord" in Swedish) (Karlsson et al. 1986) indicate that the ring friction may be 25 % of the vertical load for a sample height - diameter ratio of 0.5, as was used in the oedometer tests. This would imply that the evaluated modulus was overestimated with 25 %, which in turn would mean that the expected compression could be adjusted to 41 mm. Since the oedometer tests were performed with the lowest possible loosely-placed density, it seems unlikely that the density in the field-test would be significantly lower and thereby more compressible. An alternative explanation for the extensive compression could be that this was caused by the high pressures applied during the strength test. An advanced hydro-mechanical model would however be needed to support such an explanation.

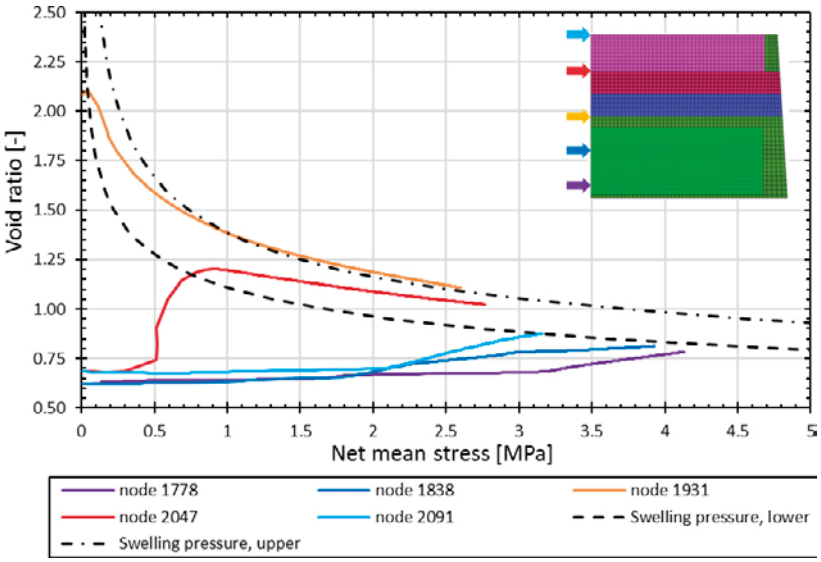

Figure 6-5. *Stress-paths in e-p plane for five nodes along the symmetry axis. An upper and lower swelling pressure curve derived from independent tests with MX-80 is shown for comparison.*

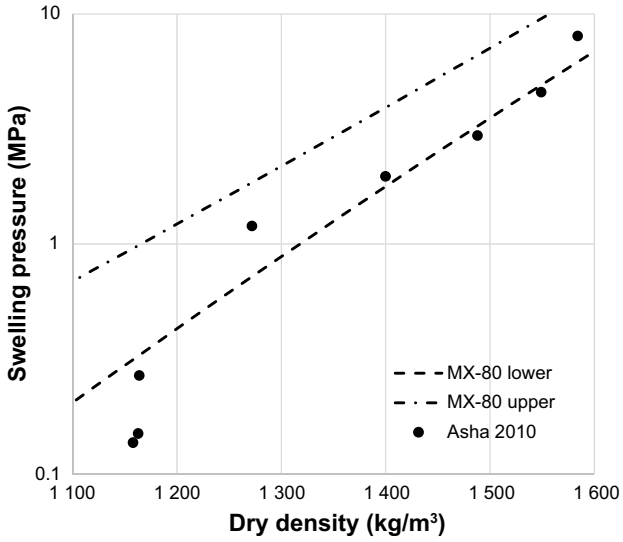

Figure 6-6. *Swelling pressure versus dry density for Asha 2010 reported by Johannesson et al. (2008). An upper and lower swelling pressure curve derived from independent tests with MX-80 is shown for comparison.*

7 Comments and conclusions

7.1 Results on monitoring of the Dome plug

The monitoring of the bentonite components has included sensors measuring Relative Humidity, Total pressure, Pore Pressure and Displacement. In addition, the applied water pressure and inflow to the filter section have been registered together with the leakages past/through the plug.

The measurements have shown that both the seal and the backfill started to take up water immediately after installation. After the filter fill-up and the later water pressure increase in the filter section up to 4 MPa, the saturation rates increased and after about two years test duration the Relative Humidity sensors indicated that both the bentonite seal and the backfill were largely saturated at the sensor positions. The registered swelling pressures in both the bentonite seal and in the backfill have in general been somewhat lower than expected, between a couple of hundreds kPa and up to 1 800 kPa. One sensor at the back of the backfill showed 5 200 kPa. The displacement sensors have registered a small movement upstream, approximately 30 mm at the end of the monitoring period, of both the bentonite seal and the filter section and these movements were later confirmed in conjunction with the dismantling that showed that the bentonite had swollen and compressed the gravel filling.

7.2 Function tests

7.2.1 Gas tightness test

A decision was made that the Dome plug experiment should be used to verify the gas tightness requirement (see description in Section 1.3.3). The test was started by draining the water from the filter section and then fill it with helium gas to an overpressure of 0.4 bar. By monitoring the gas pressure evolution and by using sniffer leak search along the entire front surface of the concrete plug it was verified that the seal was gas tight. The performed test on gas tightness is described in detail in Åkesson (2018).

7.2.2 Strength test

A preliminary design basis has been that the plug shall withstand a total pressure of 7 MPa (hydrostatic pressure of 5 MPa and swelling pressure from the backfill of 2 MPa). The total pressure during the test time has been somewhat lower, between 5 and 6 MPa, and it was therefore decided to increase the applied water pressure in the filter section to test the strength. The water pressure was increased in steps for three weeks up to 8 MPa (total pressure including the swelling pressure from the bentonite was thus > 9 MPa). No cracking or fracturing of the concrete could be observed visually. The concrete dome has also been investigated with different methods, e.g. non-destructive testing, core drilled samples etc. The results from these tests are reported in Malm et al. (2019).

7.2.3 Hydraulic tightness

The water tightness of the plug has been continuously measured during the test time (approximately day 400 to day 1 580, Figure 3-9). During this time a water pressure of 4 MPa was applied in the filter section and the leakage collected in a weir in front of the plug was determined to between one and three liters per hour. It is however not exactly known how much of this leakage that has been coming through the plug or in the interface concrete-rock and how much that has been coming via fractures in the rock. During this test period leakages were also collected from cables, about 1 l/h, and from a rock fracture positioned on the right side of the entrance to the test tunnel, 7-8 l/h.

The function tests performed after June 2nd, 2018 clearly influenced, as expected, the results from leakage measurements. When the pressure was decreased the leakages decreased and when the pressure was reset to 4 MPa the leakage increased to the same level as earlier. During the strength test of the plug, the water pressure was increased to 8 MPa. This resulted in considerably higher leakage measurements, especially from the rock fracture where the registered leakage was above 250 l/h.

The leakage from the weir increased to about 13 l/h and from the cables to about 15 l/h. When the water pressure was decreased to 4 MPa again the leakages decreased to the same level as before the pressure increase (the number of registered data is, however, limited from this period).

7.3 Sampling of components in conjunction with dismantling

7.3.1 Bentonite seal

The sampling of the bentonite seal showed that it was in general completely saturated. The bentonite had swelled and was in tight contact with the rock surface all around the tunnel contour. No empty voids or channels could be found.

The pellet filling in the periphery had been compressed by the swelling blocks. There were, however, remaining differences in density between the central parts (former block stack) and the periphery (former pellet filling) even if it was obvious that the differences had decreased when comparing with the density of the different components at the time for installation. The bentonite seal had swelled also in axial direction and compressed the gravel filling behind. The bentonite blocks had an initial thickness of 500 mm but had at the time for dismantling a thickness of between 560 and 620 mm.

The experiment design gave an opportunity to investigate how the original cation pool in the bentonite seal had been influenced of the exposure to the formation water on one side and the contact with cement on the other side. The results from the tests showed that the content of Ca-ions had increased significantly in the bentonite facing the filter section and at the same time the concentration of Na-ions had decreased correspondingly. The same redistribution could be seen on the bentonite facing the concrete beam wall albeit to a lesser content. The effect of the contact with the filter section and the concrete beams respectively, decreased significantly towards the central parts of the bentonite block where the cation pool distribution was the same as in the as-delivered material. The results indicated that the bentonite seal have had access to formation water from both sides i.e. not only from the filter section but also from the concrete beam side.

7.3.2 Filter sections

Gravel filling

In conjunction with the test dismantling it was discovered that the gravel filling had been compressed by the swelling bentonite seal. The thickness of the gravel filled section was at installation 300 mm. However, the bentonite seal had swelled and increased its thickness from 500 to between 560 to 620 mm which had resulted in that the gravel filling was compressed to a thickness between 210 to 250 mm.

No bentonite was found within the gravel filling i.e. the separating geotextile against the bentonite seal and the LECA wall against the backfill had prevented bentonite from eroding into the gravel filling.

LECA wall

The data registered during the test time had indicated that the LECA wall had moved upstream against the backfill approximately 43 mm during the peak of the strength test. Measurements during excavation verified that the LECA wall had moved upstream between 10 and 40 mm.

7.3.3 Backfill

The sampling of the backfill showed that it was largely saturated but there were some central parts with a lower degree of saturation. The differences in density between the central parts and the pellet filled parts at the periphery were similar to what was determined for the bentonite seal. The density of the pellet filling behind the LECA wall was clearly lower than the rest of the backfill although it had been compressed by the swelling backfill blocks and by the bentonite seal that had pushed the LECA wall upstream.

7.4 Modelling

The purpose of the numerical modelling of the dome plug was to predict how far the hydration and the homogenization of the bentonite seal and the backfill had proceeded at the time of the excavation. The hydro-mechanical modeling has shown a fairly good ability to predict the overall evolution of RH, swelling pressures and displacements. However, it was not possible to make a hydro-mechanical model to converge together with a hydraulic boundary condition with 4 MPa water pressure. This appears to be one of the reason for why the rate of hydration was underestimated, possibly together with a circumventing water supply to the seal from the side toward the concrete beams. The extent of homogenization was in fairly good agreement with the experimental data if the model was allowed to run to a hydration state more similar to the experiment. However, the lowest dry densities in the HM model significantly exceeded the lowest values observed in the in experimental data, which may be a consequence of the absence of wall friction in the model.

The consistency between the installed dry density, the measured effective stresses and the dismantling data were evaluated. This shows that the measured dry density distribution in the bentonite seal and the dimensions of this at the time of dismantling were in good agreement with the average dry density of the seal at the installation. A corresponding comparison for the backfill showed however that the equivalent dry density at the dismantling was 7 % lower than the average dry density at the installation, for which the main cause was the low dry densities found in the pellets filled slot adjacent to the Leca wall. The swelling pressures at the end of the monitoring period were related to the measured dry density values in samples taken close to 15 of the total pressure sensors. This was found to be consistent with established swelling pressure relations for approximately half of the sensors. However, four of the sensors in the seal close to the concrete beams showed too low pressure levels in relation to the dry density, and three of the sensors in the pellets filling close to the Leca wall showed too high pressure levels. Finally, an evaluation of the filter pressure data and the displacement at the Leca/backfill interface showed that these variables were correlated, which supports the notion that the pressurization of the filter contributed to the compression of the gravel filling.

References

SKB's (Svensk Kärnbränslehantering AB) publications can be found at www.skb.com/publications. SKBdoc documents will be submitted upon request to document@skb.se.

Belyayeva N I, 1967. Rapid method for the simultaneous determination of the exchange capacity and content of exchangeable cations in solonetzic soils. Soviet Soil Science, 1409–1413.

Börgesson L, Sandén T, Andersson L, Johannesson L, Goudarzi R, Åkesson M, 2015a. System design of Dome Plug. Preparatory modelling and tests of the sealing and draining components. SKB R-14-25, Svensk Kärnbränslehantering AB.

Börgesson L, Sandén T, Dueck A, Andersson L, Jensen V, Nilsson U, Olsson S, Åkesson M, Kristensson O, Svensson U, 2015b. Consequences of water inflow and early water uptake in deposition holes. EVA-project. SKB TR-14-22, Svensk Kärnbränslehantering AB.

Börgesson L, Hernelind J, Åkesson M, 2018. EBS TF – THM modelling. Homogenisation task. SKB P-18-05, Svensk Kärnbränslehantering AB.

Dueck A, Nilsson U, 2010. Thermo-Hydro-Mechanical properties of MX-80. Results from advanced laboratory tests. SKB TR-10-55, Svensk Kärnbränslehantering AB.

Grahm P, Malm R, Eriksson D, 2015. System design and full-scale testing of the Dome Plug for KBS-3V deposition tunnels. Main report. SKB TR-14-23, Svensk Kärnbränslehantering AB.

Johannesson L-E, Sandén T, Dueck A, 2008. Deep repository – engineered barrier system. Wetting and homogenization processes in backfill materials. Laboratory tests for evaluating modeling parameters. SKB R-08-136, Svensk Kärnbränslehantering AB.

Johannesson L-E, Sandén T, Dueck A, Ohlsson L, 2010. Characterization of a backfill candidate material, IBECO-RWC-BF. Baclo Project – Phase 3. Laboratory tests. SKB R-10-44, Svensk Kärnbränslehantering AB.

Karlsson R, Hansbo S, Andréasson L, Sällfors G, 1986. Geotekniska laboratorieanvisningar. Del 10, Kompressionsegenskaper. Stockholm: Statens råd för byggnadsforskning. (In Swedish.)

Karnland O, Olsson S, Nilsson U, 2006. Mineralogy and sealing properties of various bentonites and smectite-rich clay materials. SKB TR-06-30, Svensk Kärnbränslehantering AB.

Malm R, Enzell J, Hassanzadeh M, 2019. Full-scale test of the Dome Plug for KBS-3V deposition tunnels, structural response of the concrete dome. NDT, FE-simulations and evaluation of measurements during the leakage and strength test. SKB P-18-14, Svensk Kärnbränslehantering AB.

Posiva SKB, 2017. Safety functions, performance targets and technical design requirements for a KBS-3V repository. Conclusions and recommendations from a joint SKB and Posiva working group. Posiva SKB Report 01, Posiva Oy, Svensk Kärnbränslehantering AB.

Sandén T, Börgesson L, Dueck A, Goudarzi R, Lönnqvist M, 2008. Deep repository – Engineered barrier system. Erosion and sealing processes in tunnel backfill materials investigated in laboratory. SKB R-08-135, Svensk Kärnbränslehantering AB.

Sandén T, Olsson S, Andersson L, Dueck A, Jensen V, Hansen E, Johnsson A, 2014. Investigation of backfill candidate materials. SKB R-13-08, Svensk Kärnbränslehantering AB.

Sandén T, Karnland O, Börgesson L, Nilsson U, Hedström M, Jefferies N, 2016. Sealing Site Investigation Boreholes: Phase 2. Stage 1 laboratory programme. Amec Foster Wheeler report 202580/06 Issue A, UK.

Sellin P (ed), Åkesson M, Kristensson O, Malmberg D, Börgesson L, Birgersson M, Dueck A, Karnland O, Hernelind J, 2017. Long re-saturation phase of a final repository. Additional supplementary information. SKB TR-17-15, Svensk Kärnbränslehantering AB.

SKB, 2010. Design, production and initial state of the backfill and plug in deposition tunnels. SKB TR-10-16, Svensk Kärnbränslehantering AB.

SKB, 2014. Svar till SSM på begäran om komplettering rörande grundvattenkemi på kort och medellång sikt. SKBdoc 1437441 ver 1.0, Svensk Kärnbränslehantering AB. (In Swedish.)

SSM, 2016. Granskningsrapport Långsiktig strålsäkerhet inför yttrandet till Mark- och miljödomstolen vid Nacka tingsrätt. Stockholm: Strålsäkerhetsmyndigheten (Swedish Radiation Safety Authority). (SSM2011-1135) (In Swedish.)

Åkesson M, 2018. Full scale test of the Dome Plug for KBS-3V deposition tunnels. Gas tightness test. SKB P-17-37, Svensk Kärnbränslehantering AB.

Åkesson M, Börgesson L, Kristensson O, 2010a. SR-Site Data report. THM modelling of buffer, backfill and other system components. SKB TR-10-44, Svensk Kärnbränslehantering AB.

Åkesson M, Kristensson O, Börgesson L, Dueck A, Hernelind J, 2010b. THM modelling of buffer, backfill and other system components. Critical processes and scenarios. SKB TR-10-11, Svensk Kärnbränslehantering AB.

Arkitektkopia AB, Bromma, 2019

SKB is responsible for managing spent nuclear fuel and radioactive waste produced by the Swedish nuclear power plants such that man and the environment are protected in the near and distant future.

skb.se